



*Cruise Report*

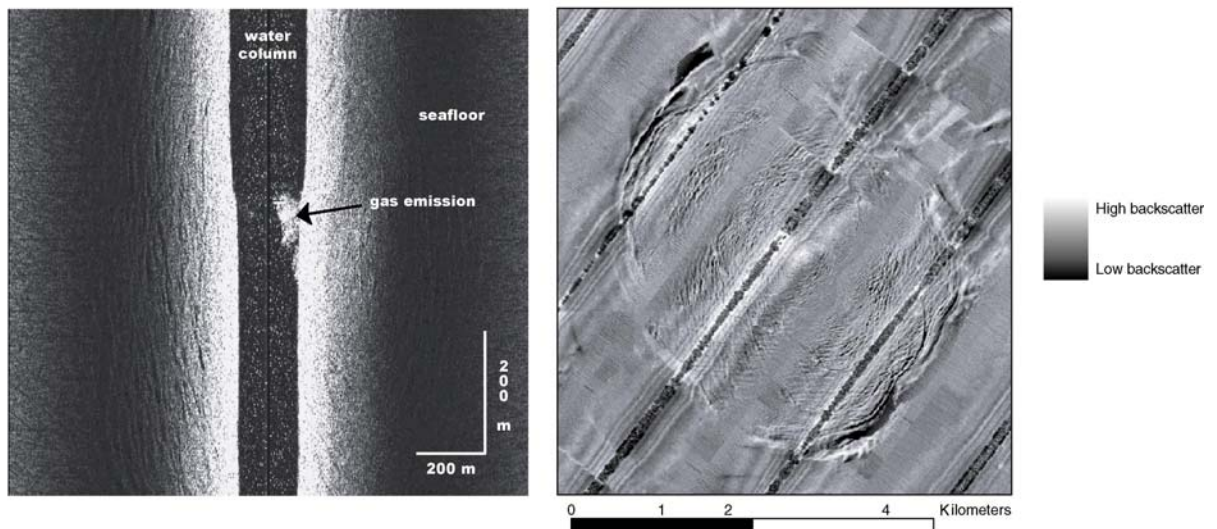


# MIMES

**An Expedition on Pelagia**

13 June 2004 -- 14 July 2004

(a contribution to the MEDIFLUX project  
of EUROMARGINS)



[Isis Mud Volcano: figure left shows unprocessed deep tow sidescan sonar data; figure right shows processed data]

ALW-NWO project 855.01.031



## Table of contents

<b>1.0.0 INTRODUCTION</b>	<b>1</b>
<b>1.1.0 BACKGROUND</b>	<b>2</b>
<b>1.2.0 DATA EXPLOITATION</b>	<b>3</b>
1.2.1 SCIENTIFIC APPROACH	3
1.2.2 RESEARCH METHODOLOGY	4
<b>2.0.0 GEOCHEMISTRY: SEA AND PORE WATER ANALYSIS</b>	<b>9</b>
<b>2.1.0 MATERIALS AND METHODS</b>	<b>9</b>
2.1.1 SEDIMENT SAMPLING	9
<b>2.2.0 ON-BOARD ANALYTICAL TECHNIQUES</b>	<b>9</b>
<b>2.3.0 CTD STATIONS</b>	<b>10</b>
2.3.1 INSTRUMENTATION	10
2.3.2 PLUME DETECTION	10
2.3.3 BRINE SAMPLING	10
2.3.4 RESULTS	11
<b>2.4.0 CORING</b>	<b>11</b>
2.4.1 INTRODUCTION	11
2.4.2 SEDIMENT SAMPLING	11
2.4.3 RESULTS – GEOCHEMISTRY OF PORE WATERS	12
<b>3.0.0 GEOCHEMISTRY: GAS COMPOSITION IN THE WATER COLUMN AND SEDIMENT</b>	<b>15</b>
<b>3.1.0 MATERIALS AND METHODS FOR GAS MEASUREMENTS</b>	<b>15</b>
<b>3.2.0 RESULTS AND PRELIMINARY DISCUSSION</b>	<b>16</b>
3.2.1 CH <sub>4</sub> CONCENTRATIONS AT AMSTERDAM MUD VOLCANO (ANAXIMANDER MOUNTAINS)	16
3.2.2 HYDROCARBONS IN THE SEDIMENT	16
<b>3.3.0 HYDROCARBON CONCENTRATIONS IN THE NILE DEEP-SEA FAN</b>	<b>17</b>
3.3.1 HYDROCARBON CONCENTRATION IN THE WATER COLUMN	17
3.3.2 HYDROCARBON CONCENTRATIONS IN THE SEDIMENT	19
<b>3.4.0 CONCLUSION</b>	<b>20</b>
<b>4.0.0 CLASTS AND CARBONATES</b>	<b>21</b>
<b>4.1.0 OBJECTIVE</b>	<b>21</b>
<b>4.2.0 SAMPLING</b>	<b>21</b>
<b>4.3.0 RESULTS</b>	<b>22</b>
<b>5.0.0 NON-SEEP SEDIMENTOLOGICAL CORES</b>	<b>31</b>
<b>5.1.0 DESCRIPTION OF CORES</b>	<b>31</b>
5.1.1 CORE MS27PT	31

5.1.2 CORE MS35PC	31
5.1.3 CORE MS43PC	32
5.1.4 CORE MS44PC	32
5.1.5 CORE MS45PC	32
5.1.6 CORE MS46PC	33
5.1.7 CORE MS51PC	33
5.1.8 CORE MS59PT	33
<b>6.0.0 DTS-1 EDGETECH DEEP-TOWED SIDESCAN SONAR</b>	<b>35</b>
<b>6.1.0 INTRODUCTION</b>	<b>35</b>
<b>6.2.0 TECHNICAL DESCRIPTION OF THE INSTRUMENT</b>	<b>36</b>
6.2.1 UNDERWATER SET-UP	36
6.2.2 LABORATORY SET-UP	37
6.2.3 SOFTWARE	38
<b>6.3.0 USBL UNDERWATER POSITIONING</b>	<b>39</b>
<b>6.4.0 DEPLOYMENT AND RECOVERY PROCEDURES</b>	<b>41</b>
<b>6.5.0 OPERATIONAL SETTINGS, EAST MEDITERRANEAN SURVEYS AND DATA QUALITY</b>	<b>42</b>
<b>6.6.0 PRELIMINARY RESULTS</b>	<b>47</b>
<b>7.0.0 HEAT FLOW MEASUREMENTS</b>	<b>57</b>
<b>8.0.0 SURVEYS WITH 3.5 KHZ ECHOSOUNDER</b>	<b>61</b>
<b>9.0.0 SUMMARY</b>	<b>65</b>
<b>9.1.0 ACKNOWLEDGEMENTS</b>	<b>67</b>
<b>10 REFERENCES</b>	<b>79</b>

## ***MIMES* CRUISE REPORT**

An Expedition aboard R/V *Pelagia* as Part of the MEDIFLUX Project  
June-July 2004, Iraklion-Limassol-Limassol

### **1.0.0 Introduction**

MIMES (a **M**ultiscale **I**vestigations of Eastern **M**editerranean **S**eep **S**ystems) was a research expedition aboard the Dutch research vessel *Pelagia*; and is a contribution to a multi-scale, multidisciplinary, multi-national exploration of seafloor areas characterized by a rich variety of fluid escape structures in the eastern Mediterranean Sea. It is an examination of the distribution and variety, emission controls, geochemistry, and biology of recently discovered fluid seeps and mud volcanoes on the Nile deep-sea fan and in the Anaximander Mountains.

The principal technical objectives of the research were

- (1) to image the fluid systems of the Nile deep-sea fan with a digital deep-tow acoustic system (combining sidescan sonar and subbottom profiling using the Edgetech DTS-1 system of Geomar, Kiel),
- (2) to obtain samples of selected seep areas using video-directed box corer, as well as standard piston and gravity corers (mostly with thermal probes attached).
- (3) to make CTD measurements through the water column and to take rosette water samples in areas of known or potential seeps using a SeaBird CTD, as well as a specially adapted CTD for use in brines and fluid mud, and
- (4) to examine the sedimentologic context of the seep areas using piston corer.

A secondary aim was

- (5) to investigate areas of related targets in the Anaximander Mountains using similar methods.

MIMES used a digital deep tow acoustic instrument (the Edgetech DTS-1 system from Geomar, Kiel, Germany) with both sidescan sonar and subbottom profiler to create mosaics of backscatter imagery over three of the different seep areas combined with digital subbottom profiling data for investigating possible shallow BSRs and mud flows from mud volcanoes (and interfingering of hemipelagic sediments with the mud flows). CTD and water chemistry measurements were made above the seeps. Sampling of the seafloor in seep areas was carried out with piston, gravity, and box corers for joint microbiological, geochemical, and sedimentological studies. The box corer was equipped with a prototype video system for observing the seafloor in the vicinity of four sampling locations and guiding the precision sampling.

Three principal areas on the Nile deep sea fan were investigated during two weeks, along with two secondary targets (in the Anaximander Mountains to the north) in a third week of work (fig 1.1). The data are being analysed in cooperating laboratories in the Netherlands, France, and Germany by partners within the longer term European project MEDIFLUX of which this expedition was a Dutch contribution within the ESF-initiated Euromargins

programme. Thus the purpose of MIMES was to contribute to the objectives of the MEDIFLUX project to (i) describe the geographical distribution, types, geological formation, and activity of fluid seeps on the Nile deep-sea fan, (ii) determine the composition of emitted fluids (including gas, liquid, and solid phases) for inferring fluid properties and processes at depth, (iii) determine the controls and mechanisms of chemical element transport and breakdown by seep biota to obtain well constrained budget of element cycling and export at fluid seeps, (iv) determine the heat flow through the seafloor, (v) measure methane concentrations in the water and sediment column, and (vi) calibrate the geophysical signature of seeps with observed seafloor characteristics in order to make it easier and quicker to map and estimate activity of fluid seeps.

This expedition was the second in a series of three. The first took place in September 2003 with the French research ship *L'Atalante* and the research submersible *Le Nautilus*. The third cruise is planned on the German research vessel *Meteor* sometime in the period 2006 to 2007. The work is a direct consequence of the cooperation established within the French-Dutch cooperative programme MEDINAUT (cruises by *L'Atalante* and *Professor Logachev* in 1998 and 1999) and based on research carried out by the French expeditions PRISMED II, FANIL, and MEDISIS.

#### 1.1.0 Background

Research into cold seeps in the eastern Mediterranean is relatively new. Little was done after the initial discovery of mud volcanoes by the Italians in the late 1970s (Cita et al., 1981), and of the first brine lake by the Dutch in the early 1980s (Jongsma et al., 1983; De Lange and Ten Haven, 1983), until the 1990s when a number of international expeditions were mounted mainly to examine the mud volcanoes and brine lakes of the Mediterranean Ridge (Cita et al., 1996; MEDINAUT/MEDINETH Shipboard Scientific Parties, 2000; MEDRIF-Consortium, 1995). Numerous structures discovered on the deep Nile Cone in the autumn of 2000 during the FANIL expedition (Bellaiche et al., 2001; Loncke, 2002) are probably the sites of active fluid seeps. Several of them are situated directly over seismically well-imaged gas chimneys. Slicks have been identified on the sea surface in connection with the suspected seeping from deep reservoirs currently the focus of petroleum company interest. The seep environment of the Nile Cone (passive continental margin) is different from that of the other seeps on the Mediterranean Ridge (the accretionary prism of the Hellenic subduction zone), the Anaximander Mountains (crustal blocks rifted southward from southwestern Turkey), and the Florence Rise (a zone of predominantly transcurrent faulting). It is therefore of interest to compare the same phenomena arising under different conditions.

In three distinct provinces of the Nile Cone and deep-sea fan, there are a number of different seep-related structures for which preliminary sampling indicates gassy ( $\text{H}_2\text{S}$ ,  $\text{CO}_2$ ,  $\text{CH}_4$ ) structureless grey sediments typical of mud volcanoes:

- (1) The **eastern province**, characterised by halotectonics, contains several large, low-relief (<50 m), sub-circular structures, 3 – 4 km in diameter which, in seismic profiles, are seen to lie directly over gas chimneys, suggesting strong degassing; pockmarks are also present. Several of these also lie to the west of a north-south escarpment of about 50 m

marking the boundary between areas underlain by Messinian evaporites (to the east) and areas apparently without salt (to the west).

- (2) A **central province** is characterised by a belt more than 100 km long of large slump and slide scars. Dozens of inferred pockmarks associated with patches of strong acoustic backscatter of the seafloor about 100 – 200 m across are found throughout this region and appear to be tectonically controlled. Seafloor instabilities may be facilitated by the seeps.
- (3) In the **western province** of the deep (2500-3000 m) fan region there are, apparently associated with growth faults, tens of small conical structures up to 1 or 2 km wide and 50 – 75 m high, some with central depressions, and a few vast sub-circular crater-like depressions up to 8 km in diameter and a few tens of metres deep with small parasitic cones.

All three provinces were investigated by the submersible *Nautilie* during the NAUTINIL expedition in September 2003 (Foucher et al., 2004) and were targets also for MIMES.

## 1.2.0 Data Exploitation

### 1.2.1 Scientific approach

The integrated multidisciplinary approach taken within MEDIFLUX combines a variable scale of observations (multi-scale) from detailed seafloor observations from *Nautilie* during the NAUTINIL expedition in 2003 (centimetric to metric scales) to a broader observational scale using deep towed devices from Pelagia in 2004 (observational scales of metres to several hundreds of metres), and up to existing multibeam maps (large scale). Sampling during MIMES also provided deeper sampling which was not possible from the *Nautilie*.

Acoustic backscatter mosaics provide information about the distribution and density of seeps and their level of long-term activity. The geophysical response of the seafloor in seep areas varies according to the age of mud flows from mud volcanoes (Volgin and Woodside, 1996), the density of shell debris and presence of benthic fauna such as tube worms and bivalves, the thickness and distribution of carbonate crusts, and the seafloor roughness and small scale relief created by the eruptive activity; and these in turn are directly related to the activity of the seeps. Digital subbottom profiles provide the necessary depth information (e.g. about flow thickness, mud volcano development, fault control and fluid migration pathways, and in some areas like the Anaximander Mountains, the presence or not of a shallow BSR indicating the base of a gas hydrate zone). Visual observations and samples provide the ground truth data for interpreting deep tow geophysical data. Moreover, detailed precision sampling is dependent on good mid-scale groundwork for determining sample locations.

The stable carbon isotope composition ( $\delta^{13}\text{C}$  of the gas molecules (methane, ethane, propane,  $\text{CO}_2$ ) analysed together with their chemical proportions reveals the origin, thermogenic versus biogenic, of the advecting gas and whether it was affected by possible post-genetic fractionation upon migration from the subsurface to the sampled seep. Interpreted along with major element geothermometry (using for example Li and B isotopes) as well as the geothermal gradient itself (to be measured by thermistors attached to the piston corer), the

source depths of fluids and any erupted mud can be estimated. The isotopic composition of dissolved Sr can help to constrain the sources and flow paths of fluids, and  $\delta^{18}\text{O}$  and  $\delta\text{D}$  analyses of the pore water will also allow us to conclude whether the fluids are related to fluvial input (e.g. in turbiditic areas), or to gas hydrates (De Lange and Brumsack, 1998), or to mineral dewatering at depth (Dählmann and de Lange, 2003; Zitter, 2004).

Only quite recently has it been realized that the process used by the microorganisms responsible for anaerobic oxidation of methane (AOM) is catalyzed by a consortium of prokaryotic organisms (Boetius et al., 2000). By combining several approaches based on 16S rDNA sequence information, isotopic composition of specific biomarkers, and radiotracer experiments, it has finally been possible to make significant progress in the identification and physiological study of these micro-organisms. Anaerobic methane oxidation is a two-step reaction carried out in syntrophy by aggregates of archaea and sulfate reducing bacteria. The archaea convert methane to a yet unknown intermediate electron carrier and the sulfate reducers oxidize that electron carrier using sulfate as an oxidant. Concomitant measurements of methane oxidation and sulfate reduction rates are proposed for different locations with high and low methane efflux, to obtain an estimate of methane emission and turnover at methane seeps and mud volcanoes.

### *1.2.2 Research Methodology*

A broad spectrum of molecular and biogeochemical approaches will be applied to the MIMES data in combination with geophysical and geochemical field studies to provide characteristic examples of how the fluid flux and its biological filter operate in marine sediments. All three phases – gas, water, and mud – are part of the study. Part of this was carried out on-board, especially for those constituents that cannot be preserved for later on-land analyses. Gas hydrates were expected at some high flux seeps on the basis of favourable stability conditions and the known presence of gas hydrates at two sites in the Anaximander area; however none were recovered during MIMES.

Seawater and sediment pore-water samples were subsampled for gas for on-board analyses, and filtered and stored for subsequent on-land analyses (see geochemistry section of this report for details). Pore waters obtained by squeezing and centrifuging sediments under inert gas atmosphere are to be analyzed for nutrients and chloride concentration. Shipboard analyses included (1) methane,  $\text{C}_2$ , and  $\text{C}_3$ , using a dedicated gas chromatograph, (2) DIC,  $\text{H}_2\text{S}$ , and nutrients, using a Technicon autoanalyser system, (3) salinity (possibly Cl), using a refractometer or possibly titration, (4) alkalinity by Gran-plot titration, (5) oxygen using Winkler titration. Intensive studies of major elements and isotopic compositions were planned to be done in the home labs, where among other gases, methane, possibly  $\text{C}_2$ ,  $\text{C}_3$ ,  $\text{CO}_2$ , and their isotopic composition will be made using conventional GCMS, and Gcirms techniques. Major and some minor elemental dissolved concentrations in pore water and vent-related seawater will be investigated using ICPAES, IC, titration, and ICPMS. Stable isotopes of water will be analysed along with dissolved carbonate, boron, HS,  $\text{SO}_4$ , and Sr, using conventional MS, CNS-MS, high-resolution-MS, and other dedicated techniques. XRD analyses will be carried out on the clay mineral composition. Petrography, SEM observations, XRD analyses, and stable isotope ( $\delta^{18}\text{O}$  and  $\delta^{13}\text{C}$ ) measurements on the

diagenetic carbonate crusts will constrain their genetic relationship with the pore fluids. Rock-Eval analyses will give information on the organic matter maturity.

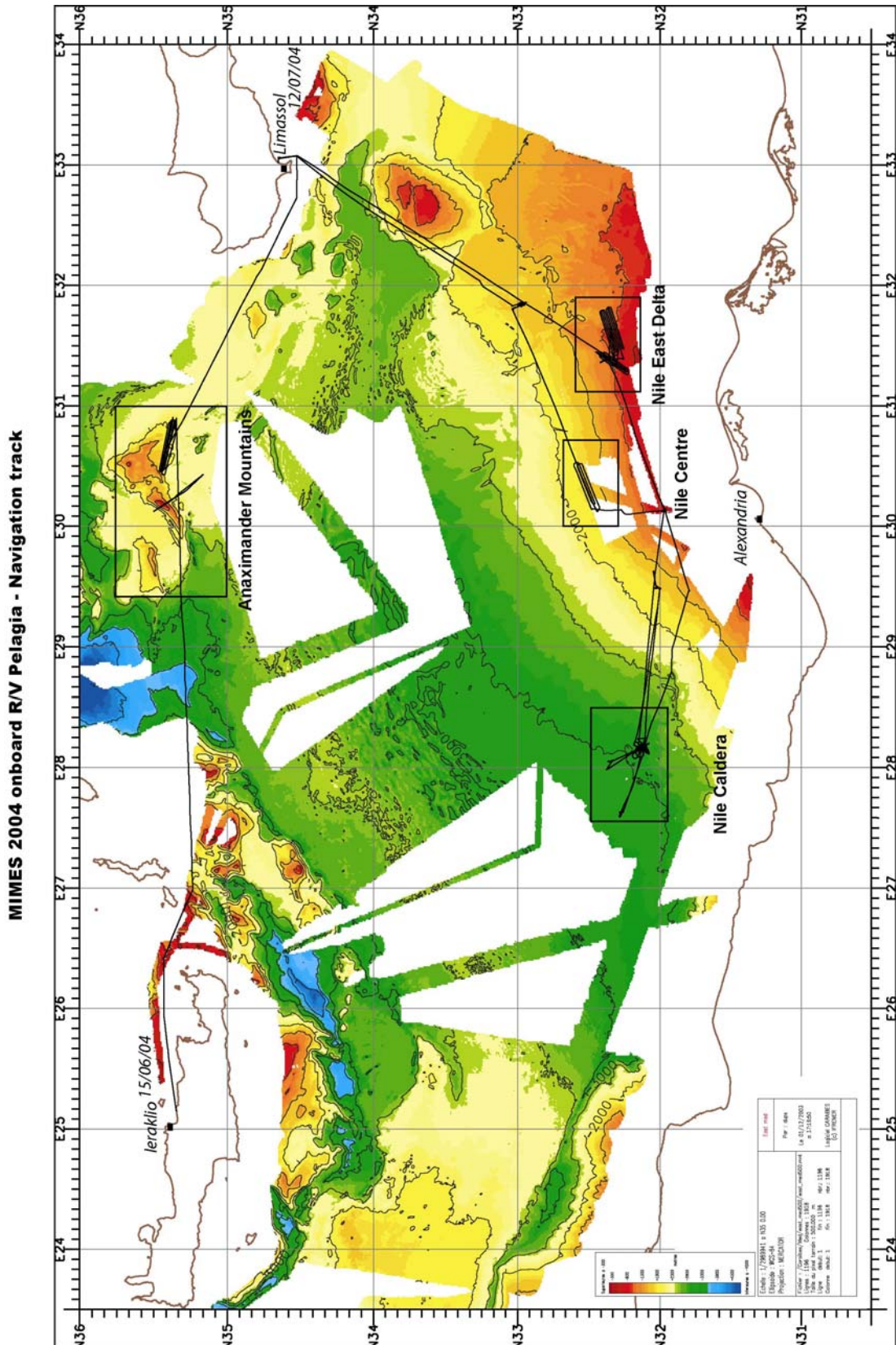
The main microbiological task is to determine the microbial turnover of methane and sulfur at the seeps. This involves carrying out concomitant measurements of methane and sulfide oxidation and sulfate reduction rates at different locations with high and low methane efflux, to obtain an estimate of methane emission and turnover at the methane seeps and mud volcanoes. Further goals are the *in situ* characterisation of the geochemical conditions for microbial methane and sulfide oxidation and its temporal and regional variation, *in situ* distribution and rRNA-based molecular diversity of microorganisms involved in methane and sulfide oxidation, and the isolation, identification and characterisation of the microorganisms involved, as well as complementary laboratory-based research into biodiversity using DNA sampled from the microbial community to amplify target metabolic genes (*csoS1A*, *cbbL* plus *cbbM*), isolation and culture of sulfur-oxidizing prokaryotes, and analysis of species diversity using genetic fingerprinting of isolates obtained from various sites and at various time intervals (using rep-PCR, AFLP). If anaerobic methane oxidation is indeed constrained by the energy yield, it should be regulated by: temperature, pH, and concentrations of sulfate, hydrogen sulfide, bicarbonate, methane, and possibly hydrogen, acetate and/or formate. All these key parameters to be analyzed in sea floor samples will be compared with other geochemical settings in gas hydrate bearing systems currently under study.

Deep tow digital geophysical observations obtained during MIMES will be analysed in combination with existing multibeam data (merged within Caribes software) along with dive observations from *Nautila* (using Adelle software with ArcView) and video-guided sampling. The DTS-1 deep tow system requires processing ashore in Kiel; shipboard work was simply data collection and storage, and preparation of navigations files.

Core descriptions were made aboard the *Pelagia* for the most part. Further sedimentology of cores, including physical properties measurements using a Geotek multitrack logger will occur ashore and provide ground truth for the analysis of seafloor acoustic backscatter variations as well as input for modeling the heat flow.



Figure 1.1 Cruise navigation tracks





## **2.0.0 Geochemistry: Sea and Pore Water Analysis**

### 2.1.0 Materials and Methods

#### *2.1.1 Sediment sampling*

The sediment was sampled for four parameters:

- Methane
- Sulphide-Fixation
- Water content / porosity
- Pore water extraction

Methane: see section on gas analysis elsewhere in this report

Sulphide-Fixation: 10 ml sediment were put into a 60ml septum bottle filled with 50 ml 0.01 M ZnAc<sub>2</sub>-solution and shaken vigorously.

Water content / porosity: 1-2 ml sediment were put into 15 ml pre-weighed glass.

Pore water extraction: Pore water (PW) extraction started as soon as possible after core recovery, generally under inert atmosphere in a glovebox and under in situ temperatures (ca. 14 C). The extraction was done either by centrifuging or by squeezing following the procedure described in De Lange (1992). The PW obtained from centrifuging was decanted, filtered over a 0.2 µm CA filter, and subsampled for various parameters. Apart from parameters directly measured on board (see below), samples were preserved for subsequent home-based analyses on N-species (nitrate, nitrite, ammonia), major elements, and isotope systems.

The remaining sediment was stored under N<sub>2</sub> in Schott glass bottles at 4°C. All pore water subsamples were stored cool, too (except if they were brines).

### 2.2.0 On-board analytical techniques

Nutrients (silicate, phosphate, DIC, hydrogen sulphide):

The samples were filtered over a 0.2 µm acrodisc filter and stored dark and cool at 4°C in polyethylene vials until analysed. All analyses were carried out on a TRAACS800 continuous flow analyser, applying colorimetric methods as described by Grasshoff et al. (1983); DIC was determined as given in Stoll et al. (2001).

In every run a mixed nutrient standard containing silicate, phosphate, ammonium, and nitrate in a constant and well known concentration was measured in triplo. This standard is used to check the performance of the analysis.

Special treatment for PW samples: DIC and sulphide samples were kept in gas-tight 5ml glass vials to prevent degassing. Due to the large variation in salinity, DIC was diluted with NaCl (41g/l) to overcome a possible matrix effect. Samples for hydrogen sulphide analysis were diluted with NaOH (5mM). Samples for phosphate analysis were acidified to pH=1 with HCl. Standards were prepared fresh every day by diluting the stock solutions of the different nutrients in nutrient depleted surface ocean water, which is also used as baseline water.

Due to the large oversaturation in dissolved gases, a substantial but unknown amount of CO<sub>2</sub> (measured as DIC) and H<sub>2</sub>S (measured as HS<sup>-</sup>) may have escaped during the ascent from the seafloor and on deck handling. The measured concentrations are therefore minimum concentrations.

Salinity: determination with a conventional refractometer.

Methane: see section on gas analysis elsewhere in this report

Total alkalinity (TA): titration with HCl and determination by a Gran plot

Chloride: potentiometric titration with AgNO<sub>3</sub>

### 2.3.0 CTD Stations

#### 2.3.1 Instrumentation

For regular water column work in order to detect methane plumes, we used a Seabird SBE9-CTD with rosette sampler (22 NOEX bottles). For the special objective of sampling a muddy brine, we used a ME33 CTD with rosette sampler (15 Niskin bottles).

#### 2.3.2 Plume detection

Seawater samples were taken from 7 successful CTD casts with the NOEX bottles and sampled for

- methane
- oxygen
- stable isotopes
- nutrients
- major elements

Methane sampling: see section on gas analysis elsewhere in this report

Oxygen: standard Winkler titration

Stable isotope ( $\delta^{18}\text{O}$ ,  $\delta\text{D}$ ,  $\delta^{13}\text{C}$ ) sampling: A 60 ml septum bottle was filled without air bubbles; the sample was poisoned with HgCl<sub>2</sub>-solution to stop bacterial activity.

Nutrient sampling: Seawater was taken directly from the bottle and filled in high density polyethylene sample bottles which were rinsed three times.

Major element sampling: A 60 ml Nalgene PE bottle was filled after having been rinsed three times with the sample. At some sites extra samples were taken for minor elements, e.g. Mn detection in the plume.

#### 2.3.3 Brine sampling

In the Menes caldera, three ME-CTD casts were carried out to sample the brine that is situated on top of Chefren and Cheops mud volcano. The saline, muddy waters were sampled for the parameters mentioned above and for sulphur and sulphur isotopes. Due to the unusual matrix, the sampling procedure was adapted so that, in addition to direct sampling, the centrifuge tubes were filled with the mud, centrifuged, and subsequently the supernatant

water was filtered (0.2 µm) and subsampled for the various parameters. From the remaining mud, a part was kept under inert atmosphere, and two centrifuge tubes were kept for geochemical (UU) and sedimentological (VU) work.

### *2.3.4 Results*

Apart from the methane concentration (see section on gas analysis elsewhere in this report), the main results will only be achieved in the home lab (major elements and isotopes). Salinity data from the brine CTD's are given in the Coring section together with the cores at the respective sites.

## 2.4.0 Coring

### *2.4.1 Introduction*

Fluid seeps are windows to the deep subsurface, as the fluid and mud emitted carry the geochemical signature of the source fluid or rock. The geochemical part of the MEDIFLUX project focusses on the methane fluxes and related carbon and sulphur species in the porewater and sediment. In particular, the concentration and gradients, as well as the isotopic composition of both C and S species will be determined.

The major objectives are:

determination of the composition of the gases, water, and mud emitted at the seeps, assessment of the relation to their origin at the various seep sites (composition, temperature, depth), evaluation of the relationship between pore water features controlled by diagenetic processes versus those controlled by seep-induced micro-biological activity (e.g. methane oxidation, sulphate-reduction, clay mineral alteration, carbonate precipitation).

### *2.4.2 Sediment sampling*

Sediment samples were mainly taken by piston and gravity corers, 21 in total, where

- 5 were pre-drilled/pre-split in order to enable a quick sampling for gasses,
- 5 were dedicated to intense pore water extraction,
- 9 were dedicated to heat flux measurements and were sampled and analyzed every meter-section for geochemical analysis,
- 2 cores were shared with the biomarker sampling (50cm-sections).

The surface sediment was sampled from three boxcorers.

pre-drilled cores: To ensure an immediate pore water sampling at sites where gas-rich sediment occurred, we used the following technique: the piston core liner was predrilled with holes of Ø 2 and 3 cm with 25 cm resolution (i.e. every 25 cm along the core liner) and sealed with tape. Upon recovery and after removing the liner from the core, it was immediately sampled with 10 and 20 ml cut-off-syringes and the sediment was transferred into vessels prepared for methane measurements, sulphide fixation, and

pore water extraction. In order to process everything rapidly, this sampling was done simultaneously by three teams of 2 persons each.

pre-split cores: These were similar to the pre-drilled liners, but with a plastic sleeve inside the PVC liner, which can be pulled out and slit open longitudinally for immediate sampling.

pore water cores: The core was cut into meter sections, that were sampled for methane at their ends and then transferred into the cool container. The upper section was sliced vertically in a glovebox and the pore water was centrifuged, all other sections were sampled horizontally in a glovebag and the sediment was squeezed (for details see De Lange 1992). Note: The latter sampling took place at in situ temperature and under inert atmosphere, which is not the case for the other cores (i.e. only pore water extraction and subsampling took place under these conditions).

heat flux cores: At the bottom of every meter section, sediment for methane and pore water analysis was taken immediately after cutting the section on deck.

biomarker cores: similar to heat flux cores, but higher resolution (50cm)

box cores: subcores were taken and sliced vertically in the glovebox (for pore water analysis) or sampled with syringes in the sediment lab (gasses and pore water).

#### *2.4.3 Results – Geochemistry of pore waters*

At Isis MV we analyzed two geochemical cores and meter-sections of six heatflow cores. The positioning of these cores and the shared data acquisition for geochemistry and heat flow measurements, provide a three dimensional insight in the fluid flow. The temperature profiles already show that the central cores (stations MS08,19 and 24PT) represent a narrow feeding channel (see section of cruise report on heat flow analysis). This general picture is also found with the pore water analysis (salinity, Fig. 2.1). However, in contrast to the heat flow measurements where all central cores have the same temperature gradient, the salinity profiles of these cores (with station MS09PC instead of MS08PT) show a more detailed picture.

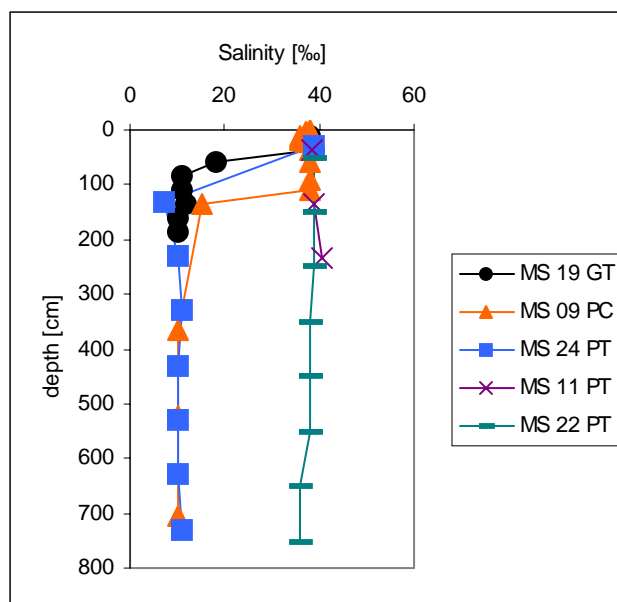


Figure 2.1 Salinity profiles of piston and gravity cores at Isis MV

Within the feeder channel (the lower parts of the cores MS 19 GT, 09 PC, 24 PT), the salinity is extremely low (about 10 ‰). Towards the sediment surface, the salinity increases, eventually reaching the value for Mediterranean seawater of around 39 ‰. The transition from low to high salinities is clearly dependent on the distance from the actual feeder channel: Core MS19GT seems to hit right in the middle of the channel, because only the very top sediment (down to 35 cm depth) shows the higher salinity. The salinity transition appears within 50 cm, so that it reaches its end member value at 85 cm. Core MS09PC is slightly off the central position, showing the salinity transition between 110 and 160 cm. Due to the low resolution in the heat flow core MS24PT, the depth cannot be determined precisely (30 to 130 cm). According to the logbook, MS19GT and MS24PT are at the same position, whereas MS09PC is a bit offset. However, regarding the calculated distance between these cores (ca. 8-9 m) the error in the positioning is in the same order of magnitude as the deduced diameter of the feeder channel.

Like the heat flow data, the geochemistry of the cores that are further away from the center of the MV ( $\geq 200$  m), do not show any difference in salinity. It is worth mentioning that there is even no difference between the core taken only ca. 220 m away from the center (MS11PT) and the reference core taken outside the caldera (MS22PT). (For the relative locations of these cores, see figure in the heat flow section of this report.)

Silicate shows a similar, but mirrored, picture as salinity (Fig. 2.2). The central cores show increasing concentration in the feeder channel (up to ca. 300  $\mu\text{M}$ ). In contrast to the salinity profiles, the maximum concentration reached is different for the three central cores. Although the transition from low Si in the surface sediments towards high values is at the same depths as for the salinity transition, the maximum concentration does not increase accordingly (i.e. highest at the very center). High Si concentrations suggest that Si is released at deeper strata, either from dissolution alone or additionally by high-temperature, metamorphic reactions.

DIC and total alkalinity also increase with depth, showing almost the same depth profiles as Si, demonstrating the low-temperature, diagenetic component.

It is worth mentioning that none of the Isis MV samples had HS in detectable concentrations.

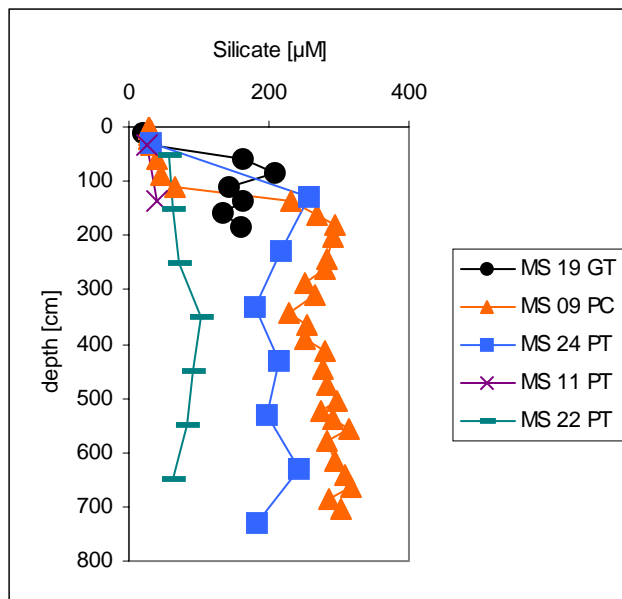


Figure 2.2\_ Si profiles of piston and gravity cores at Isis MV

In the Menes Caldera we took not only long piston and gravity cores, but also ran CTD's in order to sample the brines on top of Chefren and Cheops MV. The Caldera MV's are characterized by high salinities: ca. 150 ‰ at Chefren and ca. 300 ‰ at Cheops. At both sites, the profiles are rather constant with depth and do not differ between cores and accompanying brine-CTD's. The depth of the brine is approximately 300 meters at Chefren and 10 meters at Cheops.

The core taken on the flank of the Chefren MV (MS 34PT, ca. 620 m from the central site MS30PT) still shows 70-100 ‰ salinity, i.e. up to a third of the central sites or double as much as the background core on the Menes floor (MS59PT). Compared with the Isis MV, where no fluid influence is measured at a distance  $\geq 200$  m, this indicates a broader fluid channel or at least a more gradual transition from the central part to the outer part.

Apart from high salinities, both MV's emit warm fluids: The temperatures measured with the cores and the CTDs are the same for Chefren (57°C) and a bit more varying for Cheops (37°C, 25°C). The Si concentration in the cores reflects these temperatures with higher values at Chefren (500-600 µM) and lower values at Cheops (300 µM). Hydrogensulphide was found in higher concentrations in the central cores of Chefren MV (up to 1.5 mM), and only in minor amount at Cheops.

### **3.0.0 Geochemistry: Gas composition in the water column and sediment**

#### 3.1.0 Materials and methods for gas measurements

**Seawater sampling:** Water samples are taken from the CTD rosette sampler immediately upon arrival on deck and collected in 250 ml Schott bottles quickly sealed with a butylstopper. About 100  $\mu$ l of mercuric chloride ( $\text{HgCl}_2$ -solution, 70 g/l) is added to the samples to stop the bacterial activity. A headspace of 10 ml is made with nitrogen while simultaneously removing 10 ml of the sample. The samples are equilibrated for at least 24 hours at room temperature prior to measurement. During equilibration and storage the samples are kept up-side-down in order to prevent any gas losses through the septum.

**Sediment sampling:** Sediment samples of 10 ml are taken immediately after core retrieval with a cut syringe. The sediment is put into a 60 ml infuse bottle filled with saturated NaCl solution (ca. 300g/l) which is quickly sealed with a butylstopper, allowing no air to remain in the bottle. A headspace of 5 ml is made with nitrogen while simultaneously removing 5 ml of saltwater. The bottles are shaken very well in order to make a homogeneous suspension. The high salt concentration pushes methane almost completely into the headspace and stops bacterial activity at the same time. The samples were measured after one day of equilibration. The samples are kept up-side-down during equilibration and storage in order to prevent any gas losses through the septum.

**Gas analysis:** the analyses were carried out with a Shimadzu gas-chromatograph GC-14B with FID (Flame Ionization Detector). 2 mL of headspace were used to fill the 0.25 mL sample loop and at least 10 mL of nitrogen were used to flush the sample loop before each sample analysis. The flame ionization detector was heated to 150°C. Each gas component was separated in a Valco Plot-HayeSep D capillary column (30 m, 0.53 mm i.d., 20  $\mu$ m film thickness). The GC oven was kept at 60°C for 2 min, ramped to 180°C at 35°C per min, and finally held at 180°C for 8 min.

The following standards have been measured three times prior to a set of samples: 15, 100 and 100 ppmv  $\text{C}_1$ - $\text{C}_6$  mixture, 1000 ppmv methane, 1% (10000 ppmv) methane (all from Scotty), and Nitrogen (zero ppmv). The precision of the method is about 3%.

The concentration of each gas component in the headspace ( $\text{ppmv} = L/106L$ ) is calculated off-line from the peak areas using linear regression of the standards and no intercept. The concentration of each component in the liquid phase (in L/L) is calculated from the headspace concentration using the Bunsen solubility coefficient  $\beta$  (Wiesenburg and Guinasso (1979)). Finally, each gas concentration in the sediment (in  $\mu\text{mol/L}$  of wet sediment) is calculated considering the volume of wet sediment sampled.

Due to the large oversaturation in dissolved gases, a substantial but unknown amount of gas may have escaped during the ascent from the seafloor and on-deck handling. The concentrations measured for those samples are therefore minimum concentrations.

### 3.2.0 Results and preliminary discussion

#### 3.2.1 $CH_4$ concentrations at Amsterdam mud volcano (Anaximander Mountains)

##### $CH_4$ concentration in the water column

The first hydrocast was run above Amsterdam mud volcano in the Anaximander area. The profile shows clear methane enrichment in the water column (Figure 3.1A). The methane concentration ranges from 7 ppmv at 500 m depth to 450 ppmv at 1980 m depth (the seafloor depth is about 2020 m). Compared to the sea background, considered to range from 0.4 to 0.8 ppmv, these values are very high. This result indicates that Amsterdam mud volcano has remained active since its discovery during the MEDINAUT cruise in 1998 (Charlou et al., 2003). The highest methane concentration is obtained at 1980 m, i.e. 42 m above the seafloor, whereas the deepest samples have a lower methane concentration. This observation suggests that the cast might have been not exactly above the most active part of the mud volcano.

An ethane plume was also detected at 1980 m depth with a concentration reaching 4 ppmv.

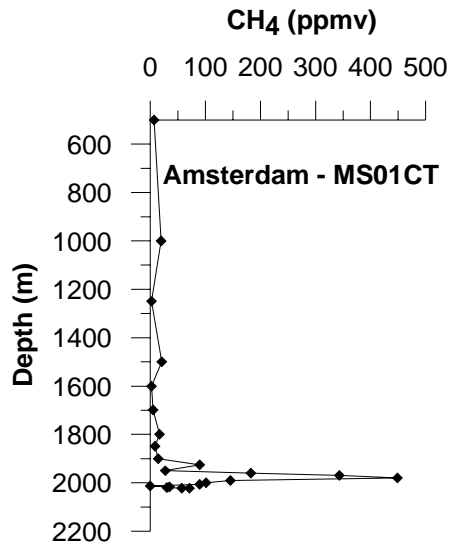


Figure 3.1  $CH_4$  concentrations (ppmv) versus depth (m) in the water column above Amsterdam mud volcano.

##### 3.2.2 Hydrocarbons in the sediment

One piston core has been taken at Amsterdam mud volcano (station MS04PT). Below 40 cm depth the methane concentration remains more or less constant with a  $CH_4$  concentration of 71,000 ppmv. Heavier hydrocarbons until *n*-butane are also present with concentrations leading to a  $C_1/(C_2+C_3)$  ratio of 70 on average, suggesting that gases have a mixed bacterial-thermogenic source.

### 3.3.0 Hydrocarbon concentrations in the Nile deep-sea fan

#### 3.3.1 Hydrocarbon concentration in the water column

In the Nile deep-sea fan, five casts were carried out at four locations: one station located above Isis mud volcano (station MS23CT), two in the central province, above North Alex mud volcano (stations MS25CT and MS60CT), and one each above Chefren and Cheops mud volcanoes in the Menes Caldera, western fan province (stations MS28CT and MS56CT).

##### A. Eastern fan province: Isis mud volcano

In the eastern part of the Nile fan, we focussed on Isis mud volcano which appeared to be the most active volcano of the area during the NAUTINIL cruise (2003) and where free gas bubbles have been observed in the water column (Station MS23CT). The methane concentration reaches 614 ppmv just above the seafloor (989 m depth). However, the geometry of the plume obtained differs completely from those usually observed above mud volcanoes. The numerous peaks observed may be explained by the presence of gas bubbles rather than by discrete plumes of dissolved methane. This suggestion is supported by the sidescan sonar data showing high acoustic anomalies in the water column above Isis: these anomalies are preferentially explained by the presence of gas bubbles since there is a larger acoustic impedance contrast associated with gas bubbles in the water column than with dissolved CH<sub>4</sub> (or any other gas).

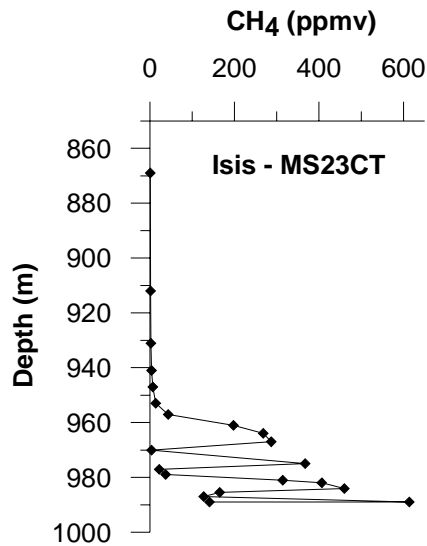


Figure 3.2 Example of CH<sub>4</sub> concentrations (ppmv) versus depth (m) in the water column above Isis mud volcano, eastern fan province.

In addition to methane, heavy hydrocarbon gases have been also detected in the water column with concentrations reaching 180 and 20 ppmv for ethane and propane, respectively. These values are rather high and may reflect a high thermogenic hydrocarbon imprint at Isis mud volcano.

The results obtained during the MIMES cruise are similar to those obtained during the 2003 NAUTINIL cruise (station NLCTD6) even though the methane concentration measured this year (614 ppmv at 989 m depth) is twice as high as the one measured in 2003 (315 ppmv at 1000 m depth). However, in both casts, the vertical profile is the same with a 50 m thick plume detected between 950 and 1000 m depth.

#### *B. Central fan province: North Alex mud volcano*

In the central part of the Nile deep-sea fan two hydrocasts were run above North Alex mud volcano (stations MS25CT and MS60CT). At MS25CT, the methane concentration measured just above the seafloor (7,100 ppmv at 498 m depth) is high compared to the background. Moreover the methane distribution shows a 200 m thick plume between 50 and 250 m depth with a methane concentration ranging from 1,500 ppmv to 5,500 ppmv. Between 250 m and 450 m depth, the methane concentration decreases to reach 8 ppmv at 440 m depth. These two distinct plumes at 498 m and 250 m depth observed at North Alex may be explained by episodic gas expulsions.

At MS60CT, the methane pattern is similar to that at the station MS25CT, showing two methane plumes. However, the methane concentration measured at MS25CT is four times higher than the one measured at MS60CT.

Moreover, high ethane and propane concentrations have been measured with concentrations at 498 m depth of ~1600 ppmv for ethane and ~50 ppmv for propane (station MS25CT).

#### *C. Western fan province: Chefren and Cheops mud volcanoes*

In the western fan province, two hydrocasts were carried out above Chefren and Cheops mud volcanoes in the Menes Caldera (stations MS28CT and MS56CT, respectively). Brine pools surrounded by whitish and orange mats were discovered there during the 2003 NAUTINIL cruise.

The methane concentration measured just above Cheops is very high (3,200 ppmv at 2992 m depth). Like at Isis mud volcano, the profile shows numerous peaks with a maximum methane peak of 6,200 ppmv at 2972 m depth.

At Chefren mud volcano, the profile shows the highest methane concentrations ever measured in the water column of the Nile fan. The methane distribution shows the presence of two plumes: a first one at 2882 m depth with a methane concentration of 14,400 ppmv and a second one close to the seafloor at 2951 m depth with a methane concentration of 16,400 ppmv. Just above Chefren at 2955 m depth the methane concentration decreases suddenly to 13 ppmv. Like at North Alex mud volcano, this particular pattern with several plume layers suggests that Chefren expulses huge amounts of gas more episodically rather than continuously.

At Chefren the brine has been sampled as well and a high methane concentration of 356,000 ppmv has been measured (station MS48CT).

High ethane and propane concentrations have also been measured in the water column above Cheops and Chefren mud volcanoes. At Chefren, ethane and propane concentrations reach 3,800 and 152 ppmv at 2951 m, respectively. At Cheops, C<sub>2</sub>H<sub>6</sub> and C<sub>3</sub>H<sub>8</sub> concentrations are much lower: at 2992 m depth, ethane and propane concentrations reach 185 and 14 ppmv, respectively. In the Chefren brine, the high ethane and propane concentrations measured give a C<sub>1</sub>/(C<sub>2</sub>+C<sub>3</sub>) ratio of 114, suggesting a mixed bacterial-thermogenic in origin.

### 3.3.2 Hydrocarbon concentrations in the sediment

The large methane plume obtained above Isis mud volcanoes is in concordance with the high CH<sub>4</sub> concentrations measured in the sediments. Figure 3.3 shows the methane profile in sediment at the centre of Isis mud volcano. Close to the surface, the CH<sub>4</sub> concentration is relatively low (94 µmol/L of wet sediment at 25 cmbsf). Then, the concentration gradually increases with depth to reach 4200 µmol/L of wet sediment at 730 cmbsf.

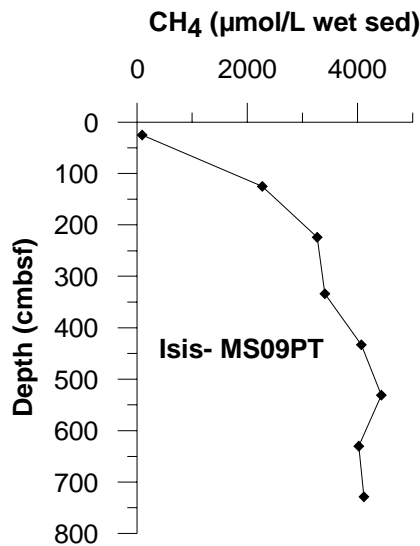


Figure 3.3 Example of CH<sub>4</sub> concentration (µmol/L of wet sediment) versus depth (cm below the seafloor) in sediment at the centre of Isis mud volcano.

Moreover, high concentrations of heavier hydrocarbons have been measured. The C<sub>1</sub>/(C<sub>2</sub>+C<sub>3</sub>) ratio of 40 on average indicates a mixed bacterial-thermogenic mixture in origin.

Several cores have also been taken nearer the outer edge of Isis (stations MS11-, 12-, 13-, and 17PT) as well as one for reference just off the mud volcano (MS22PT). At all of these stations, the methane concentration is very low compared to the concentrations measured at the centre: at station MS11PT, the closest station to the centre, the methane concentration is less than half the concentration measured at the centre (1000 µmol/L wet sediment at 250 cmbsf). At stations MS12-, 17- and 13PT the methane concentrations range from 0.2 to 4 µmol/L of wet sediment and at station MS22PT, which is the furthest from the centre, to the

east of the mud volcano, the CH<sub>4</sub> concentration ranges from 0.04 to 0.2 μmol/L of wet sediment. Therefore, at Isis, gases are most likely escaping from a narrow conduit located in the centre of the mud volcano.

These results are in agreement with those from heat flow measurements showing decreasing temperature gradients from the centre to the edge of the mud volcano.

At North Alex, the methane concentration in the sediment is also very high (5,800 μmol/L wet sediment at 525 cmbsf). However, the C<sub>1</sub>/(C<sub>2</sub>+C<sub>3</sub>) ratio is much higher with a constant value of 900, suggesting, here as well, a mixed biogenic-thermogenic origin.

In the Menes Caldera, high methane concentrations have been measured. At Chefren, the measured methane concentration reaches 15 mmol/L of wet sediment (station MS49GC) which is 150,000 times the concentration measured in the north of the Menes Caldera, in an area considered to be inactive and taken as the background. High ethane and propane concentrations have also been measured at the centre of the Chefren mud volcano and the C<sub>1</sub>/(C<sub>2</sub>+C<sub>3</sub>) ratio of 100 on average supports a mixture of both bacterial and thermogenic sources.

At Cheops mud volcano, the same observations were made. The methane concentration is also very high (~ 4000 μmol/L of wet sediment, station MS41PT) and the C<sub>1</sub>/(C<sub>2</sub>+C<sub>3</sub>) ratio of 160 on average suggest as well a bacterial-thermogenic mixture in origin.

#### 3.4.0 Conclusion

The main result is that the Nile deep-sea fan is characterised by expulsion of huge amounts of gases (not only methane but also ethane and propane) into the water column. The low C<sub>1</sub>/(C<sub>2</sub>+C<sub>3</sub>) ratio measured both in the seawater and in the sediment suggests that gases have a bacterial-thermogenic mixture in origin, which is commonly observed at cold seeps environments.

## **4.0.0 Clasts and Carbonates**

### 4.1.0 Objective

During the MIMES cruise (15 June-12 July 2004), we will taken clasts and carbonate concretions to understand more accurately the mechanism of mud volcanoes. The carbonate concretions are also important to understand which biogeochemical processes induce precipitation of the authigenic carbonates under various cold seep environments. In addition to a complete suite of biomarkers in the authigenic carbonates in order to reveal “currently” active biogeochemical processes fuelled by fluids migrating from depths, inorganic chemical studies (mineralogy, petrography and stable isotopic compositions) of authigenic carbonates will bring us to better understand the “record” of the palaeo-environments in which they formed.

### 4.2.0 Sampling

Clasts and carbonate samples were taken from different parts of Eastern Mediterranean (Anaximander area (Amsterdam and Kazan Mud Volcanoes), East Delta area (Isis and Osiris Mud Volcanoes), the North Alex area, and the Caldera area). They were found within the sediment obtained from:

- **Box Core (MS-03-BV)** (35.33348N, 30.2662E)  
in Amsterdam Mud Volcano at 1991m
- **Piston Core (MS-09-PT)** (32.36098N, 31.38947E)  
in the centre of Isis Mud Volcano at 978m
- **Box Core (MS-18-BV)** (32.36107N, 31.38938E)  
in the centre of Isis Mud Volcano at 977m
- **Gravity Core (MS-19-GT)** (32.36097N, 31.38952E)  
in the centre of Isis Mud Volcano at 986m
- **Piston Core (MS-26-PT)** (31.9695N, 30.13617E)  
in the centre of North Alex Mud Volcano at 495 m)

Sediments were also sampled each centimetre in piston core MS-09-PT in order to observe and pick under a binocular microscope both the carbonate micro-concretions and other authigenic minerals such as benthic foraminifera. The mineralogic composition of carbonate micro-concretions and other authigenic minerals will be studied later by scanning electronic microscope. The carbon and oxygen isotope compositions of carbonate micro-concretions will also be studied later.

The biggest clasts and carbonate concretions in the sediment were taken before the sieving of the bulk. We recovered the smaller clasts and carbonate concretions with a sieve of 250µm, and the fine fraction of sediment with a sieve of 150µm. These different fractions of bulk sediment were also examined under a binocular microscope and the authigenic minerals and benthic foraminifera were picked for later study.

#### 4.3.0 Results

Once the clasts and carbonate concretions were dried, they were classified according to their colour, their shape and size, their texture, their structure, and their admixture. We found 17 main categories (siltstones, polymictic siltstone, claystones, mudstones, mudstone with high terrigenous admixture, marlstones, limestones, micritic limestone, carbonatous rocks, chimneys, cemented shells debris, polymictic sandstones, cemented mud breccia, argillites, argillitous rocks, fragments of calcite and gypsum veins, terrigenous rocks) which were then further sub-divided. Tables 4.1a, 4.1b, 4.1c, 4.1d, and 4.1e give a summary of the shipboard descriptions of these clasts and concretions and table 4.2 gives a summary for all the samples studied from Isis Mud Volcano.

Some carbonate chimneys have been found in sediment sampled from Isis Mud Volcano and the North Alex structure. They could indicate the occurrence of past seepage activity in these different areas. In these chimneys, several analyses (mineralogy, isotopic composition and biomarkers) will be done to understand the processes of formation of the authigenic carbonates.

Table 4.1 North Alex mud breccia description (following page)

SUMMARY INFORMATION ON ROCK CLASTS FROM MUD BRECCIA  
*North Alex Mud Volcano*  
 Sampling site: MS 26 PT

Group	subgroups	Number	Lithology	Colour	Shape	Texture	Structure	Admixture	Notes	
1	a	1	mudstone	brownish grey	planar, isometric, subangular to angular; 2.5x1.5x0.7 cm	silty-grained	massive, planar	silt, clay, sulphidic minerals (pyrite?)	indurated on the top and in the bottom; the middle part is hard; the reaction with HCl is from none to weak	
	e	e(1)		13	brownish grey	subrounded, subangular; from 2.5x3x1.7 cm to millimetric size		massive	silt, foraminifera, carbonate	firm; weak reaction with HCl
	f			86	dark grey	subrounded, subangular; from 4x2.5x2.5 cm to millimetric size		massive	silt, carbonate, foraminifera	firm; the reaction with HCl is from none to weak
	g			7	grey	isometric, subangular; from 1.7x1.5x0.7 cm to millimetric size		massive, planar lamination	silt, carbonate-bearing layers, foraminifera	firm, fissured; partially dissolved foraminifera; in light laminated layers with semi-strong reaction with HCl. In clayey layers, there is none reaction with HCl
	m	m(2)		4	bicolor: grey and dark grey	subrounded, subangular; from 2x1.3x0.7 cm to 1x1x0.4 cm	polymictic of the lighter part and no texture for the darker part	massive	polymictic for the lighter part, carbonate for both parts	indurated; the upper boundary is sharp and irregular; the lower boundary is gradual; the contrast between colors is more visible; weak reaction with HCl for both parts of the clast
2	e	2	marlstone	light brownish color	tabular; from 2x0.7x0.3 cm to 1.5x0.7x0.3 cm	irregular	massive, planar	silt	hard; from weak to semi-weak reaction with HCl	

3	c	c(2)	1	carbonatous rock	light grey, similar to the outer part of the c(1) in the MS09PT	isometric, angular to subangular; 2x1.5x0.8 cm	porous, micritic	massive	mud breccia clasts from 1 cm diameter to millimetric sizes	hard; the reaction with HCl is strong; probably part of the bigger carbonate chimney (?)
	e	e(2)	5		light brownish grey	isometric, irregular; 2x1x0.5 cm		massive	mud breccia clasts, clay	hard; probably inner part of carbonate chimney; strong reaction with HCl
	e	e(3)	6		brownish grey	probably piece of chimney; from 3x1x0.5 cm to 1.2x0.7x0.4 cm	irregular and sometimes porous	massive	mud breccia clasts from 0.3 cm to millimetric sizes in diameter	hard; most probably pieces of chimney; strong reaction with HCl
	m		1	Chimney	light brownish grey	smooth chimney, fingers-shape; from 9x2.5x2.5 cm to 2.2x0.8x0.7 cm	micritic with some pores	massive	clay, foraminifera	hard; no hole inside; occasional shell debris; heavy with smooth surface; "finger-shape"; strong reaction with HCl
	n		6	Cemented shell debris	from dark grey to light liege	irregular, subangular, shape of cemented shells; from 5x4x1 cm to 1x1.3x0.3 cm	micritic	massive	clay, mud breccia matrix	solid; strong reaction with HCl
	o		19	Pieces of carbonates	light brownish grey	round, smooth; from 2.7x1.4x1 cm to 1x0.5x0.5 cm	micritic with inclusions of mud breccia	massive	clay, silt, shell debris, dark minerals	firm; similar to group 3e(2) but more brownish; inclusions of mud breccia are smaller in diameter; reaction with HCl is from strong to semi-strong
	p		5		from dark to light grey (color is patched)	irregular, subangular to angular; from 6x2.3x2.5 cm to 1.4x0.6x1 cm	partially micritic	massive	clay, shell debris	hard; most probably piece of chimney but significantly different from these observed before; strong reaction with HCl
	q				light brownish grey	irregular, angular to subangular; from 5.5x4x2.5 cm to 1.5x1x0.6 cm	micritic, sometimes porous with inclusions of mud breccia clasts		clay	hard, shape of some edifices is similar to these observed in the same area during the NAUTINIL 2003 cruise. The difference is size: these clasts are much bigger; strong reaction with HCl
	r		>200		from brown to grey	irregular; from centimetric to millimetric size	from micritic to sand-coarsed	massive, porous	mud breccia clasts, shell debris	firm; the same as those which are found in the same structure during NAUTINIL 203 cruise; strong reaction with HCl
	s		6		light brownish grey	tabular, from angular to subangular; from 2x1.7x0.4 cm to 1.5x0.9x0.2 cm	micritic	massive, planar	clay	firm; strong reaction with HCl
t		1	light biege		subrounded, subangular; 2.5x1.7x1.5 cm		massive	clay, occasional mud breccia clasts of millimetric sizes	firm; strong reaction with HCl	

4	a		2	claystone	very dark grey	isometric to subrounded; from 2.5x1.5x1.3 cm to millimetric size		massive, sometimes planar lamination	silt, foraminifera	indurated; soapy; no reaction with HCl
5	a		1	polymictic sandstone	brownish grey	isometric, angular; 3x1.7x0.3 cm	sandy coarsed, medium sorted	massive	well-sorted silt, dark minerals	hard; small slicken slide surfaces coated by polymictic stones
8			12	Cemented mud breccia	dark grey	irregular			carbonate, shell debris	soft and fragile; cemented mud breccia by probably carbonate material; medium reaction with HCl

Table 4.2 Isis mud breccia description (following page)

SUMMARY INFORMATION ON ROCK CLASTS FROM MUD BRECCIA

*Isis Mud Volcano*

Sampling sites: MS 03 PT, MS 18 BV and MS 19 GT

Group	subgroups	Number	Lithology	Colour	Shape	Texture	Structure	Admixture	Notes	
1	a		mudstone	brownish grey	planar, isometric, subangular to angular; from 10x3.5x4 cm to 1x1x0.7 cm	silty-grained	massive, planar	silt, clay, sulphidic minerals (pyrite?)	indurated on the top and the bottom; the middle part is hard; from no to weak reaction with HCl	
	b			light grey	irregular, subrounded, angular to subangular; from 1.5x1.5x0.7 cm to 1x1x0.8 cm		massive	silt	indurated; weak reaction with HCl	
	c	c(1)			greenish grey	subrounded, subangular; from 2x1.5x0.5 cm to 1.5x1.5x1 cm		massive	foraminifera	indurated; well-preserved and recrystallised foraminifera
		c(2)			light greenish grey	subrounded, subangular; from 2x1.5x0.5 cm to 1.5x1.5x1 cm		massive	foraminifera	indurated; well-preserved and recrystallised foraminifera and less foraminifera than the mudstone group c (1)
		c(3)			dark greenish grey	subrounded, subangular; from 2.5x1.5x1.5 cm to 1.5x1.3x1.3 cm		massive	foraminifera	indurated; well-preserved and recrystallised foraminifera
	d			light brownish grey	subrounded, isometric; from 2x1x1 cm to 1x1x1 cm		massive	carbonate, silt	firm; high carbonate rocks; from no to weak reaction with HCl	
	e	e (1)			brownish grey	subrounded, subangular; from 3.5x2.5x1.5 cm to 0.5x0.5x0.5 cm		massive	silt, foraminifera, carbonate	firm; weak reaction with HCl
		e (2)			light brownish grey	subrounded, subangular; from 3.5x2.5x1.5 cm to 1x0.5x1 cm		massive	more silt than group e(1), carbonate	firm; from strong to semi-strong reaction with HCl
	f			dark grey	subrounded, subangular; from 5x2x1.5 cm to 0.5x0.5x0.7 cm		massive	silt, carbonate, foraminifera	firm; from weak to no reaction with HCl	
	g			grey	isometric, subangular; from 3.5x3.5x2 cm to 0.7x1.2x0.3 cm		massive, planar lamination	silt, carbonate bearing layers, foraminifera	firm, fissured, dissolved foraminifera; covered by well-sorted silt; in lighter layers of laminated sediment, there is a semi-strong reaction with HCl and in clays, there is no reaction with HCl	
	h			grey	isometric, angular; 5x4x3 cm		massive	carbonate, sulfid minerals (pyrite?)	hard; layer of sulphid minerals all around the clast; strong reaction with HCl	
	i			light brownish grey	subrounded, subangular; 3.5x2x1 cm		micritic	massive	clay, silt, carbonate	firm; high content of sulfid minerals (pyrite??); strong reaction with HCl
	j			j(1)	light brownish grey to dark brownish grey	isometric, subangular; from 3x2x1 cm to 2x1.5x1.2 cm		thin lamination	silt, dark minerals, carbonate, clay, light minerals	indurated; gradual boundary between two colors of the mudstone; strong reaction with HCl
k			polymictic mudstone	greenish grey	isometric, subangular; from 2x2x1.5 cm to 1.5x1x0.5 cm	"conglomerate-like"	massive	polymictic, dark minerals, carbonate, various mud- and claystones	indurated with high admixture of rocks on different lithologies and grained-size which makes the clast looking like conglomerate; strong reaction with HCl	
m			mudstone	bicolor: grey and dark grey	subrounded, subangular; 4x4x2.5 cm	polymictic of the lighter part and no texture for the darker part	massive	polymictic for the lighter part, carbonate for both parts	indurated; the upper boundary is sharp and irregular; the lower boundary is gradual; weak reaction with HCl for both parts of the clast	
n				light to dark greenish grey	isometric, subangular; 3x2x1 cm	irregular	massive	carbonate, dark minerals, silt	indurated; probably burrows in the darker parts infilled with light material; strong reaction with HCl for both parts of the clast	

2	a		marlstone	light brownish grey	subrounded to rounded: from 2.5x2x1 cm to 1x0.7x0.7 cm		massive	silt	firm; high carbonate rocks; strong reaction with HCl
	b			light grey	subrounded, subangular to angular; from 4x3x1 cm to 1.5x2x0.5 cm	micritic	massive	clay, silt	from hard to firm; from strong to semi-strong reaction with HCl
	c			light brownish grey	isometric, subrounded, from 3x1x0.5 cm to 1x0.8x0.5 cm	micritic	massive	silt, shells (diameter = 0.5 cm)	firm; from strong to semi-strong reaction with HCl
	d	d(1)		light greenish grey	isometric, angular; from 3x1.7x1 cm to 2x1.5x0.3 cm	micritic	laminated, massive	silt, foraminifera, clay	firm; some clay cover; strong reaction with HCl

3	a		limestone	very light grey almost white	isometric, angular; from 4x3x3 cm to 1.5x1x1 cm		massive	silt, foraminifera, clay	firm; well-preserved and recrystallised foraminifera; the biggest clast is characterised by presence of burrows infilled with grey mud		
	b		carbonatous rock	light brownish grey	isometric, angular; from	micritic	massive	foraminifera, silt, clay	hard; some veins of light grey material; some crack on the surface		
	c	c(1)		Piece of chimney	light brownish grey (the inner part is light brown and the outer part is light grey)	chimney-like, angular on the edges; 5x3x1 cm	the inner part is porous and cracked; the outer part is porous, more smooth and micritic	massive	claystone inclusions from 0.5 cm diameter to millimetric sizes	hard; two different lithologies: the inner and the outer parts; the reaction with HCl is strong and similar for both surfaces	
		c(2)		carbonatous rock	light grey, similar to the outer part of the c(1) in the MS09PT	isometric, angular to subangular; from 9x5x3 cm to 1.2x0.8x0.2 cm	porous, micritic	massive	claystone inclusions from 1 cm diameter to millimetric sizes	hard; the reaction with HCl is strong; probably part of the bigger carbonate chimney (?)	
	d		carbonatous rock	brownish grey	isometric, angular; from 4x5.3x1.5 cm to 2x1.5x0.5 cm	sandy coarsed	massive	clay, pyrite	hard; one of the pieces has a shape of chimney; strong reaction with HCl		
	e	e(1)		entire carbonate chimney	brownish grey	chimney (diameter in the inner of hole is 1.5 cm); 2x2x3 cm	irregular and sometimes porous	massive	inclusions of claystones and mudstones from 0.3 cm to millimetric sizes in diameter	hard; strong reaction with HCl	
		e(2)		Carbonatous rock	brownish grey	probably pieces of chimney; from 3.5x2x0.5 cm to 1x1x0.5 cm	irregular and sometimes porous	massive	inclusions of claystones and mudstones from 0.3 cm to millimetric sizes in diameter	hard; most probably pieces of chimney; strong reaction with HCl	
		e(3)			brownish grey	isometric, irregular; 2x1.3x0.3 cm		massive	clay	hard; probably inner part of carbonate chimney; weak reaction with HCl	
	f		Carbonatous rock	light grey	isometric, angular; from 2.5x2x1 cm to 1x1x0.3 cm	irregular rough from sand to grave coarsed		rough	inclusions of mudstones and claystones at different sizes, foraminifera, subhedral	firm; rocks are full of inclusions of mudstones and claystones; strong reaction with HCl	
	g			light brownish grey	subrounded, subangular; 2x1.3x1 cm		micritic	massive	silt, clay	firm; strong reaction with HCl	
	h			light brownish grey	isometric, subangular; 2x1x0.5 cm		micritic	massive	silt, dark minerals, clay	firm; interacted with the lighter in color carbonate; strong reaction with HCl	
	i			micritic limestone	light brownish grey	tabular, angular; 16x12.5x4 cm	micritic with silty to sandy coarsed		massive	clay, silt, foraminifera ( <i>Globigerina sp. ??</i> )	hard; strong reaction with HCl
	j	j		Carbonatous rock	light grey	subrounded, subangular; 3x2x1.5 cm		micritic	massive	clay, foraminifera	firm; strong reaction with HCl
		k			brownish grey	subrounded; 1.5x1x0.5 cm	sandy and silty coarsed		massive	polymictic	firm; crystals of calcite (?); crystalline rock; weak reaction with HCl
		l			brownish grey	subrounded; 1.5x1x1.2 cm	recrystallised		massive	calcite, clay	hard; covered by calcite; strong reaction with HCl

4	a		claystone	very dark grey	isometric to subrounded; from 5x4x2.5 cm to 0.7x1x0.3 cm		massive, sometimes planar laminated	silt, foraminifera	indurated; soapy; no reaction with HCl
	b			dark brown	isometric, subangular; 2x1.5x1 cm		massive		hard; no reaction with HCl
	c			light brownish grey	isometric, subangular; 1.5x1x1 cm		massive		hard; no reaction with HCl
5	a		polymictic sandstone	brownish grey	tabular, isometric, angular; from 6.5x5x1.5 cm to 3x2x0.6 cm	sandy coarsed medium sorted	massive	well-sorted silt, dark minerals	hard; small slicken slide surfaces coated by polymictic stones
	b		terrigenous rocks	brownish grey	isometric and planar; from 2.5x1.5x0.3 cm to 1x1.5x0.5 cm	sand coarsed	planar and massive	silt, dark minerals, carbonate, clay, light minerals	firm; medium sorted; from weak to no reaction with HCl
	c		medium-sorted siltstone	light brownish grey	angular, irregular; 1x1x0.7 cm	silty coated	massive	clay, dark minerals, mica	firm; medium sorted; polymictic medium-sorted; no reaction with HCl
	d		polymictic siltstone	grey	isometric, subangular; from 3x2x1.5 cm to 1.5x1x1 cm	silty to sandy coarsed	massive	polymictic, probably cemented by clay (?)	soft; easy to break; no reaction with HCl
6	a		argillite	dark to light brownish grey	angular, planar; 3x2x0.2		planar and massive	carbonate	hard; weak reaction with HCl
	b		argillitous rocks	light brownish grey	planar and angular; from 2.5x1.5x0.3 cm to 2x1x0.5 cm	very thin laminations	laminated, massive		hard; very thin planar laminations; no reaction with HCl
	c			light brownish grey	angular, irregular; from 3x1.5x1 cm to 2x1x0.5 cm		massive	carbonate, silt	hard; slicken side; from weak to semi-weak reaction with HCl
7	a		mudstone with high terrigenous admixture	from light to medium brownish grey	isometric, subangular to angular; from 3.5x3x1.5 cm to 0.7x1x0.4 cm	silt coarsed	massive	silt, sulphid minerals, mica (?)	firm; from weak to no reaction with HCl
	b			light brownish grey	isometric, subangular to angular; from 1.5x1.2x1.3 cm to 1.4x1x0.5 cm		silt coarsed	massive	silt, sulphidic minerals, mica



## **5.0.0 Non-seep sedimentological cores**

### 5.1.0 Description of cores

Eight cores were collected for sedimentological purposes over the whole Rosetta turbidite system (western Nile deep-sea fan) during the MIMES cruise. The locations of the cores were chosen to allow the study of the dynamics of sediment transport and deposition in several areas of the turbidite system, and to provide a stratigraphic framework allowing the study of the relationship between climate and sediment-supply variations. This also provided the sedimentological framework in which the cold seeps and mud volcanoes occur.

Name	Position	Location	Length (m)	Number of sections	Water depth (m)
MS27PT	N31 47'.90 E29 27'.70	Slope, west of Rosetta canyon	7,34	8	1389
MS35PC	N32 16'.00 E27 38'.00	Distal lobe	5,19	6	3051
MS43PC	N32 00'.10 E29 28'.90	Channel floor	2,90	3	1695
MS44PC	N32 01'.89 E29 29'.00	Right-hand levee	8,43	9	1683
MS45PC	N32 02'.73 E29 36'.65	Head of a slope failure, east of Rosetta channel	5,29	6	1606
MS46PC	N32 00'.06 E29 28'.87	Channel floor	7,23	8	1700
MS51PC	N32 21'.70 E28 03'.00	Distal lobe	0,76	1	2938
MS59PT	N32 09'.80 E28 08'.50	Northern part of Menez Caldeira	5,80	7	2925

Total length of cores : 42,94 m

#### *5.1.1 Core MS27PT*

This core was collected on the continental slope, west of the Rosetta canyon. It consists of highly bioturbated hemipelagic layers, few decimetres to one metre thick, and sapropel deposits. The top of the core consists of a classical orange-coloured muddy interval overlying the sapropel layer S1, 30 cm thick. Then, the most interesting facies consists of well-laminated muds. They are observed between 60 and 205 cm, and 650 and 734 cm depth. Laminae are less than 1 mm thick. They are alternatively lighter and darker, and probably correspond respectively to bloom episodes and hemipelagic supplies from the Nile delta. A thin sapropel is interbedded with those laminated muds in the second section, and 2 sapropel layers are also observed in the fifth and sixth section.

#### *5.1.2 Core MS35PC*

This core was collected in the very distal part of the most recent distal lobe. The first 2 metres consist of whitish carbonate-rich muddy layers alternating with 6 light-grey, carbonate-rich silty-sandy turbidites, 5 to 20 cm thick. Below this a sharp change of colour and sediment facies occurs at 159 cm depth. The interval ranging from 159 to 510 cm depth consists of one sapropel layer on top, then 30 sequences of sandy turbidites, 2 to 15 cm thick, interbedded with 3 debris-flow deposits, 1 m thick. Sandy turbidites are commonly laminated and cross-stratified. Wood fragments are abundant in both turbidite and debris-flow deposits.

#### 5.1.3 Core MS43PC

This core was collected in the floor of the Rosetta channel. The first 15 cm corresponds to the typical orange-coloured holocene muddy deposits. Then a sharp change of colour occurs at 15 cm depth and the interval ranging from 15 to 290 cm depth consists of debris-flow deposits alternating with slumped intervals. Debris-flow deposits consist of mud clasts displaying various colours and sizes supported by a dark muddy matrix. Surprising angular pieces of indurated sand were found in the top of the first debris-flow deposit. Slumped deposits consist of inclined layers displaying rapid changes of dip.

#### 5.1.4 Core MS44PC

This core was collected on the right-hand levee of the Rosetta channel, close to the site of core MS43PC. Holocene deposits in the first 15 cm consist of highly bioturbated orange-coloured mud with abundant foraminiferas and Pteropod fragments. Then, a sharp change of colour and sediment facies occurs at 15 cm depth. The interval ranging from 15 to 843 cm consists of silty to sandy turbidites and hemipelagic deposits. Sandy turbidites are less abundant near the base of the core. From 75 to 445 cm, turbidite deposits alternate with well-laminated muddy intervals, similar to those described in core MS27PT. Sedimentary structures like laminae and ripples are not abundant in the turbidites. Organic matter is quite abundant, and the 2 last (bottom) sections of the core are highly disturbed by gas decompression when corer was brought to the surface.

#### 5.1.5 Core MS45PC

This core was collected on the continental slope, east of the Rosetta channel, in the head of a huge submarine landslide. The first 280 cm consist of homogeneous dark bioturbated muds probably deposited by low-concentrated flows. The interval ranging from 330 to 529 cm depth corresponds to the landslide *sensu stricto*. The silty and sandy turbidites previously deposited on the slope have been highly disturbed by the sliding process. Most of the layers show a dip of about 40-50°, and some are affected by micro-faults.

#### *5.1.6 Core MS46PC*

This core was collected in the channel floor, near the site of core MS43PC, but using a 12 m long core barrel. The first 224 cm are similar to core MS43PC. We observed the same debris-flow deposits and slumped intervals but they are thinner than in core MS43PC. Then, from 224 to 723 cm depth, deposits consist of thin silty to sandy turbidites, alternating to thicker laminated silty-clayey, and dark muddy turbidites. Light hemipelagic layers are interbedded with turbidite deposits, allowing a clear discrimination of individual turbidites. Greenish muddy intervals, with abundant foraminiferas and Pteropod fragments, are observed on top of section number 8. They are interpreted as potential sapropel layers.

#### *5.1.7 Core MS51PC*

We tried to collect a core in the most recent distal lobe of the Rosetta system, in an area where small channels are observed on the backscatter imagery, but unfortunately, the coring failed and we only recovered 76 cm of sediments in the trigger core. The first 57 cm consist of carbonate-rich muddy intervals, 5 to 10 cm thick, and a sandy turbidite, 10 cm thick. Then, the sapropel layer S1 is observed from 57 to 72 cm depth. The base of the core corresponds to the top of a sandy turbidite.

#### *5.1.8 Core MS59PT*

This core was collected in the northern part of the Menez caldeira, in an attempt to calibrate a dark-grey backscatter facies observed on the EM300 imagery. The core was not split aboard during the cruise.



## **6.0.0 DTS-1 EdgeTech deep-towed sidescan sonar**

### 6.1.0 Introduction

Cartographic maps based on multibeam echo-sounder data have been produced in the Eastern Mediterranean (Fanil 2000 and PrisedmedII 1998 cruises) (Sardou & Mascle, 2003). These bathymetric and imagery maps were completed last year during the Nautinil cruise, the first part of the Mediflux project. In the Anaximander Mountains, a few deep-towed sidescan sonar lines are also available (single OreTech swaths obtained during the Medineth project in 1999 and some MAK-1 lines obtained during the Anaxiprobe expedition in 1996). These datasets were used to identify the best targets for more detailed, high-resolution studies during this cruise.

Sidescan sonar mapping is a well-established technique based on the interaction of an acoustic beam with the seafloor. The underlying principle of sidescan sonar is that an acoustic beam is scattered at targets on the seafloor and the amount of scattering that is directed back to the instrument is recorded (Fig. 6.1). This amount of back-scattering is related in decreasing order to the regional slope, the microtopography of the seafloor, and the physical properties of the material on the seafloor. Knowing the regional slope, it is in principle possible to relate the backscatter signal to lithology of the seafloor, as long as the backscatter return is correctly calibrated. For more detailed information about sidescan sonar principles and data processing, please refer to Blondel & Murten (1998).

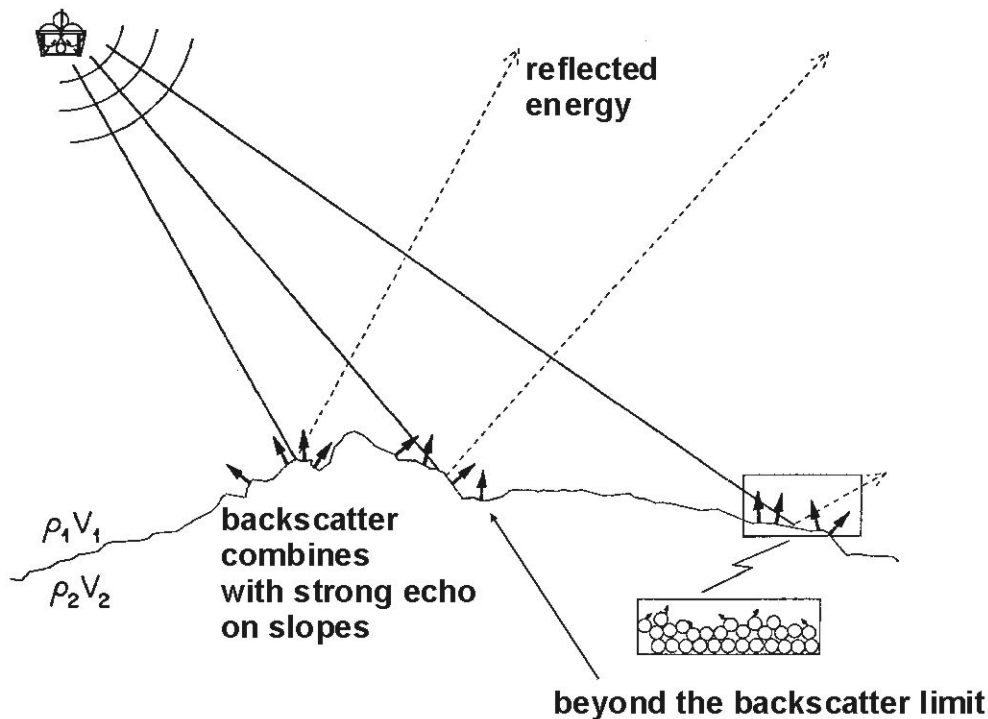


Figure 6.1 General principles of backscattering of acoustic energy at the seafloor from (Johnson & Helferty, 1990).

Compared to the previous low-resolution instruments used to obtain backscatter imagery in the Nile deep sea fan region (EM12-Dual, EM300), the high-resolution DTS-1 data should provide the possibility to identify and map fluid emission areas associated with mud flows, carbonate crust and gas plumes. This surface information can then be integrated with very high-resolution subbottom information from the uppermost sedimentary layer, thereby allowing volume estimates to be made of sedimentary units at the seafloor, mud breccia layers, and carbonate crust thickness. Using maps resulting from such an approach it will be subsequently possible to more clearly relate these features to the underlying structures that are believed to act as fluid conduits.

## 6.2.0 Technical description of the instrument

### 6.2.1 Underwater set-up

The DTS-1 sidescan sonar (Fig. 6.2) is an *EdgeTech Full-Spectrum (FS-DW)* dual-frequency, chirp sidescan sonar working with 75 and 410 kHz centre frequencies. During the present cruise, the sonar was mainly operated with the lower frequency (75 kHz), with the exception of line MS14DT5 (East Delta, Isis mud volcano). The 410 kHz sidescan sonar emits a pulse of 40 kHz bandwidth and 2.4 ms duration (giving a range resolution of 1.8 cm) and the 75 kHz sidescan sonar provides a choice between two pulses of 7.5 and 2 kHz bandwidth and 14 and 50 ms pulse length, respectively. They provide a maximum across-track resolution of 10 cm. Due to towing speeds in the range of 2.3 to 2.6 knots and a range of 750 metres to each side during this cruise, maximum along-track resolution is on the order of 0.75 metres. In addition to the sidescan sonar sensors, the DTS-1 contains a 2-16 kHz, chirp subbottom penetrator providing a choice of three different pulses of 20 ms pulse length each: a 2-10 kHz pulse, a 2-12 kHz pulse and a 2-15 kHz pulse giving nominal vertical resolution between 6 and 10 cm. The sidescan sonars and the subbottom penetrator can be run with different trigger modes: internal, external, coupled and gated triggers. Coupled and gated trigger modes also allow the trigger delays to be specified. The sonar electronics provide four serial ports (RS232) in order to attach up to four additional sensors. One of these ports is used for a Honeywell attitude sensor providing information on heading, roll, and pitch. Finally, there is the possibility of recording data directly in the underwater unit through a mass-storage option with a total storage capacity of 30 Gbyte.

The sonar electronics are housed in a titanium pressure vessel mounted on a towfish of 2.8m x 0.8m x 0.9m in dimension (Fig. 6.2). The towfish houses a second titanium pressure vessel containing the wet-end of the *SEND DSC-Link telemetry system* and the bottom PC of the seismic streamer data acquisition system. In addition, a Posidonia capable *OCEANO releaser* with separate receiver head and a *NOVATECH emergency flash and sender* are included in the towfish.

The towfish is connected to the sea cable via a depressor (2 tons weight) through a 40 m long umbilical cable (Fig. 6.2). The umbilical cable is tied to a buoyant rope that takes up the actual towing forces. An additional rope has been taped to the buoyant rope and serves to pull in the instrument during recovery.

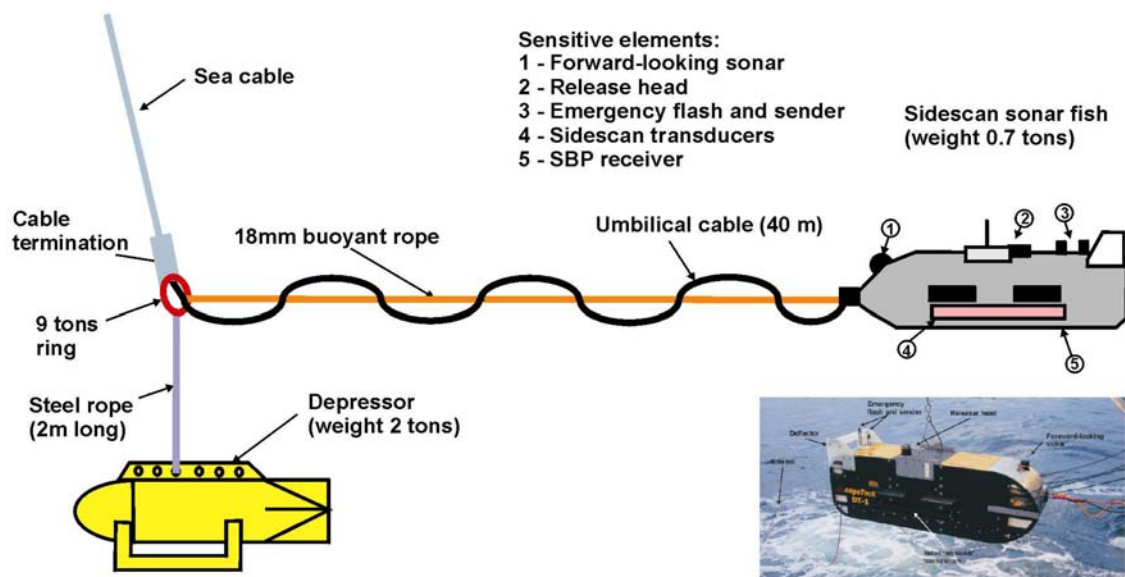


Figure 6.2 The DTS-1 towing configuration and towfish.

### 6.2.2 Laboratory set-up

The laboratory set-up consists of four elements: the dry-end of the *SEND DSC-Link telemetry*, the topside PC of the streamer acquisition system, the *EdgeTech surface interface unit FS-IU*, and the topside unit running *ELAC Hydrostar Online* software (Fig. 6.3). In the absence of the deep-towed seismic streamer, the only function of the bottom and topside PC of the streamer acquisition system is to provide a serial link between the *OCEANO* releaser operating in responder mode and the *Posidonia* topside unit. *Hydrostar Online* carries out general running of the sidescan sonar and subbottom penetrator operations as well as onscreen display of a subset of the acquired data. Unfortunately some additional settings such as the trigger mode or data window size can only be changed by accessing the underwater electronics directly via the *FS-IU*. The *FS-IU* also runs *JStar*, a diagnostic software tool for running some basic data acquisition and data display functions.

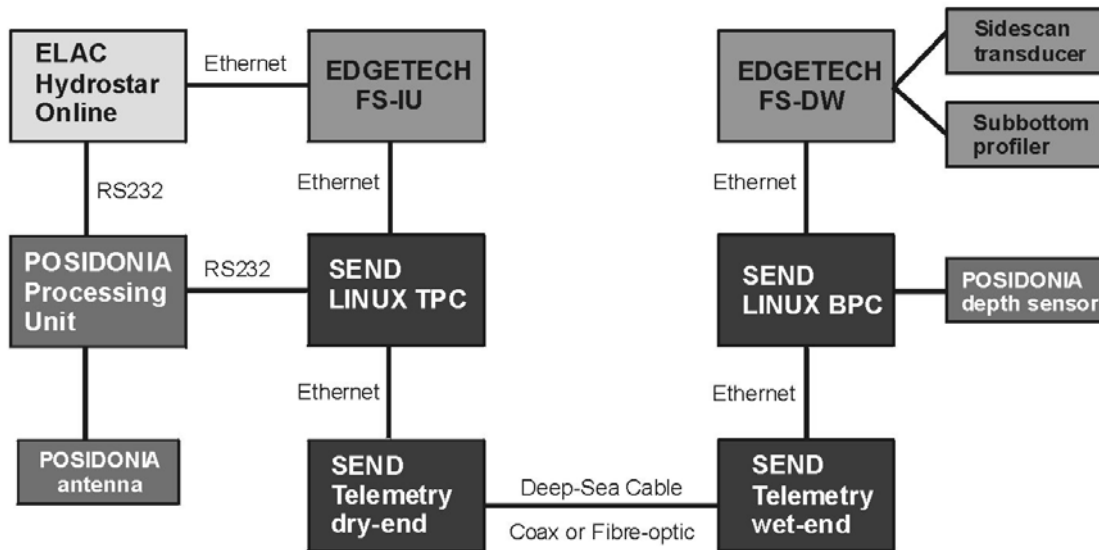


Figure 6.3 The DTS-1 laboratory and electronics set-up.

### 6.2.3 Software

The main operations of the DTS-1 sidescan sonar are essentially run using *Hydrostar Online*, a multibeam bathymetry software developed by *ELAC Nautik GmbH* and recently adapted to the acquisition of *EdgeTech* sidescan sonar data. *HydroStar Online* version 3.3.4 with improved onscreen data representation and time synchronisation was used during the cruise. This software package allows onscreen representation of the data, of the fish's attitude, and of the towfish's navigation when connected to the POSIDONIA system. It also allows setting some principle parameters of the sonar electronics, such as the selected pulse, the range, the power output, the gain, the ping rate, and the range of registered data. However, this version does not allow setting of the trigger mode or the master subsystem in coupled trigger mode. *HydroStar Online* is also used to start and stop data storage either in XSE-format on the *HydroStar Online* computer or in JSF-format on the *FS-DW*. Simultaneous storage in both XSE and JSF-formats is also possible. *HydroStar Online* creates a new XSE-file when a file size of 10 Mb is reached, while a new JSF-file is created every 20 Mb. How fast this file size is reached depends on the amount of data generated, which in turn essentially depends on the use or not of the high-frequency sidescan sonar. The amount of data generated is also a function of the sidescan sonar and subbottom pulses and of the data window that is specified in the sonar.ini file on the *FS-DW*. The data window specifies the range over which data are sampled. Proper selection of this parameter strongly depends on the selected range of the sidescan sonar system in order to avoid good data to be cut-off, or to prevent too large amounts of useless data using up storage space. It also proved practical to switch off data recording during turns. During the present cruise a new file was created every 2 minutes, resulting in a total of 43 Gbyte of data. Two datasets were recorded, one directly in the fish and another one transmitted in real time to the ship. The data were then copied onto DVDs.

Further handling of the data is still problematic as neither the XSE nor the JSF data format can be read directly by our sidescan sonar and seismic (for the subbottom penetrator) processing software. At present patches have been developed to read sidescan sonar data into both *PRISM* (a software package from Southampton Oceanography Centre) and *CARAIBES* (a software package from IFREMER) and to read subbottom profiler data into *SEISMOS*. The data processing could not have been fully completed onboard due to some difficulties with the latest developments of a new version of Caribes (v3.0). However, the data were converted into a format readable by Caribes and some tests have been performed in order to improve the processing chain of Caribes. During the cruise, continuous contact with the development team of Caribes in Brest (Ifremer) was possible via emails, resulting in the creation of new patches. Navigation, sonar image, and subbottom profiler data will be processed in Kiel (Geomar) and in Amsterdam (VU). Processing will include slant range correction, beam correction, positioning of the fish and geographic representation of the sidescan in mosaic.

### 6.3.0 USBL Underwater positioning

For the MIMES expedition, underwater navigation of the towfish could not be carried out using the *POSIDONIA* deployable acoustic array from *OCEANO Technologies*. The *POSIDONIA* system is based on a bi-directional exchange of submarine acoustic signals between one or several acoustic transponders and the acoustic array consisting of 1 transmission transducer and two pairs of hydrophones (Fig. 6.4). The acoustic transponders are interrogated by an acoustic signal and will send a 25ms M-FSK (multi-frequency shift keying) reply. The 25ms M-FSK signal is a succession of ten monochromatic pulses (each 2.5ms long) of ten different frequencies ranging from 14.5 to 17.5 kHz. The order of frequencies during the pulse is determined by the M-FSK code. For best detection of the signal with Posidonia, codes 22 or 23 should be selected. The four reception hydrophones of the array receive this signal that is then transmitted to the processing unit, which measure the phases of the signals and the time between interrogation and reply in order to deduce the relative position of the transponder and calculate its geographical position. The minimum ping interval depends on the range of the transponder (5 or 10 s).

The *POSIDONIA* positioning system runs in two different modes: the free mode and the towed-fish mode. In the free mode all four hydrophones are used to calculate the position of the transponder. In the towed-fish mode only the hydrophones aligned with the towed vehicle are used together with depth information provided by a built-in depth sensor. The free mode should be used when the transponder is located in a cone of 60 degrees underneath the ship, but this mode will work fine up to an angle of 120 degrees. Beyond this angle the towed-fish mode should be used.

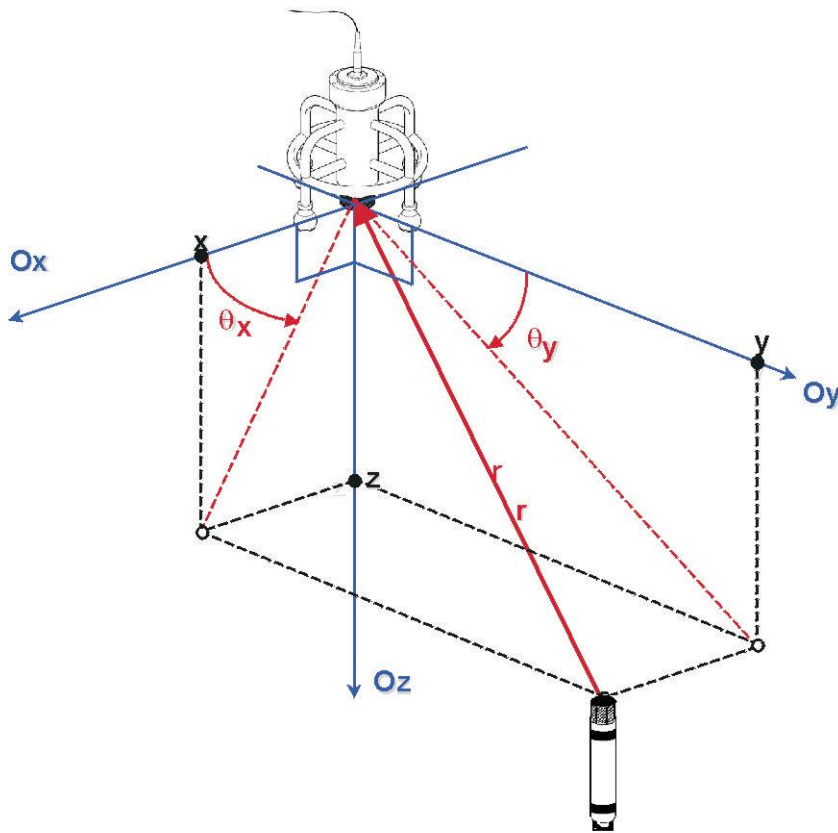


Figure 6.4 The operating principles of the Posidonia USBL system.

As the Posidonia antenna is not fixed to the hull of the ship, the antenna has to be calibrated prior to using the Posidonia system. For such a calibration (not performed during the cruise) an acoustic transponder has to be moored on the seafloor in water depths ranging from 1000-2000 metres, but should be free from any acoustic shadows, i.e. ideally several metres above ground. The ship then describes a figure of eight above the mooring point in order to interrogate the transponder at any angle and from either side of the vessel. The dimension of this figure of eight depends on the water depth and is designed to obtain a minimum of 1000 data points. The Posidonia software then calculates correction factors of roll, pitch, and yaw in order to correctly position the transponder. The latest version of the software Abyss also allows filters to be set in order to eliminate bad navigation points from the final data file. This filter function also allows smoothing of the underwater navigation, a feature particularly useful for towed instruments.

The Posidonia system was neither calibrated nor deployed during this cruise because of chronic problems. There were problems in communication between the integrated PC unit and the processing unit and possibly also problems with the Abyss software. The time needed to calibrate the system was therefore not thought useful in view of lack of confidence in the operation of the complete system which would shut itself down regularly during the

running of lines. It was always turned on in order to observe its behaviour and better document these difficulties or test possible solutions.

#### 6.4.0 Deployment and recovery procedures

Operations for deployment and recovery of the sidescan sonar are a bit demanding and require relatively calm sea for handling that is safe for both crew and instrument. Five persons were on deck during the deployment, which is ideal for safe operation. The sidescan sonar instrument should ideally be towed via the A-frame. With the ship underway at the lowest speed (i.e. propellor just turning over), the kite tail is first thrown into the water and let to drift away. Then the sidescan towfish is heaved into the water (Fig. 6.5) and released with a special hook to detach it from the crane cable. The sidescan fish then also drifts astern with minimal speed made by the ship. Meanwhile, the buoyant rope is secured. Then the depressor is put in place below the A-frame, the buoyant towing rope fitted to the end termination of the sea cable and the umbilical cable connected to the sea cable. Any loose ends are securely tied up and the depressor, with the towfish attached to it, is heaved into the water. At this stage it is important that no strain is exerted on the cable connection.



Figure 6.5 The DTS-1 towfish and the depressor weight during deployment and recovery (Courtesy of Klaucke and Foucher).

During recovery, first the depressor is pulled in and secured on deck. Then the towfish is pulled close to the stern of the ship with the additional rope taped to the umbilical cable. In this way the towfish can be recovered with the air-pressure winches on the A-frame. This technique proved practical under good weather conditions, but for a short time during recovery, the sidescan sonar fish is only secured at one point and can turn freely along its long axis.

### 6.5.0 Operational settings, East Mediterranean surveys and data quality

The DTS-1 was deployed six times during the cruise (MS02-05-10-14-20 and 65). All the deployments were successful (see Table 6.1 for a brief summary of the different surveys). These several surveys resulted in the acquisition of data along 26 profiles in total, 7 across the Anaximander Mountains namely Amsterdam, Athina, Kazan and Tuzlukush mud volcanoes (Fig. 6.6a), 15 in the East Nile Delta across Isis, Osiris and Amon mud volcanoes (Figs. 6.6b, c and d) and 4 in the Centre Nile area where pockmarks are present (Fig. 6.6e). The western part of the Nile deep sea fan, including the Caldera area lying at ~ 3000 m water depth (Chefren, Cheops, Mykerinos mud volcanoes), could not be investigated with the DTS due to the restricted cable length (4450 m), which allows only for surveying in 2000 m water depth at maximum.

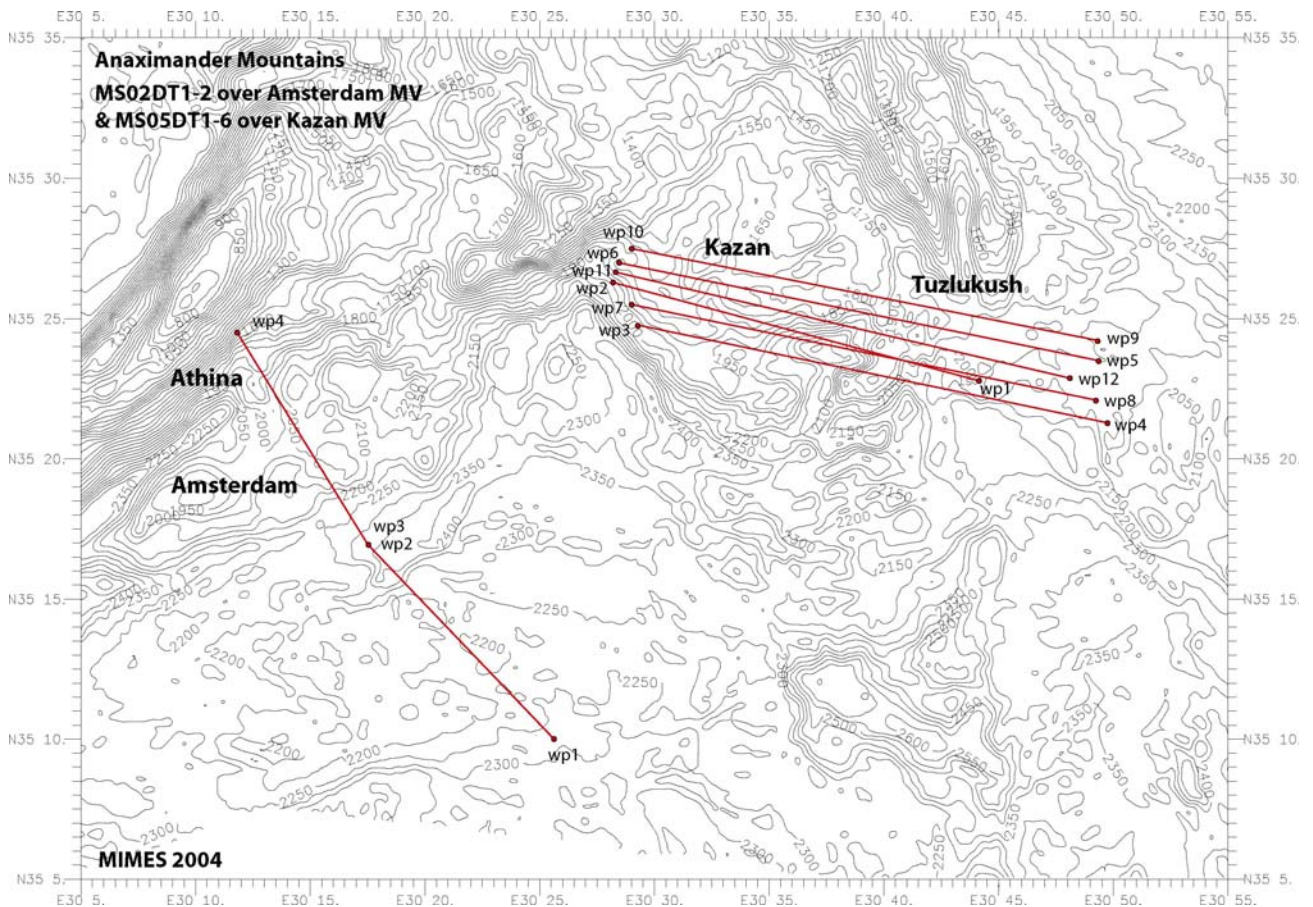


Figure 6.6a Track-plan for MS02DT1 and MS05DT1-6.

**DTS survey  
23-25 June  
East Delta  
Isis mv and  
surroundings**

**MS10DT1 to 6**

**Legend**

- MS10DT1-5
- mv south
- eastdeltabathy20
- eastdeltabathy5
- MS10TD2 no record
- MS10TD6 WP11&12

0 5,000 Meters

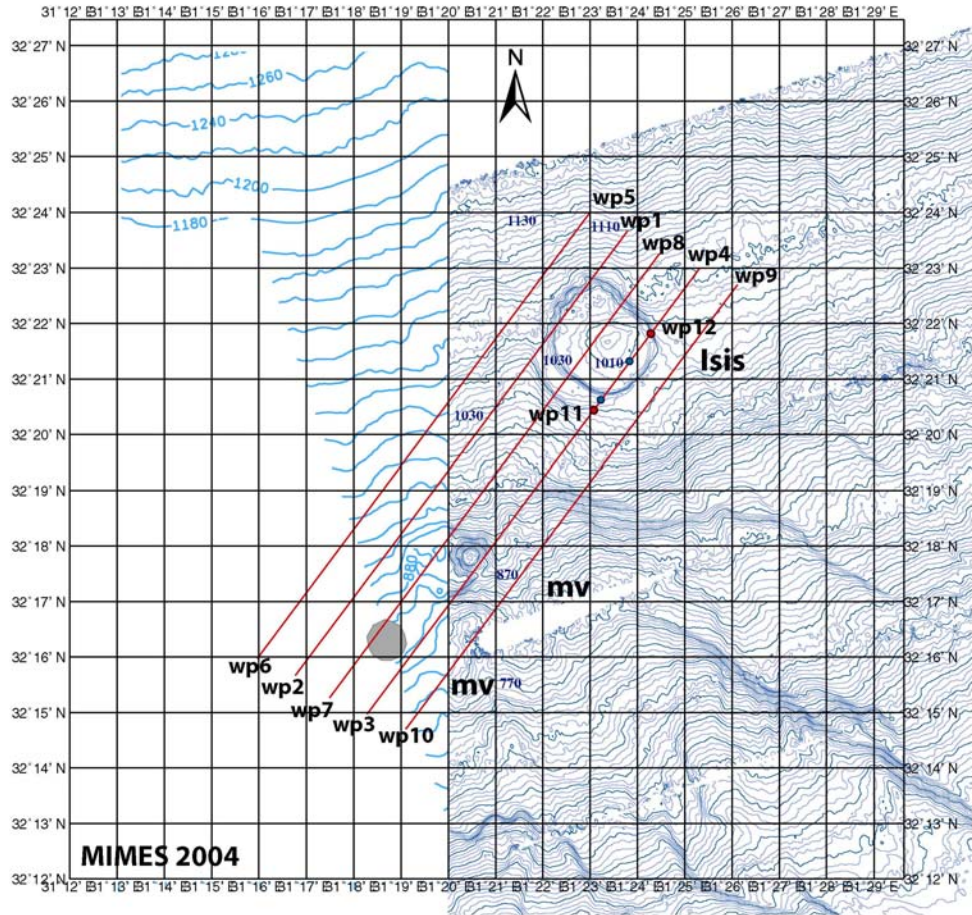


Figure 6.6b Track-plan for MS10DT1-6.

**Osiris and Amon MVS  
MS14DT1-5**

**Survey A**  
**Lines 1 to 5**  
Friday 25th evening  
-->Sunday 27th morning

**Legend**

- WP
- dts2
- eastdeltabathy20metres

0 5.000 Meters

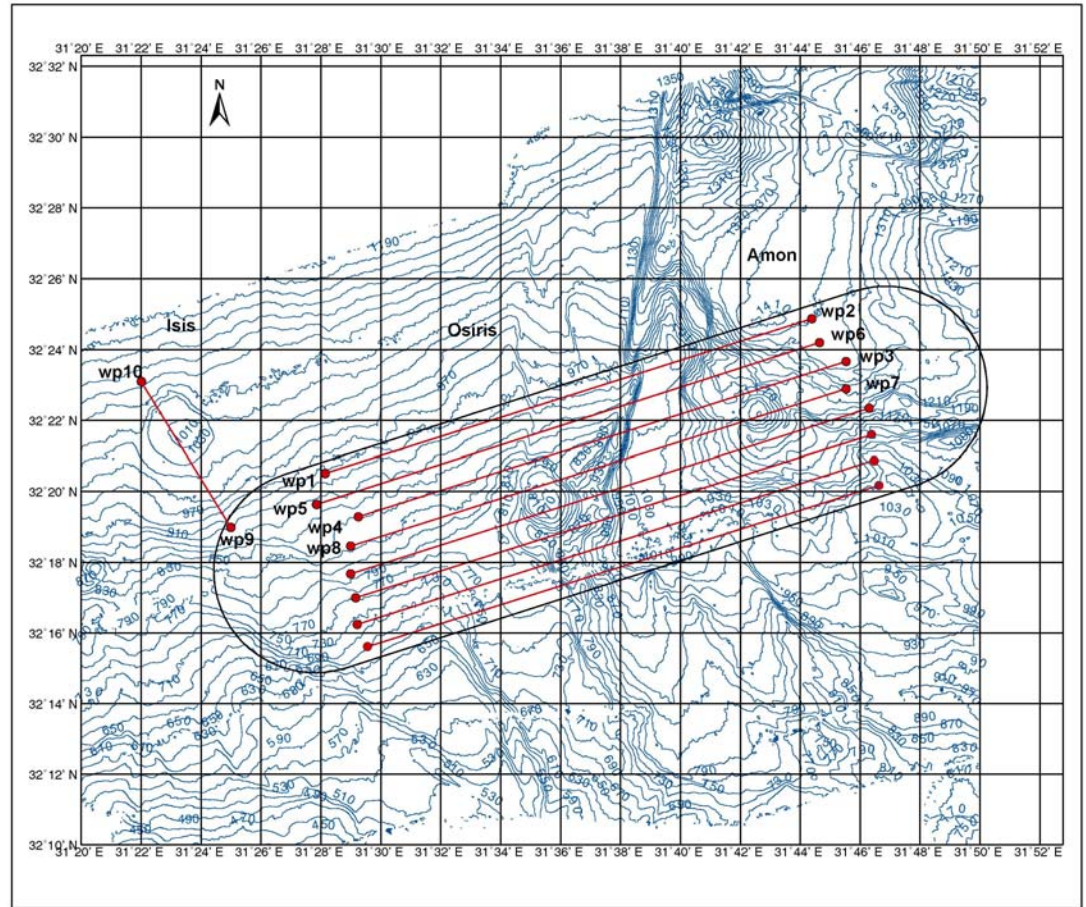


Figure 6.6c Track-plan for MS14DT1-5.

**Osiris and Amon MVS  
MS20DT1-4**

**Survey B**  
**Lines 1 to 4**  
Sunday 27th evening  
-->Tuesday 29th morning

**Legend**

- WP
- dts2
- eastdeltabathy20metres

0 5,000 Meters

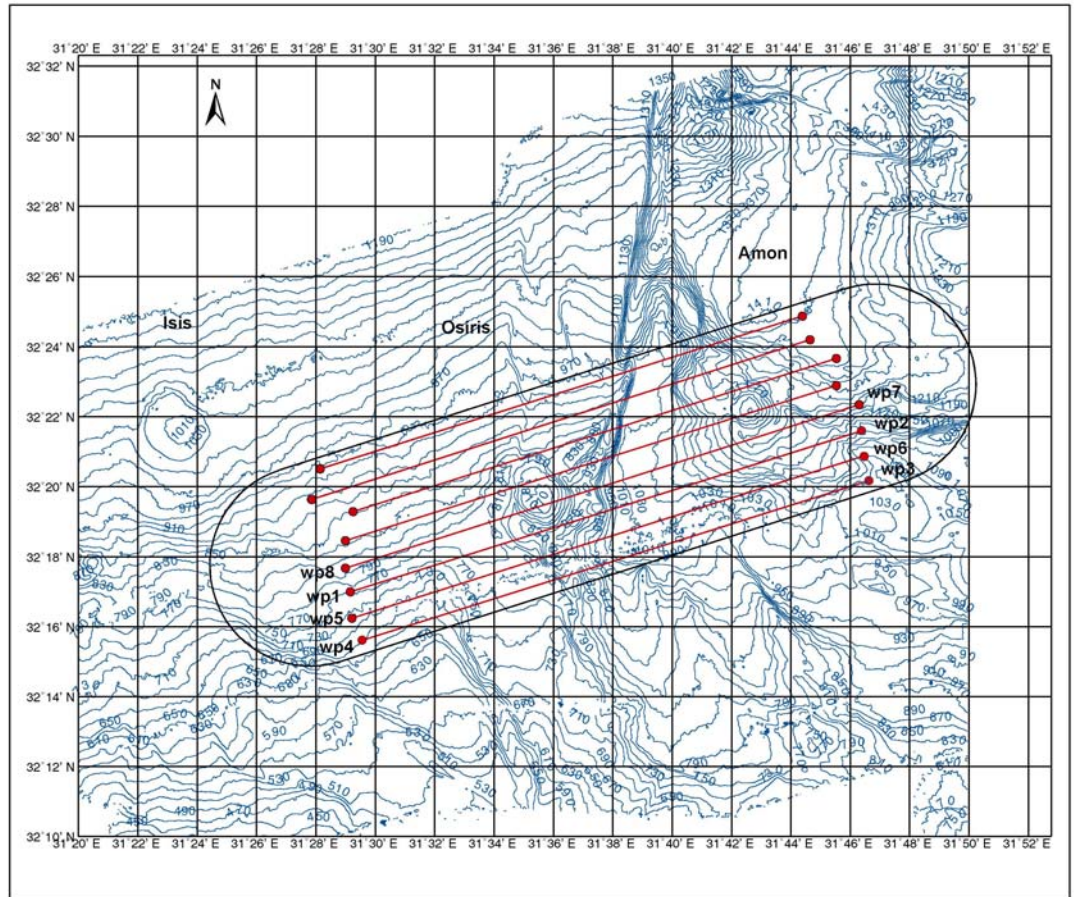


Figure 6.6d Track-plan for MS20DT1-4.

### MS65DT1-4 Centre Nile - Pockmarks area

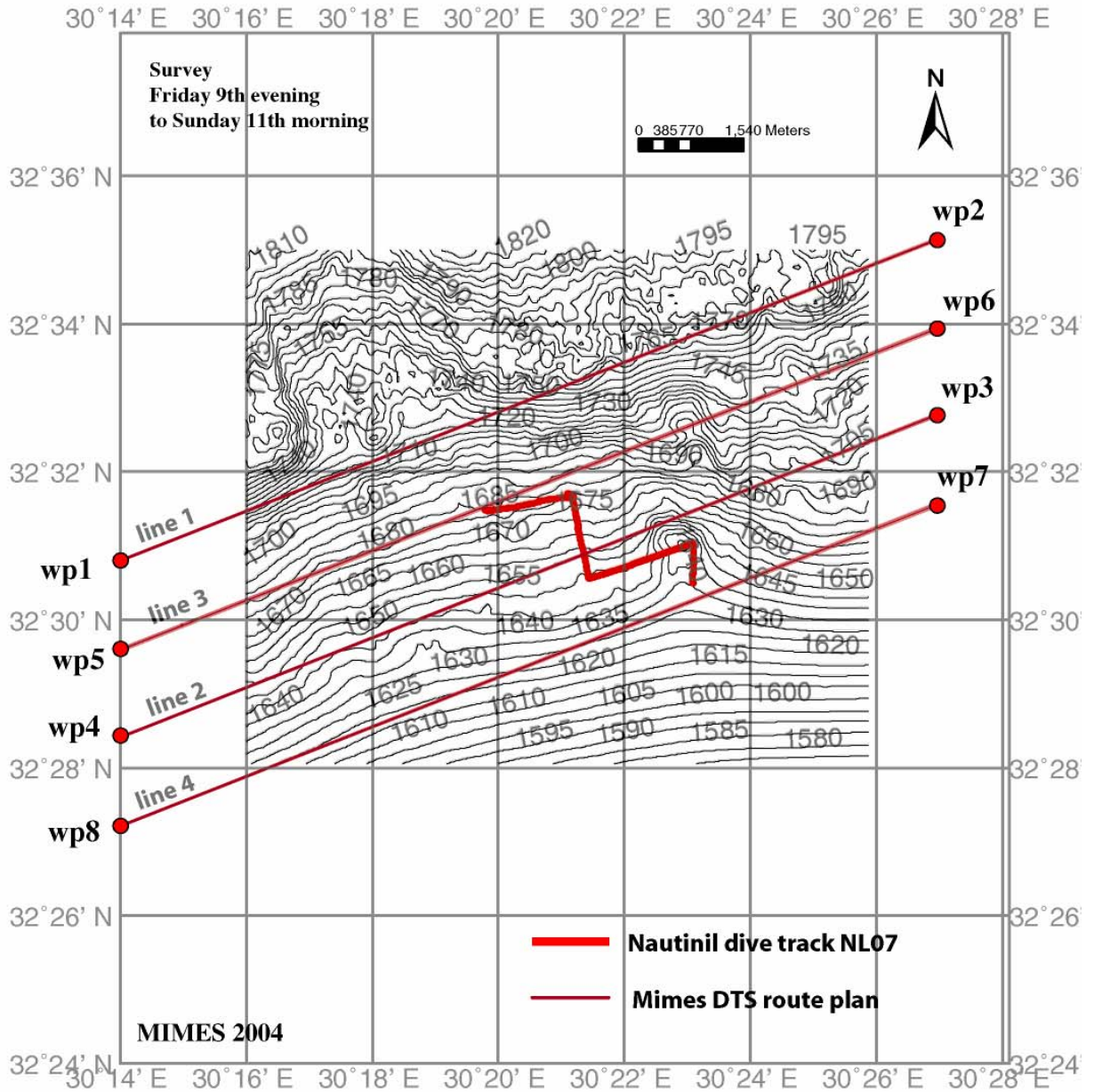


Figure 6.6e Track-plan for lines MS65DT1-4.

The orientations of the lines were chosen carefully in the areas of interest. As much as possible, they follow the isobaths in order to minimize cable length changes, and therefore to obtain good quality data. The line spacing of 1.2 to 1.3 km provided for overlap between adjacent lines. During the quasi-majority of the surveys, the sonar was operated with low

frequency (75 kHz) (with an exception made for line MS14DT5 when a frequency of 410 kHz was also tried). The tow elevation depth should be around 100 m for low-resolution and 20 m for high-resolution.

Site	Survey	Lines	Distance (km)	Time (days)
Amsterdam	MS02DT1	1	52	1.5
Kazan	MS05DT1-6	6	225	2.5
Isis	MS10DT1-6	6	90	1.5
Osiris-Amon	MS14DT1-5	5	118	1.5
Osiris-Amon	MS20DT1-4	4	108	1.5
Centre Nile	MS65DT1-4	4	90	1.5
<b>Total</b>		<b>26</b>	<b>683</b>	<b>10</b>

Table 6.1 DTS surveys summary

During all deployments the principal parameters or operational settings were kept constant in order to obtain data of similar characteristics. These settings were as follows:

- Sidescan pulse: 7.5 kHz bandwidth, 14 ms duration
- Sidescan sonar range: 750 m (or 150 m for high resolution)
- Sidescan sonar data window: 26000 samples
- Subbottom profiler pulse: 2-10 kHz bandwidth, 20 ms duration
- Subbottom profiler data window: 6000 samples
- Trigger mode: coupled (sidescan was master trigger)
- Ping repetition rate: 1 s

The quality of the data obtained during these deployments was overall rather satisfactory (see Figs. 6.7). Strong acoustic interference resulted from the interrogation of the Posidonia transponder although the latter works at much lower frequencies (14.5 - 17.5 kHz) than the 75 kHz sidescan sonar. These Posidonia pings are also present in the subbottom profiler data (2-10 kHz). This high-amplitude interference at fixed intervals can be easily filtered during processing of the data.

#### 6.6.0 Preliminary results

Processing and interpretation of the high-resolution sidescan sonar data are still going on; however a few important statements can be made at this point.

→ High-backscatter patches related to the features we are interested in have been observed in the explored sites. Structures associated with mud flows (Figs. 6.7 a, b, d and e) and the presence of carbonate crusts (Figs 6.7c and g) were identified on numerous lines.

→ High variability in the backscattering is observed in most of the sites, allowing a good post-processing interpretation (e.g. seafloor geological mapping, statistical analysis) (e.g. Figs. 6.7d and f)

→ Gas plumes have been detected in the water column at three sites, in the East Nile delta on Isis and Amon mud volcanoes (Figs. 6.7b and d) and in the Centre Nile in the region of the pockmarks (Fig. 6.7g). Such observations confirm the intensity of the present-day activity of the Nile deep sea fan in terms of seepage associated with gas emissions.

The correct correspondence between different backscatter intensities and mud breccia/carbonate crust related facies can only be determined after full processing of the data and integration with ground-truth=data. This will also be investigated further in the coming months.

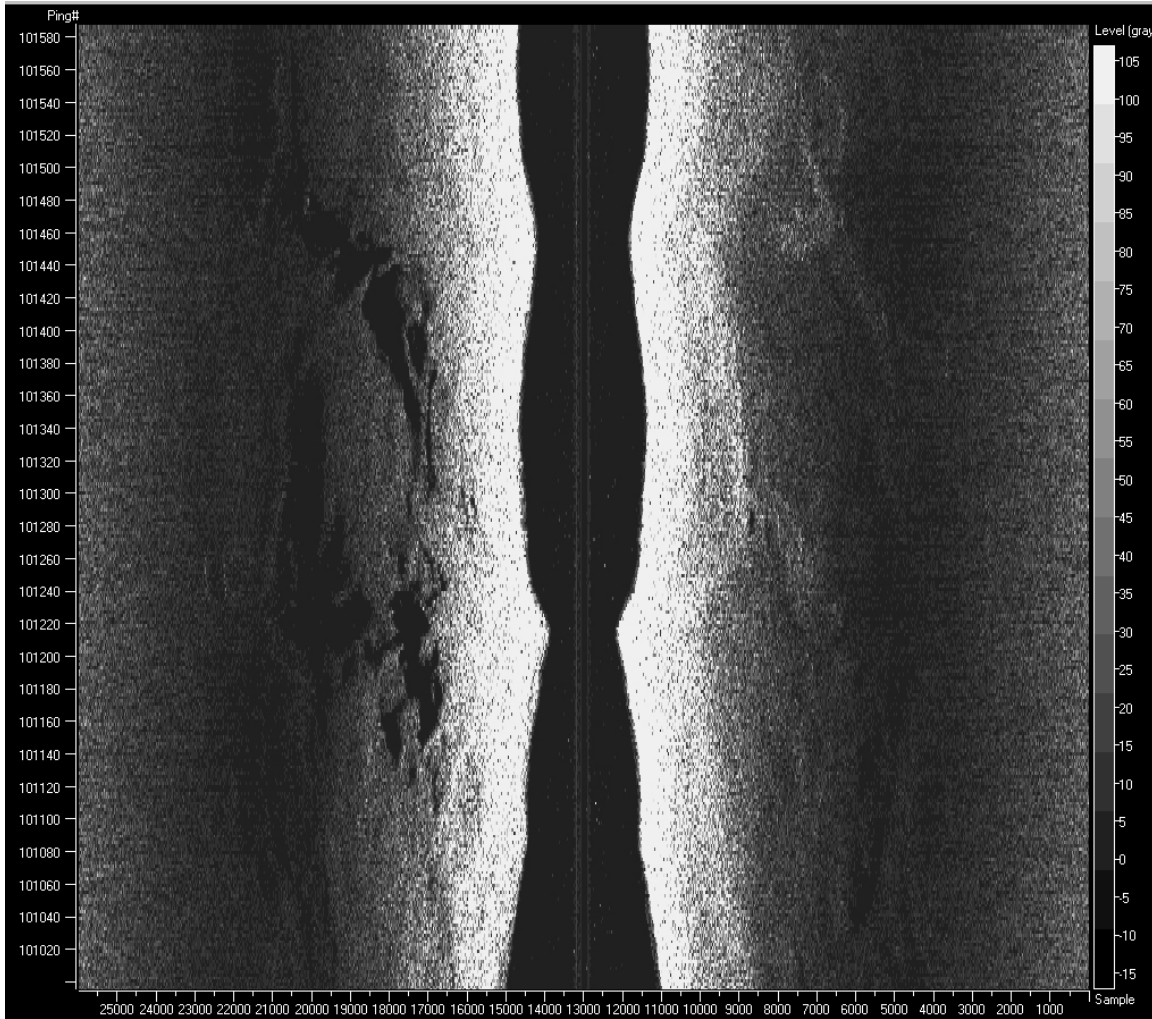


Figure 6.7a MS05DT3 – over Kazan mud volcano

On the left side, dark areas are interpreted as the shadows of ridges associated with mud flows. Variability in the backscattering on the right side could possibly be related to several mud flow events.

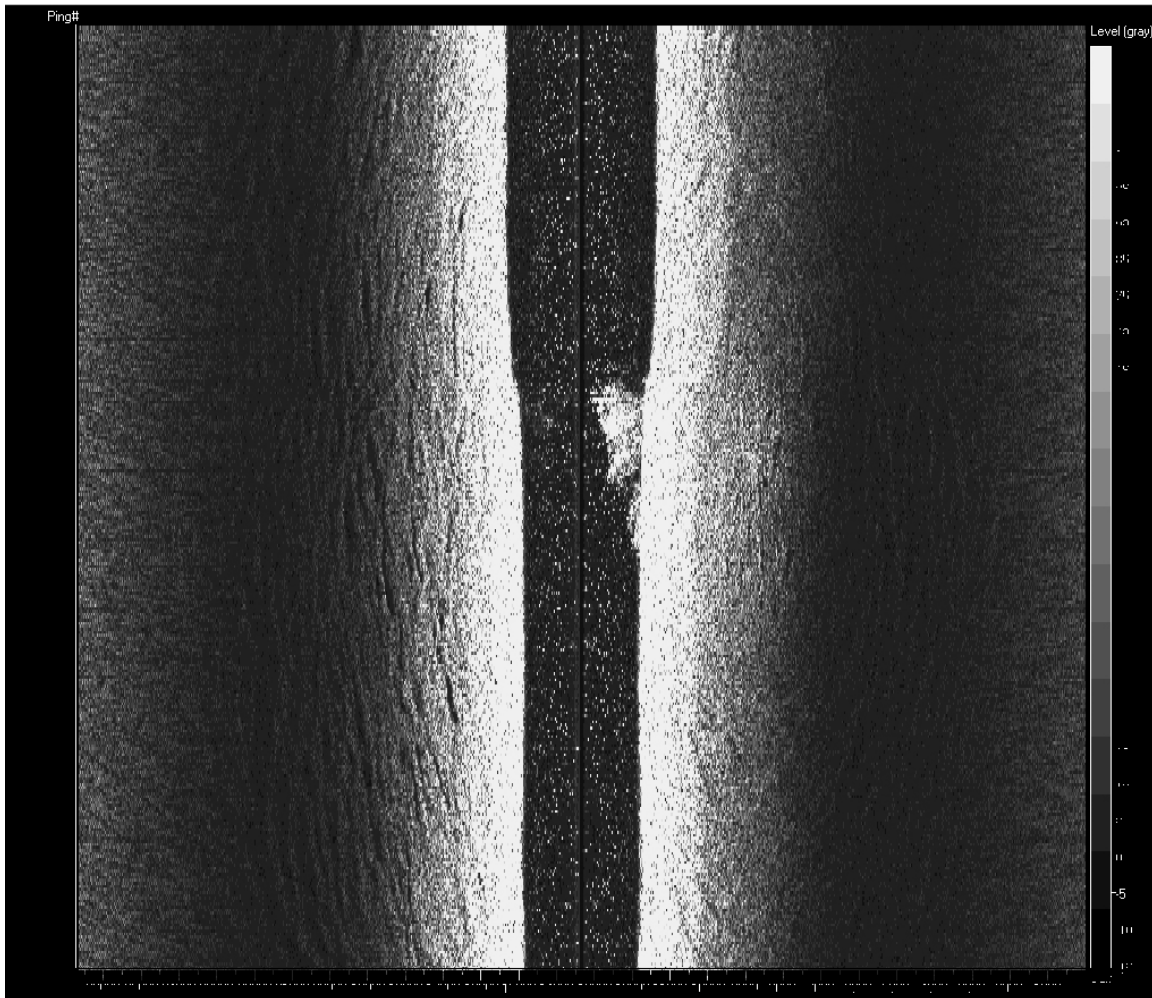


Figure 6.7b MS10DT3 – over Isis mud volcano

Concentric ridges formed by radial mud flows are visible on the left hand side of the sonar image. A gas plume can be observed in the water column, attesting to the present-day activity of the mud volcano.

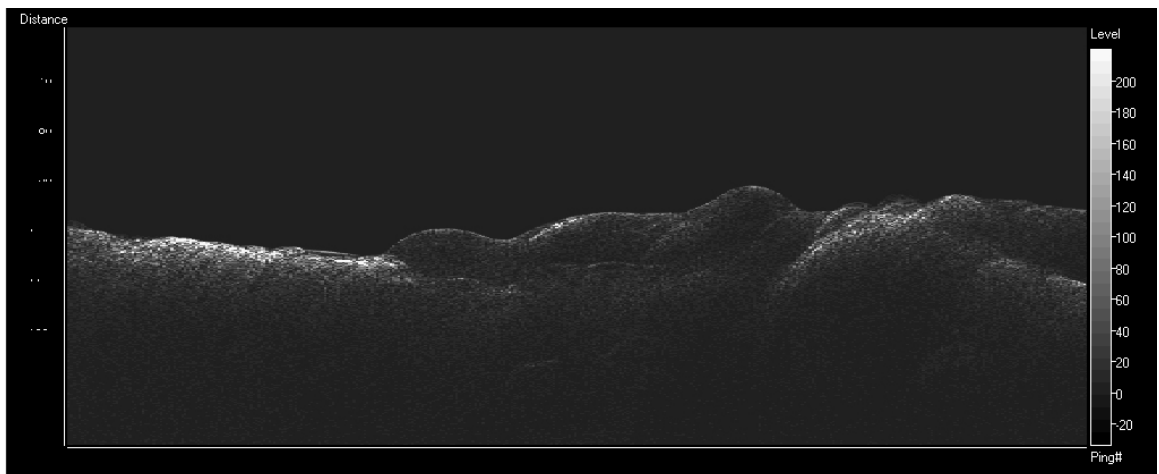
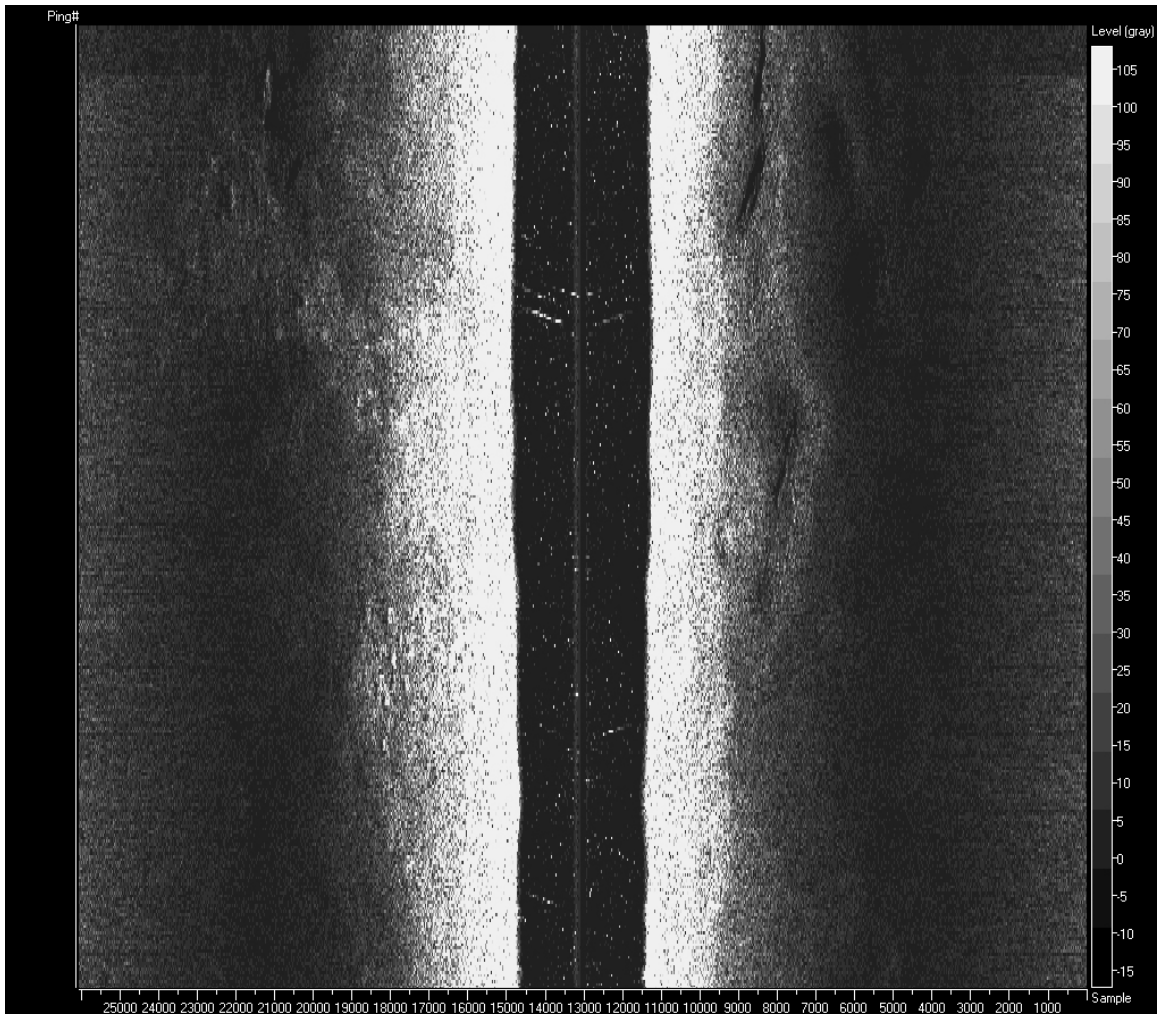


Figure 6.7c MS14DT2 – over Amon mud volcano

On the subbottom profiler (lower panel), bumpy reflectors at the seafloor represent mud breccia and the strong and bright subsurface reflectors on the left side are most probably caused by carbonate crust.

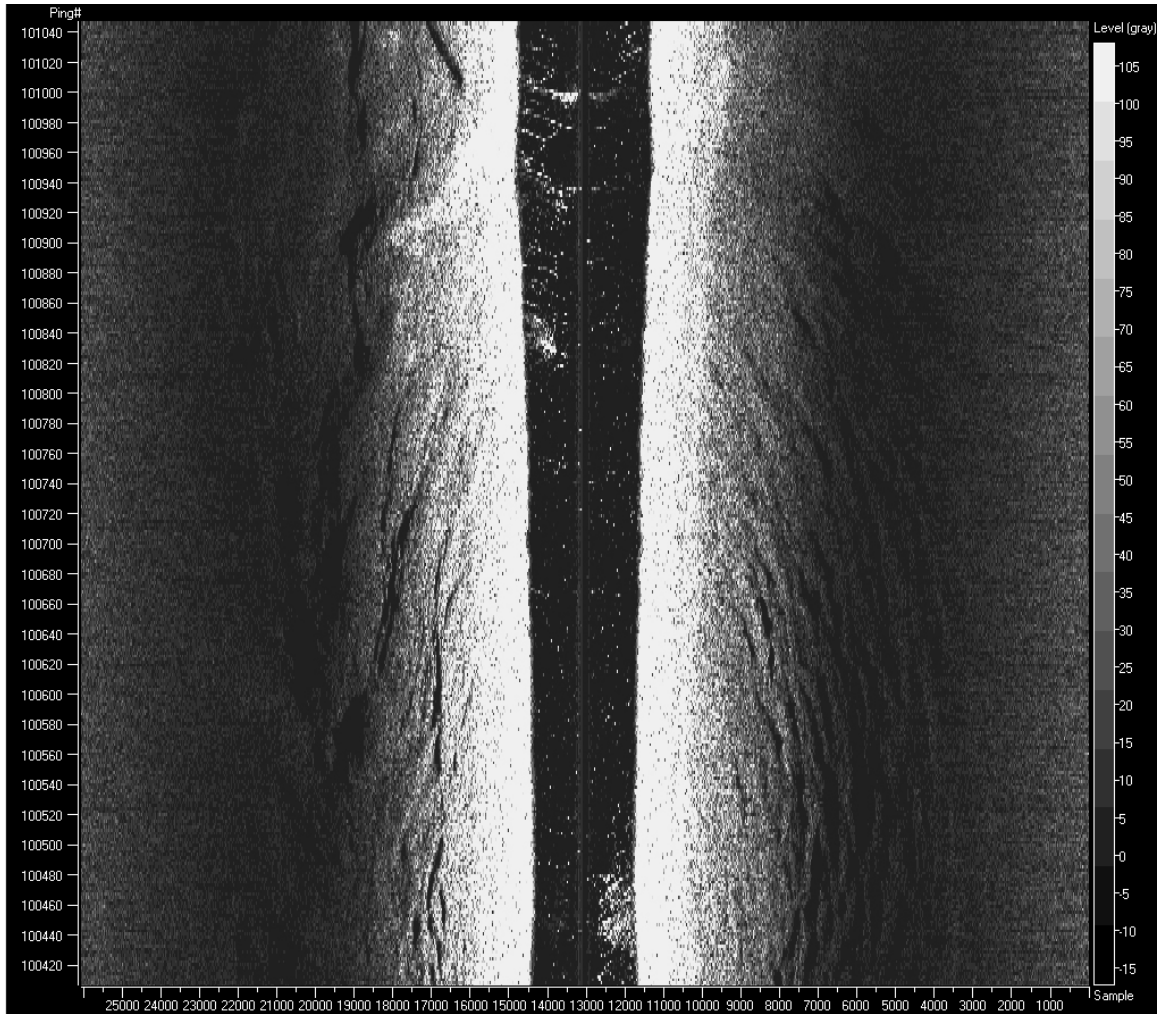


Figure 6.7d MS14DT4 – over Amon mud volcano

Gas plumes in the central part of the mud volcano as well as near one edge are visible in the water column in the unprocessed sidescan record (lower and upper parts). The seafloor is very much disturbed and non-uniform leading to high variability in backscattering, with the presence of concentric ridges suggesting radial pressure from mud eruptions in the centre.

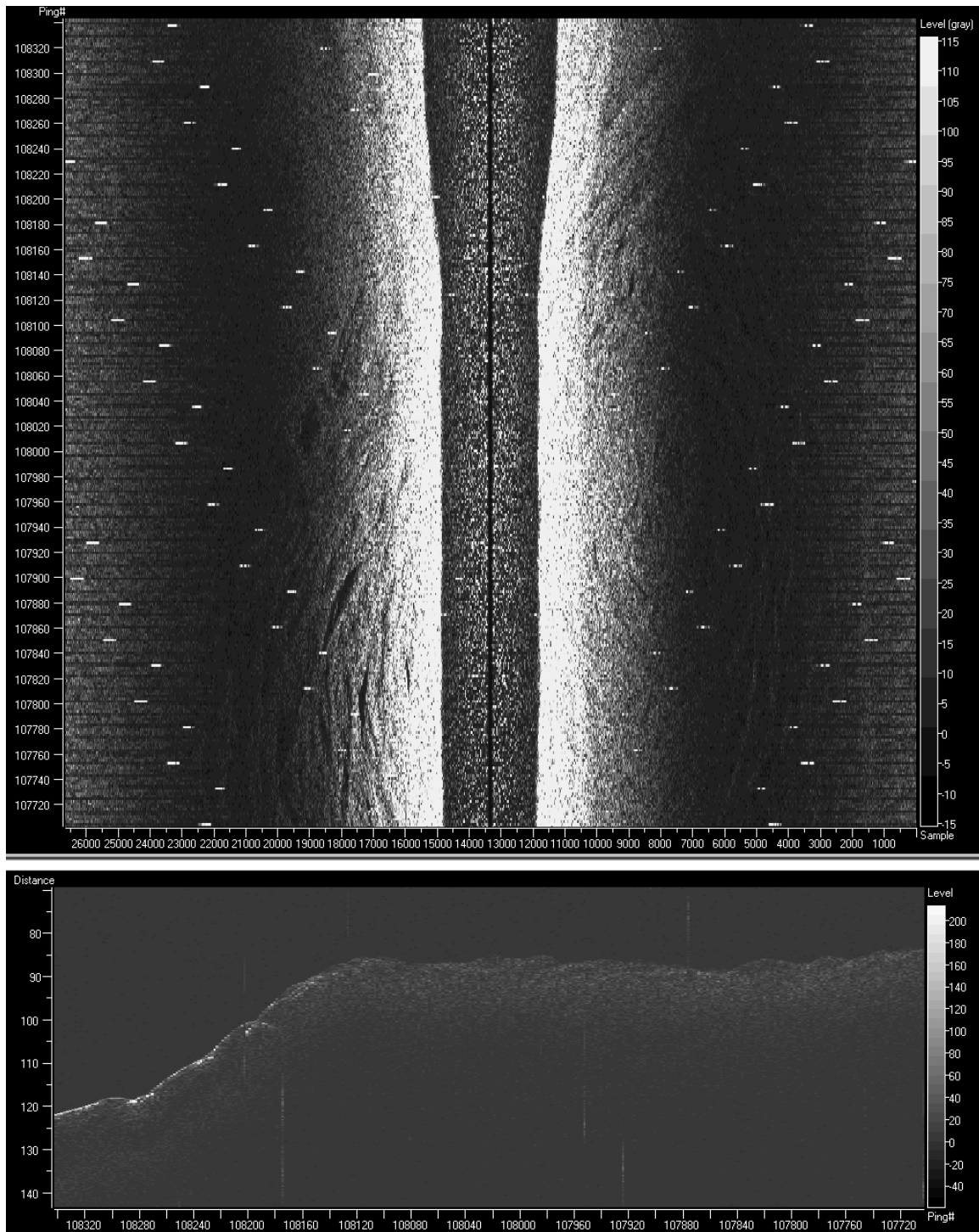


Figure 6.7<sup>e</sup> MS20DT4 – over Osiris mud volcano

A diffuse seismic facies, representing the mud breccia, characterizes the positive topography of the mud volcano (right side of the subbottom profiler). This surface is composed of a succession of small-scale mounds and depressions (of a few metres high). The transition between the mud volcano and the surrounding (hemipelagic sediments) is rather sharp. The seafloor seismic expression outside Osiris is characterized by clear and continuous reflectors (left side).

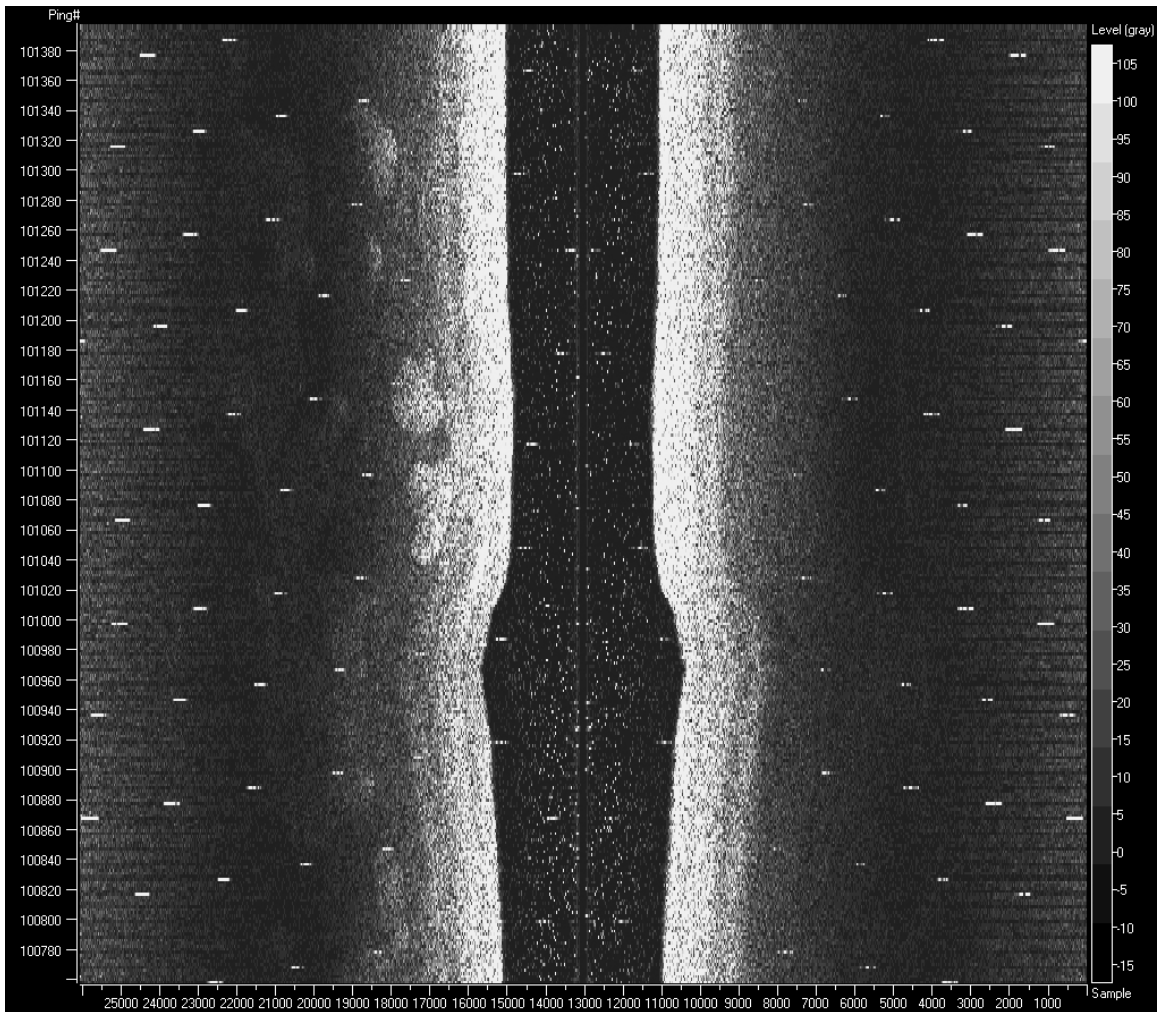


Figure 6.7f MS20DT4 – over Amon mud volcano

Numerous high backscattering patches (white spots on the left side) are observed on Amon mud volcano and are interpreted as mud breccia structures. Their geometry and variable backscattering contrast with the surroundings and might suggest that they could correspond to distinct mud eruptions events.

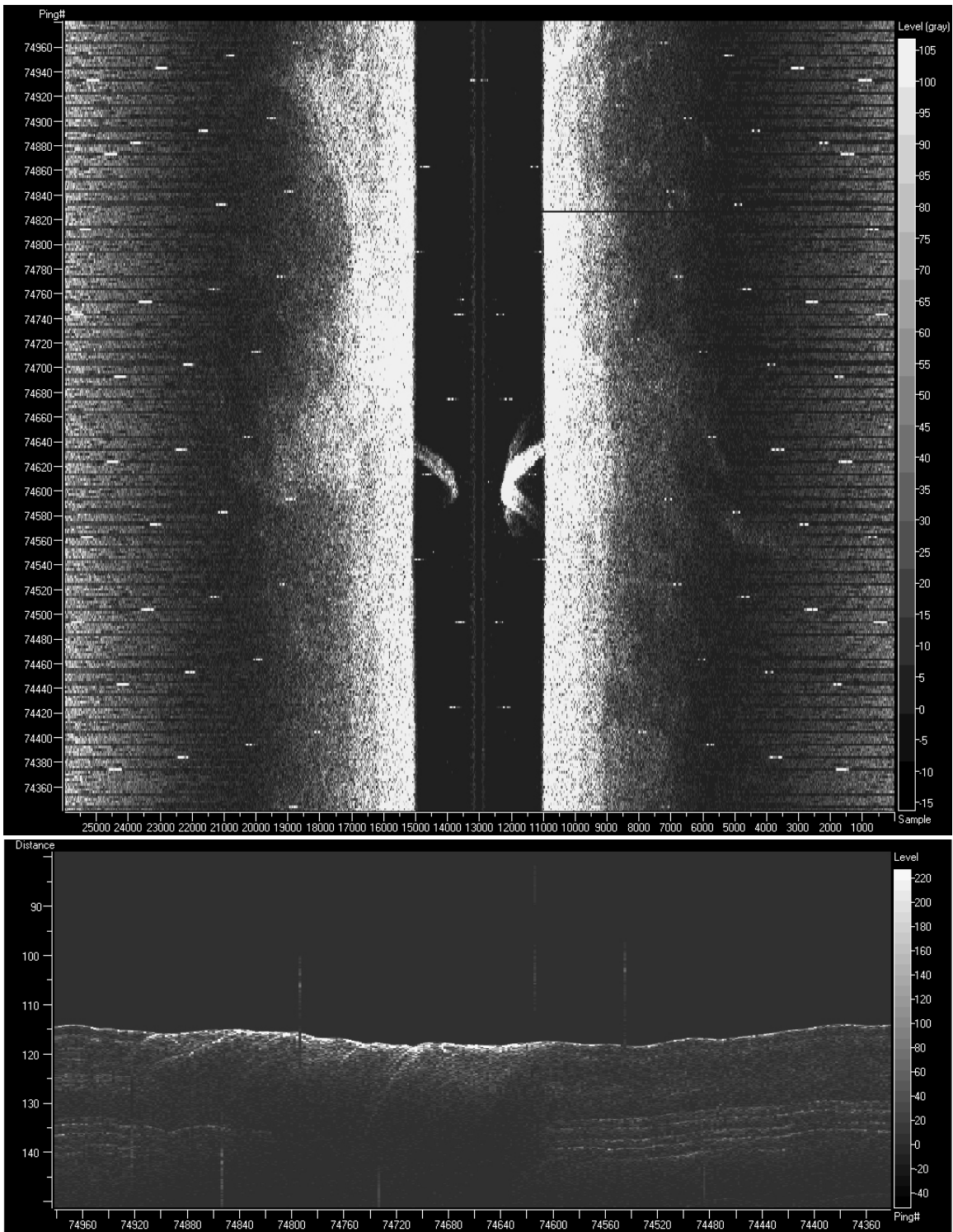


Figure 6.7g MS65DT3 – over the Centre Nile

Very reflective zones are observed on the sonar image and sometimes are associated with white patches in the water column. Such features are interpreted to be gas plumes. The subbottom profiler shows strong reflections at the surface associated with gas and most probably carbonate crust. Transparent seismic facies characterizes the subsurface below.

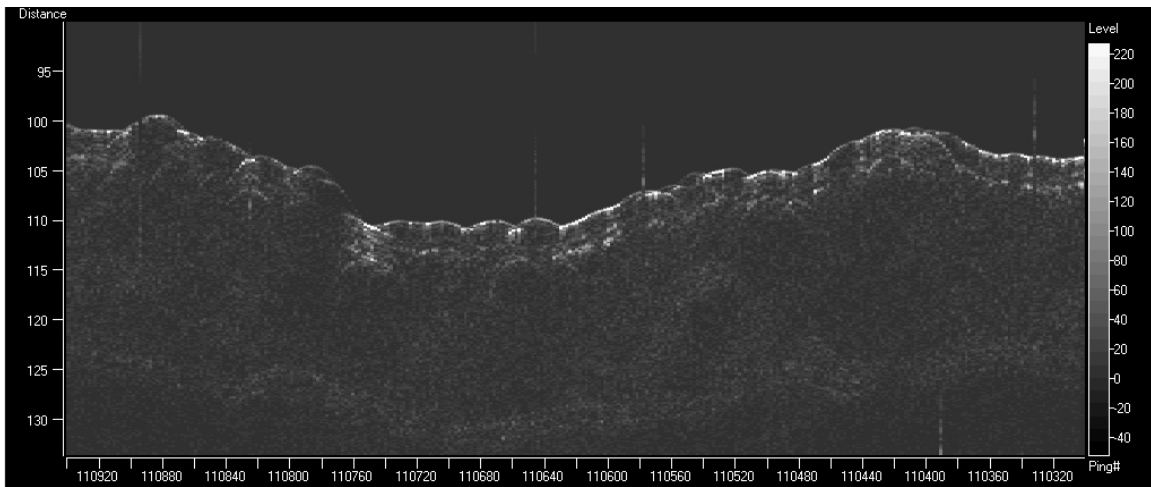


Figure 6.7h MS65DT4 – over the Centre Nile

The subbottom profiler shows an area of pockmarks localised in a depression of ~10 metres. The subsurface is very much disturbed, associated with bumps and bright internal reflectors in its upper part. Below the surface, no clear reflectors are visible but rather a transparent facies. The geometry and the seismic facies suggest the presence of ascending material, partially associated with gas.



### **7.0.0 Heat flow measurements**

Warm fluids escaping at seeps create heat flow anomalies which in turn, when detected and quantified, provide information on the nature and strength of fluid venting at those seeps. Measurements of temperature at several depths below the seafloor allow determination of temperature gradients. Heat flow is defined as the simple product of the vertical temperature gradient and sediment thermal conductivity measured either in situ or on recovered core samples. Measuring heat flow at the surface of several mud volcanoes was an important objective of MIMES. A main goal is to use heat flow anomalies to constrain models of fluid flow through those mud volcanoes.

All temperature measurements taken during MIMES were made with Ifremer/Micrel thermistor thermometers mounted on outrigger-type probe holders that were welded to the outer surface of a standard 9 cm diameter NIOZ piston coring barrel (fig 7.1). Up to seven thermometers were attached to a 12 m long core barrel. After penetration, the corer was usually kept 10 minutes in the sediment, thus allowing for thermometers to closely approach in situ seafloor temperatures. Each individual thermometer has an internal memory to record the in situ temperature data according to a pre-set acquisition schema. Recorded data were downloaded to a laptop on the ship's aft-deck after completion of each coring station combining heat flow measurement, on return of the corer to the ship. Thermal conductivity was measured in situ at a few sites by an newly-developed Ifremer probe. Thermal conductivity data will be processed ashore.



Figure 7.1 (a) Leon Wuis welds outrigger probe thermal holders on core tube. (b) Tomas Feseker attaches a thermal probe to one of the probe holders.

Table 7.1 summarizes all 22 heat flow measurements taken during MIMES, including three in the Anaximander study area (1 on Amsterdam MV, 2 on Kazan MV), eight in the Isis study area (7 on Isis MV, 1 at a reference site further east), two on North Alex MV, eight in Menes Caldera (5 on Chefren MV, 3 on Cheops MV, 1 on the caldera floor), and one on the western upper slope of the Nile fan. In addition, Ifremer/Micrel temperature and pressure sensors were attached to the ME CTD frame at three CTD stations on Chefren and Cheops MV also reported in Table 7.1 (MS48CT, MS52CT, MS58CT).

*Anaximander study site:*

No geothermal anomaly was detected on Kazan MV. In contrast, MS04PT in the centre of Amsterdam MV revealed a significant warming of the mud (temperature increase of over 3°C in the upper ten meters of mud). This measurement, the first ever made on Amsterdam MV to our knowledge, is viewed as a strong indication of the high current activity of fluid and/or mud emission at the surface of this mud volcano.

*Isis study site:*

Isis MV was the site of a particular focus of heat flow measurements during MIMES. This was because we planned to develop thermo-hydrodynamic modeling of Isis MV taken as a case example of a pie-type mud volcano formed above a gas chimney. Measurements at the centre of the volcano indicate an exceptionally high level of activity, with a temperature gradient up to 21.9 °C per 10 meters, although apparently in decline with respect to an even higher gradient of 26.6 °C per 10 meters measured during NAUTINIL in september 2003 (Fig 7.2). Away from the centre, measurements were taken at increasing distances in several directions to check on the axisymmetric nature of the temperature distribution in the mud pie (Fig 7.3). Rapidly decreasing temperature gradients from the centre to the outer part of the mud volcano, with no apparent influence of the direction, are consistent with the hypothesis of a narrow feeding channel and an axisymmetric dynamic functioning and growth of Isis MV. Porosity and permeability will be measured in the Ifremer laboratory on dedicated sediment samples to contribute constraints on hydrogeological modeling.

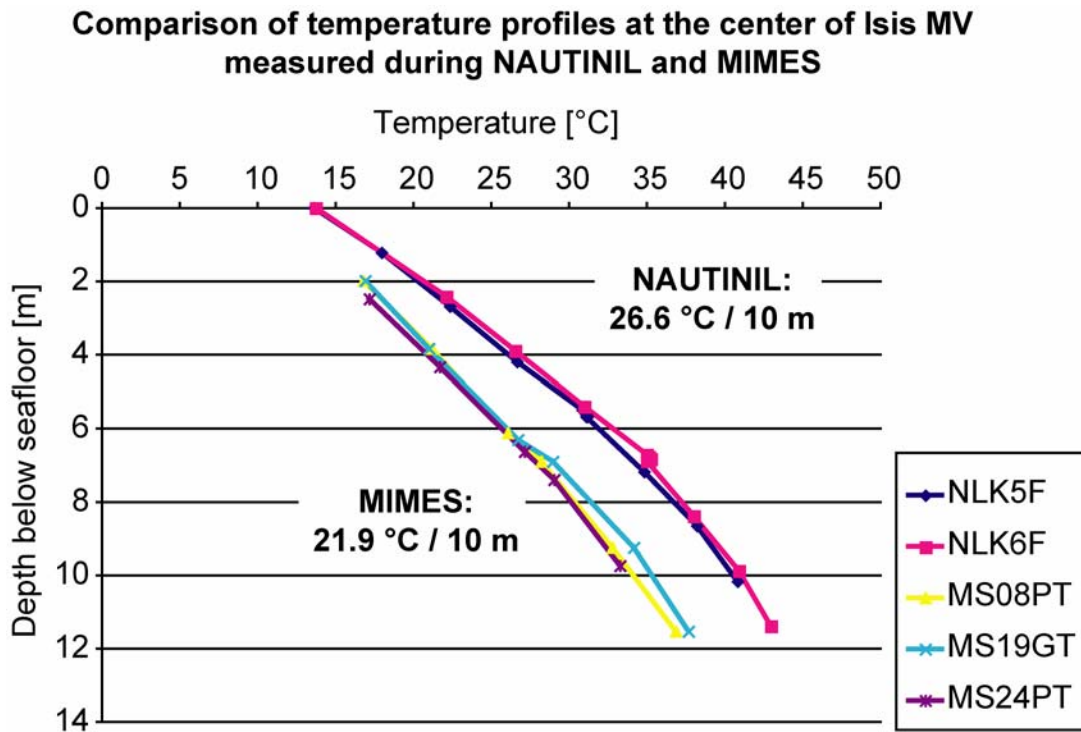


Figure 7.2 Thermal gradients in the centre of Isis Mud Volcano measured 9 months apart.

## MIMES - Heat flow stations on Isis MV

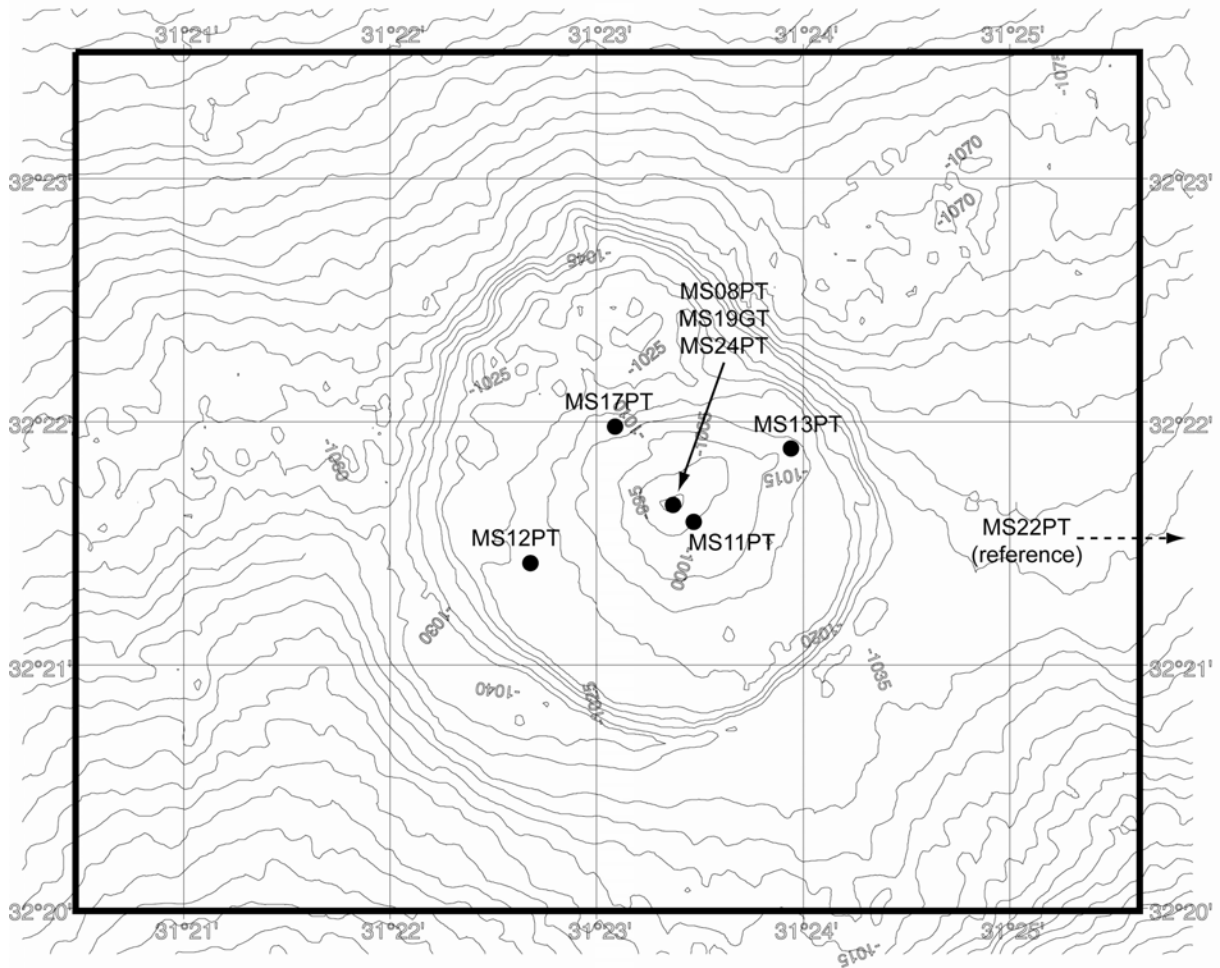


Figure 7.3 Pattern of heat flow measurements on Isis Mud Volcano. Note that MS22PT was a reference measurement taken away from the mud volcano at a position not shown here.

### *North Alex site:*

The two heat flow measurements made on North Alex MV indicate a high level of current activity of mud and/or fluid emission, with an apparent similarity to the situation on Isis MV. Free gas release adds buoyancy to the erupting mud and fluids. This effect is expected to be more pronounced at this shallow water mud volcano than at other deeper sites and might have a considerable thermal signature, which will need investigations.

### *Menes caldera site:*

Temperature and pressure measurements made during lowering at coring stations and on CTD profiling indicate that over 200 meters of warm brine, with temperature up to 57°C, occupy the crater of Chefren MV. When the seafloor at the bottom of the brine could be penetrated by the corer, temperature in the sediment below the brine was observed to remain close to the brine temperature, with low positive or negative gradients (less than a few tenths

of °C per ten meters). This also applies to Cheops MV, but the brine thickness on the summit of Cheops MV does not exceed a few meters and the brine temperature is lower than on Chefred MV (25 to 42°C depending on location). Heat flow measurements on the flank of the Chefred MV (MS34PT) and at a site away from volcanoes on the bottom of the caldeira (MS59PT) indicate low amplitude geothermal anomalies.

Site	Station N°	Latitude		Longitude		Water Depth m	T sensors in sediment	In Situ Conductivity	Penetration of deepest T sensor, m	Prelim Tgrad °C/10m	CI measurement Hydro sample
		N	E	N	E						
Amsterdam MV	MS04PT	35°20.006'	30°15.951'	1995	1 no	3.50	3.4	no			
Kazan MV	MS06GT	35°25.85'	30°33.90'	1688	3 no	4.17	0.15	no			
Kazan MV	MS07GT	35°25.92'	30°33.72'	1664	3 yes	4.17	0.15	no			
Isis MV (center)	MS08PT	32°21.66'	31°23.37'	978	6 yes	11.54	21	no			
Isis MV (SE)	MS11PT	32°21.59'	31°23.47'	986	4 no	5.40	1.4	yes			
Isis MV (SW)	MS12PT	32°21.42'	31°22.68'	1017	4 no	5.40	0.1	yes			
Isis MV (NE)	MS13PT	32°21.89'	31°23.94'	1005	5 no	8.50	0.3	yes			
Isis MV (NW)	MS17PT	32°21.98'	31°23.09'	990	3 no	7.50	0.5	yes			
Isis MV (center)	MS19GT	32°21.66'	31°23.37'	977	7 yes	11.54	22	no			
Ref East Isis MV	MS22PT	32°21.40'	31°26.70'	1007	7 yes	12.24	0.25	yes			
Isis MV (center)	MS24PT	32°21.65'	31°23.38'	980	6 yes	9.75	22	yes			
N. Alex MV (center)	MS26PT	31°58.16'	30°08.16'	495	6 no	11.54	10	no			
Slope W	MS27PT	31°47.90'	29°27.70'	1389	6 no	12.04	0.35	no			
Chefred MV (center)	MS30PT	32°06.53'	28°10.66'	2898	6 no	no mud smear	0. (T= 57°C)	no			
Chefred MV (edge)	MS34PT	32°06.74'	28°10.33'	2949	6 no	no mud smear	0.5	yes			
Chefred MV (center)	MS36PT	32°06.53'	28°10.68'	2898	2 no	no mud smear	0. (T= 57°C)	no			
Chefred MV (center)	MS37PT	32°06.53'	28°10.68'	2898	2 no	no mud smear	0. (T= 57°C)	no			
Cheops MV (center)	MS40PT	32°08.18'	28°09.43'	2923	6 no	no mud smear	0. (T= 42°C)	no			
Cheops MV (center)	MS41GT	32°08.17'	28°09.41'	2923	6 no	no mud smear	0. (T=37.1°C)	no			
Chefred MV (center)	MS47GT	32°06.54'	28°10.66'	2906	2 no	no mud smear	0. (T=57°C)	no			
Chefred MV (center)	MS48CT	32°06.54'	28°10.67'	2906	1, on CTD	0.	T=up to 57°C	no			
Chefred MV (center)	MS52CT	32°06.54'	28°10.67'	2900	2, on CTD	0.	T=up to 57°C	no			
Cheops MV (center)	MS58CT	32°08.17'	28°09.43'	2925	1, on CTD	0.	T=up to 25°C	no			
Menes Caldeira North	MS59PT	32°09.80'	28°08.50'	2925	4 yes (in water?)	5.41	0.5	no			
N. Alex MV (center)	MS64PT	31°58.18'	30°08.18'	495	7 yes	11.54	7.6	yes			

Table 7.1 Heat flow summary

### **8.0.0 Surveys with 3.5 kHz echosounder**

The 3.5 kHz bottom profiler was used principally in the Menes Caldera area where the depth was beyond the reach of the deep tow system on the ship. It was also used to check the bathymetry on the Isis mud volcano (figure 8.1) before we started coring there and for providing additional (deeper penetration) information during the deep tow survey in the pock marks area. It was not working properly for the first lines (up to the Isis survey) but thereafter provided some very useful information.

In the Menes Caldera, the survey lines concentrated only on crossings of targets for further sampling and measurements (figure 8.2). During Nautinil in September 2003 a grid of survey lines was completed over the Menes Caldera by the 3.5 kHz system on the L'Atalante; thus this survey was not intended as duplication but as complement as well as to provide context for work during MIMES. Thus several lines were run across the caldera in different directions to provide profiles crossing Chefren, Cheops, and Mykerinos mud volcanoes from different directions. The fault control of these features was clearly visible in the lines. The specific form of each of the mud volcanoes was visible, with both Chefren and Mykerinos having deep crater depressions extending to below the surrounding seafloor; however, the crater of Mykerinos is empty whereas the Chefren crater is filled with fluid mud and brine. Cheops mud volcano also has a summit crater filled with brine and fluid mud but it does not appear to be deeper than about 15 to 20 m. The depth of the crater at Chefren can not be observed in the 3.5 kHz echosounding profiles but lowerings of cores and CTDs into the crater indicate a depth of at least 250 m. Both Cheops and Chefren had relatively flat tops probably as a result of the fluid muds and brines in their craters.

During one of the surveys, two strange reflectors were noticed in the water column to the northeast of the main summit region of Cheops, in the vicinity of a small subsidiary centre of eruption indicated by a northeastward elongation of the mud volcano (figure 8.3). The reflectors appear as low amplitude diffractions, one shallower than the summit of the mud volcano and the other a little deeper. Because there was not thought to be any unmapped peak of Cheops or other shallower source of reflections, it was inferred that this might be a cloud of recently erupted muddy gassy brine in the water column. To check this, a duplicate of one of the survey lines was run a day later; and the two reflectors were in the same place and had the same character. To decide if there was physical source for the reflectors as, for example, a new or unknown and shallower peak of Cheops, two further surveys were run across Cheops during following nights, with lines placed so as to locate as best as possible the true source of the reflectors or diffractions. The results were still inconclusive. We did not manage to find a location where the reflection/diffraction was any stronger (i.e. we could not find a source with a similar acoustic contrast to the seafloor) or any better defined. All that can be concluded is that there was a source of reflection or diffraction in the water column above the seafloor defining the northeast elongation of Cheops, and that the source had a low acoustic contrast. The easiest way to explain is as a cloud of fluid in the water column with such an acoustic contrast, and that this might perhaps be a cloud of muddy brine emitted from Cheops.

ISIS - 3.5kHz survey - MIMES 2004 - MS07aES1-4

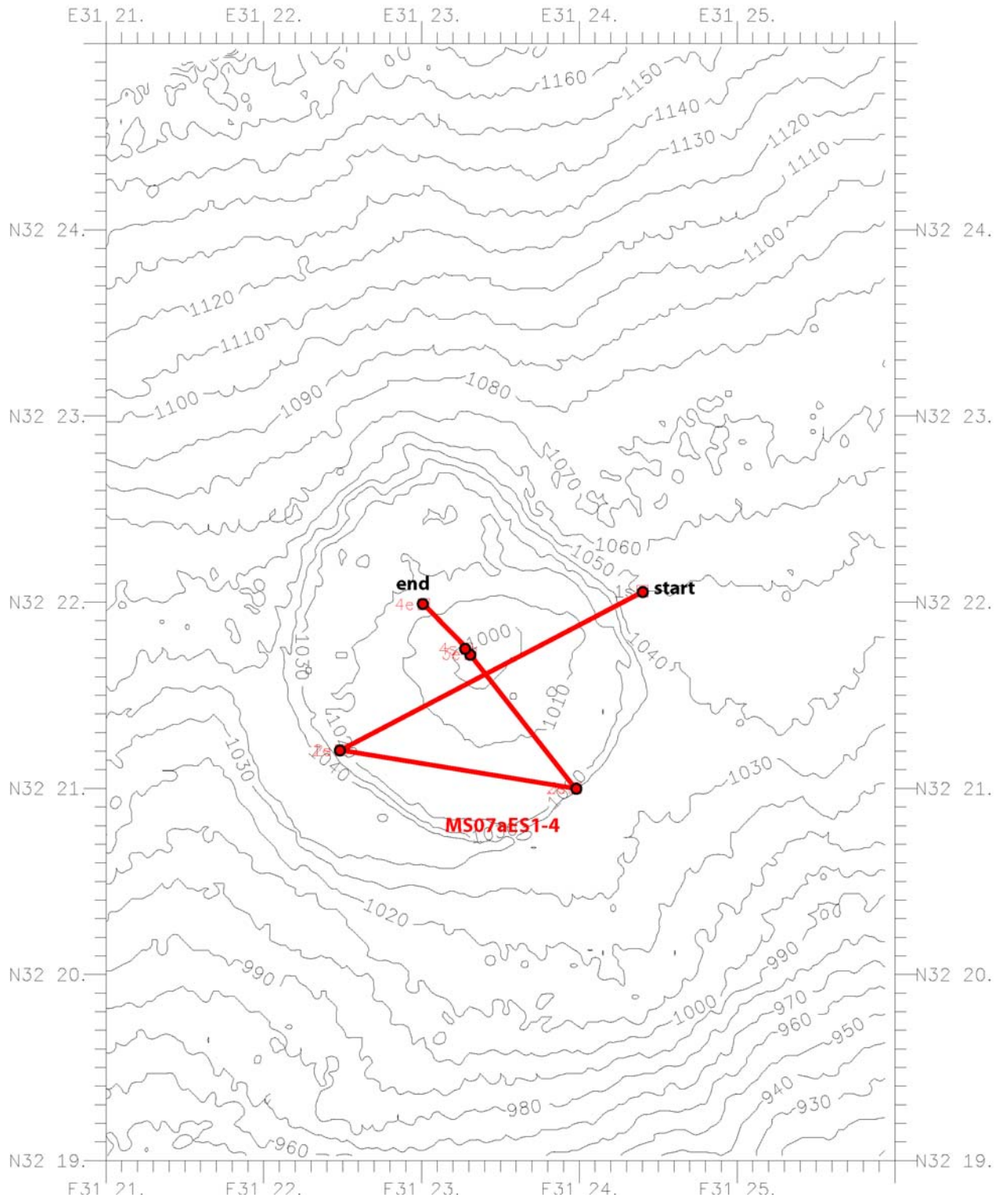


Figure 8.1 MS07aES1-Isis

CALDERA - 3.5kHz surveys - MIMES 2004

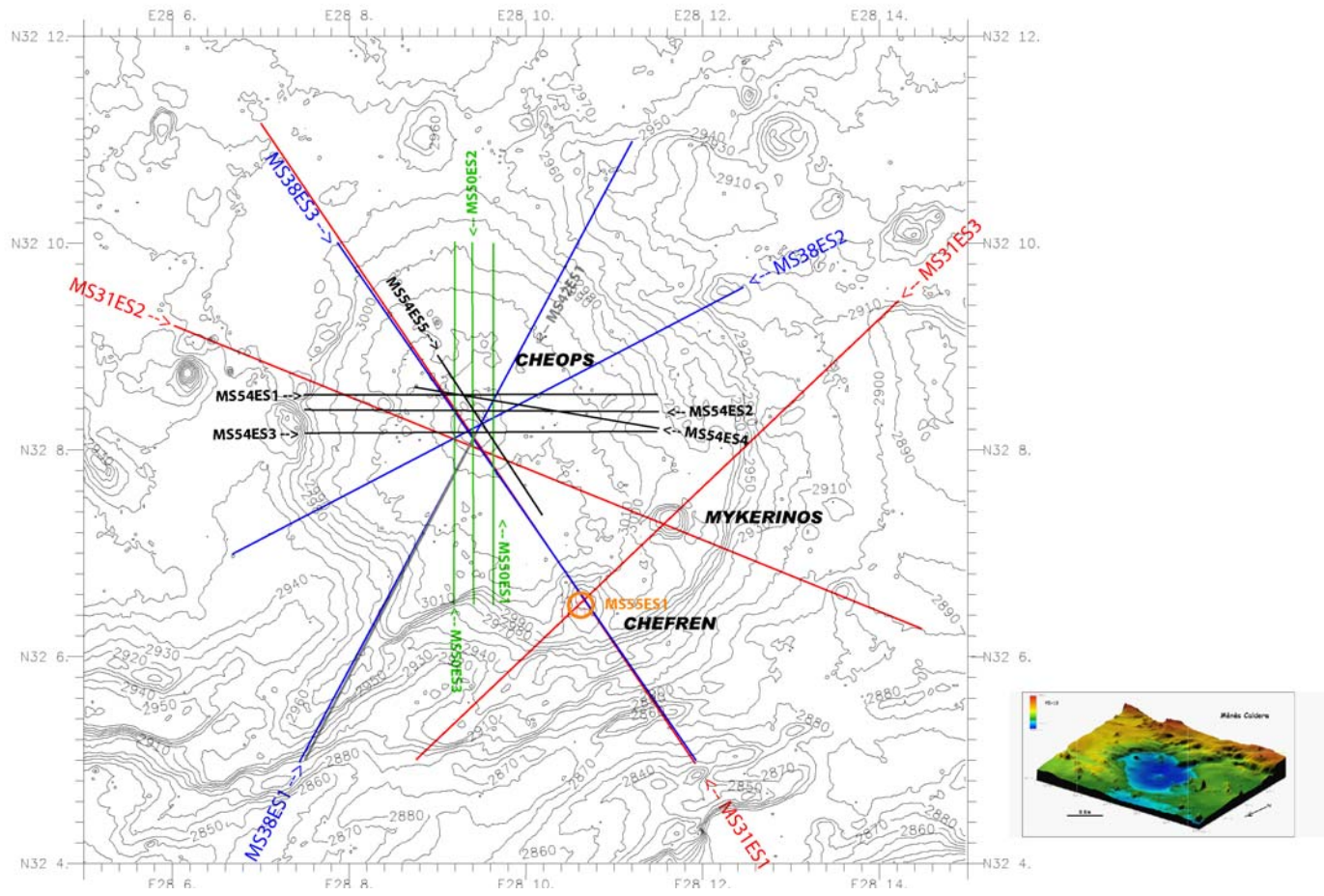
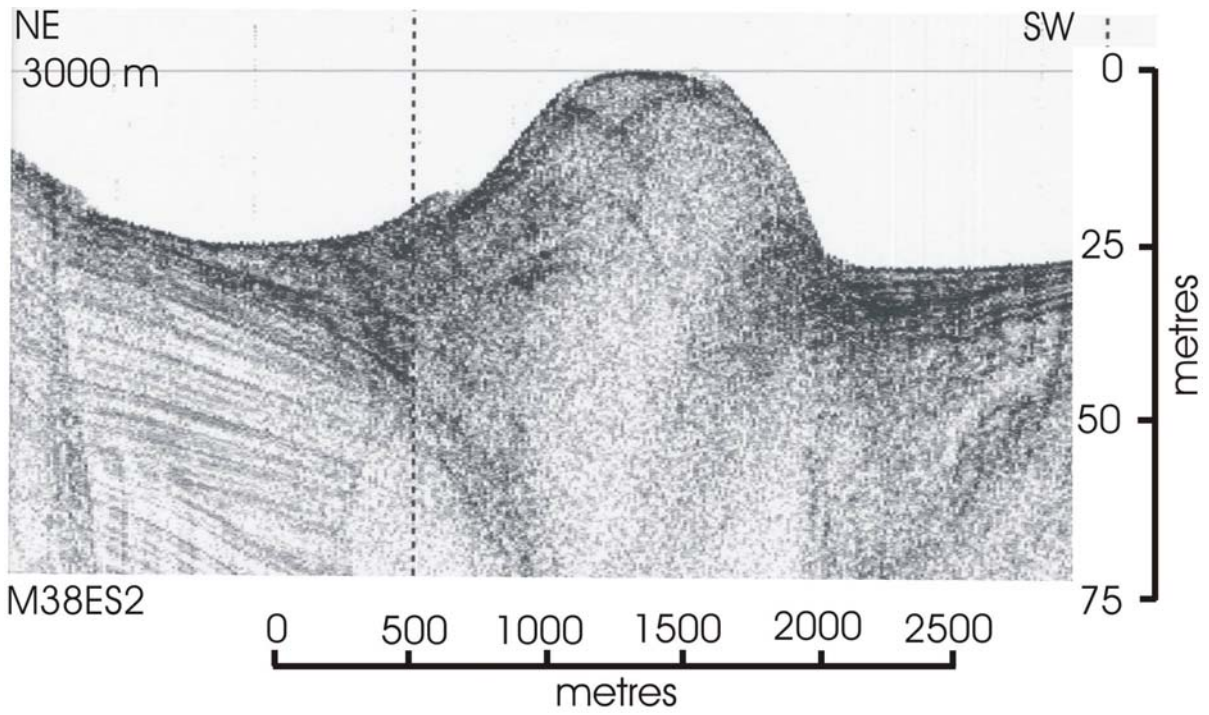


Figure 8.2 MS ES Caldera



### Cheops Mud Volcano (centre of Menes Caldera)

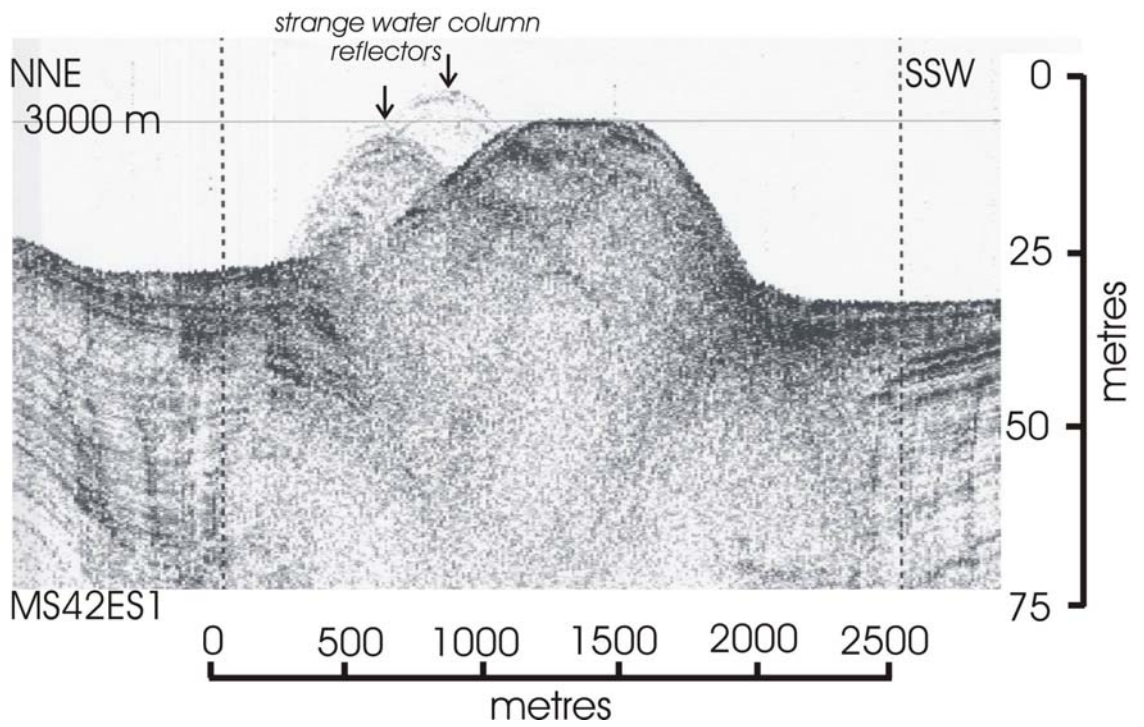


Figure 8.3 Cheops MS38ES2&MS42ES1

## **9.0.0 Summary**

The MIMES Expedition on R/V *Pelagia* docked in Limassol on 12 July after a successful mission to investigate seafloor seeps and mud volcanoes in the eastern Mediterranean Sea, mainly on the Nile Deep Sea Fan. MIMES (a **M**ultiscale **I**vestigations of **E**astern **M**editerranean **S**eep **S**ystems) is a Dutch (NWO) funded contribution to the four year MEDIFLUX project in which France, Germany, and the Netherlands cooperate under the ESF umbrella of Euromargins. As a follow-up to NAUTINIL, a French-coordinated expedition in September 2003 with the French submersible *Nautile*, MIMES aimed to add deeper sampling at locations examined and sampled by *Nautile*, provide detailed water column and sedimentary geochemical analyses, and use geophysical methods (principally the Edgetech DTS-1 deep tow system owned and operated by Geomar, Kiel, with additional 3.5 kHz echosounding) to characterize the seafloor in areas where ground truth observations from *Nautile* had been made. Table 9.1 lists all participants on the ship who contributed to MIMES during the expedition.

During the period between 16 June when the *Pelagia* departed Iraklion to the end of the cruise on the 12 of July, 26 piston and 11 gravity cores were made – 19 of these core stations with thermal probes mounted on the core barrel, 5 box cores were taken with a video system mounted to provide guidance for reconnaissance and selected sampling of the seafloor, 10 SeaBird CTD casts and 3 CTD casts in briny mud pools on two mud volcanoes using an instrument adapted to this extreme environment (and with thermal probes attached), 6 deep tow deployments with 26 lines for a total of roughly 700 line kilometers, and 7 surveys of mud volcanoes with the 3.5 kHz echosounder totaling about 130 line kilometres (Table 9.2). The work was carried out in 5 general areas with the concentration on two different environments on the Nile fan system – one over large gas chimneys in the east and one over a large caldera structure near the base of the fan in the west. Table 9.3 provides a summary of all activities with their locations, as extracted from the electronic logbook maintained on the bridge during the work.

The brine pools on two mud volcanoes (Chefren and Cheops) in the 3000 m caldera site were particularly interesting. On the summit of Chefren there is a brine pool that is about 250 m across accompanied by soupy mud with a depth as great as 250 m, thus deeper than the seafloor surrounding the mud volcano. The temperature of the mud is as high as 57°C throughout indicating both good mixing of the briny mud but also relatively high advection of fluids into the pool from below. Strangely, however, there is some density stratification with the pool related to salinity and suspended matter variations. Cheops has a much shallower pool with lower temperature brine (25°-42°C depending on location) suggesting less vigorous activity than at Chefren; however there is a much higher concentration of methane in the water column above Cheops. The sources of fluids appear to be different between Cheops and Chefren also, with Chefren having a much higher sulphide content and lower salinity than Cheops.

Above all the mud volcanoes where CTD casts were made are plumes of water enriched in methane and extending tens of metres upwards from the seafloor in association with elevated levels of turbidity in the water. Where a CTD cast was repeated during MIMES after an

interval of a week, the levels of turbidity and methane were different which suggests variable activity of fluid emission, perhaps as short bursts at regular intervals, rather than as a continuous release of fluids at a constant rate at the seafloor. Plumes of free gas bubbles were observed in the water column above two mud volcanoes on sidescan sonar records where deep-tow surveys were done utilizing the Geomar DTS-1 Edgetech system. One surprising observation from the deep tow survey in the pockmarks region of the central Nile fan was large gas plumes observed in the raw sidescan sonar data, which indicates an unexpected high level of activity from some of the structures.

Preliminary observations from deep tow surveys completed over mud volcanoes in the eastern province of the Nile deep sea fan system show small scale concentric seafloor relief to be characteristic of these rather low conical-shaped structures over large gas chimneys imaged previously in seismic data. They give the impression of ripples in a pool. The heat-flow measurements on one of these (Isis mud volcano) show axisymmetric values with a strong central peak (where the thermal gradient in the upper 10 m exceeds  $2^{\circ}\text{C}/\text{m}$  ( $2.2^{\circ}\text{C}/\text{m}$ , down from the value of  $2.7^{\circ}\text{C}/\text{m}$  measured during Nautinil last year) and a rapid decrease outwards towards the margins of the structure. Similarities in structure, morphology and high central gradients in other mud volcanoes of this type would indicate similar mechanisms of fluid release if not also similar fluxes.

A prototype video camera system mounted on the box corer showed great promise for the future as well as providing us with a way of examining the seafloor at sample sites and taking samples exactly where desired. This was especially important in order to try to sample small areas of seafloor observed from the French submersible Nautile last year where different types of bacteria or fluid emissions were found. We could also use the video to monitor possible changes in the seeps systems since last September, in much the same way that repeat observations on mud volcanoes south of Crete show relatively rapid changes for example in location of brine pools. The development of this system should be fully supported with integration of fibre optic cable for true real-time observations with good resolution, as well as provision of more sensitive heave compensator and better lighting.

### 9.1.0 Acknowledgements

The success of any cruise is dependent on good team work, good support, good equipment, and good communications. MIMES would not have been as successful as it was without the excellent officers and crew of Research Vessel *Pelagia* under the fine command of John Ellen. The ship had larger numbers of people on board than are normal (see table 9.1) but coped very well thanks to everybody's mutual efforts and understanding. Although there were some difficulties with some equipment, everybody pitched in to help solve the problems including many people not on the ship who worked hard behind the scenes to trace spare parts and send information and advice; among these shore-based supporters who are here thanked for their efforts during the expedition were Jack Schilling, Jean-Marc Siquin, and Marieke Rietveld, to name only three.

Table 9.1

**PARTICIPANTS ABOARD R/V PELAGIA DURING MIMES (MEDIFLUX)****SCIENTIFIC AND TECHNICAL STAFF**

<b><u>name</u></b>	<b><u>affiliation</u></b>	<b><u>function</u></b>	<b><u>email</u></b>
Marcel Bakker	NIOZ	marine technician	Marcelb@nioz.nl
Dietmar Bürk	Geomar	DTS-1 deep tow	dbuerk@ifm.geomar.de
Anke Dählmann	UU	geochemistry	A.Daehlmann@geo.uu.nl
Gert de Lange	UU	co-chief scientist, geochemistry	gdelonge@geo.uu.nl
Emmanuelle Ducassou	Geoazur	sedimentology	e.ducassou@epoc.u-bordeaux1.fr
Stéphanie Dupré	VU	geophysics	stephanie.dupre@falw.vu.nl
Tom Feseker	Ifremer	heat flow	feseker@uni-bremen.de
Jean-Paul Foucher	Ifremer	MEDIFLUX coordinator, geophysics	jean.paul.foucher@ifremer.fr
Swanne Gontharet	UPMC	foram signature of seeps	Swanne.Gontharet@lodyc.jussieu.fr
Sanela Gusic	UU	geochemistry	s.gusic@geo.uu.nl
Cheryl Melati van Kempen	UU	geochemistry	c.m.vankempen@students.uu.nl
Ingo Klaucke	Geomar	DTS-1 deep tow, Geomar	iklaucke@geomar.de
Martin Laan	NIOZ	electronics/CTD technician	martin@nioz.nl
Vincent Mastalerz	UU	geochemistry	v.mastalerz@geo.uu.nl
Sebastien Migeon	Geoazur	sedimentology	migeon@obs-vlfr.fr migeon@geoazur.unice.fr
Shauna Ni Fhlaithearta	UU	geochemistry	shauna.ni@wur.nl
Jan van Ooijen	NIOZ	AA technician	ooyen@nioz.nl
Patrick van Santvoort	UU	geochemistry	p.v.santvoort@hccnet.nl
Torsten Schott	Geomar	DTS-1 deep tow	<a href="mailto:tschott@ifm-geomar.de">tschott@ifm-geomar.de</a> <a href="mailto:schriever@biolab.com">schriever@biolab.com</a>
Alina Stadnitskaia	NIOZ	biomarkers	alina@nioz.nl
John Woodside	VU	chief scientist, geophysics	john.woodside@falw.vu.nl
Leon Wuis	NIOZ	marine technician	wuis@nioz.nl

**OFFICERS AND CREW**

John Betsema	NIOZ	AB 4	
Piet Boon	NIOZ	AB 2	
John Dresken	NIOZ	Cook	
John Ellen	NIOZ	Master	<a href="mailto:jce@pelagia.nioz.nl">jce@pelagia.nioz.nl</a>
Marcel de Kleine	NIOZ	Chief Engineer	
Niels Knuth	NIOZ	2nd Officer	
Niels Meijer	NIOZ	AB 1	

Bert Puijman	NIOZ	Chief Officer
Emanuel Vermeulen	NIOZ	2nd Engineer
Ger Vermeulen	NIOZ	AB 3
Jose Victoria	NIOZ	Assistant Cook

**Affiliation addresses**

Geoazur	Géosciences Azur Observatoire de Villefranche Port de la Darse 06235 Villefranche-sur-Mer France
Geomar	IFM-GEOMAR Wischhofstr. 1-3 24148 Kiel Germany
Ifremer	Ifremer DRO-GM BP 70 29280 Plouzané France
NIOZ	NIOZ Landsdiep 4 1797 SZ 't Horntje (Texel) The Netherlands
UPMC	LODYC (tr. 45-55, 4 <sup>ème</sup> étage) Université Pierre et Marie Curie 4 Place Jussieu 75252 – Paris Cedex 5 France
UU	Utrecht University Faculty of Geochemistry Department of Earth Sciences P.O. Box 80021 3508 TA Utrecht The Netherlands
VU	Faculteit Aard- en Levenswetenschappen Vrije Universiteit De Boelelaan 1085 1081 HV Amsterdam The Netherlands

Table 9.2 Science operations summary

<b>MIMES overview of scientific activities</b>										
MS number	piston core	thermal probes	gravity core	box core	video	SB CTD	ME CTD	deep tow	3.5 kHz	line kms
1							1			
2								1		52
3				1	1					
4	1	1								
5								1		225
6			1							
7			1							
extra (7a)									1	10 km
8	1	1								
9	1									
10								1		90
11	1	1								
12	1	1								
13	1	1								
14								1		118
15										
16							1			
17	1	1					1			
18					1					
19		1	1							
20								1		108
21	1									
22	1	1								
23							1			
24	1	1								
25							1			
26	1	1								
27	1									
28										
29				1	1		1			
30	1	1								
31										1 50 km
32										
33				1	1		1			
34	1	1								



Table 9.3 Cruise logbook

MEDIFLUX04 - 64PE227		MIMES										
Station Label	Type	Event	Date/Time	Lat	Lon	LAT(DEG)	LAT(MIN)	LO(DEG)	LO(MIN)	Depth	Remarks	Where
1 MS01CT	CTD sal- nutrients- en oxygen samples	Begin	Jun 17 2004 15:04:11	35.33333	30.26663	35	19.9998	30	15.9978	1987		Amsterdam mv
1	CTD sal- nutrients- en oxygen samples	Bottom	Jun 17 2004 15:38:45	35.33335	30.26662	35	20.0010	30	15.9972	1991		
1	CTD sal- nutrients- en oxygen samples	End	Jun 17 2004 17:03:17	35.33322	30.26673	35	19.9932	30	16.0038	1991		
2 MS02DT1	DTS	Begin of line	Jun 17 2004 18:51:33	35.16673	30.42702	35	10.0038	30	25.6212	2213	DEPLOYMENT OF DTS	Amsterdam mv
2	DTS	End of line	Jun 17 2004 23:20:11	35.28270	30.29230	35	16.9620	30	17.5380	2286	END OF DEPLOYMENT LINE	Where
3 MS02DT2	DTS	Begin of line	Jun 17 2004 23:20:13	35.28270	30.29230	35	16.9620	30	17.5380	2290		to
3	DTS	End of line	Jun 18 2004 03:04:48	35.40835	30.19668	35	24.5010	30	11.8008	1491		Athina mv
4 MS03BV	Boxcorer	Bottom	Jun 18 2004 08:11:12	35.33348	30.26620	35	20.0088	30	15.9720	1991		Amsterdam mv
5 MS04PT	Pistoncorer	Bottom	Jun 18 2004 12:53:57	35.33398	30.26570	35	20.0388	30	15.9420	1991		Amsterdam mv
6 MS05DT1	DTS	Begin of line	Jun 18 2004 21:33:14	35.37978	30.73567	35	22.7868	30	44.1402	1950	LINE 1	Kazan mv survey
6	DTS	End of line	Jun 19 2004 03:21:11	35.43835	30.47005	35	26.3010	30	28.2030	1922		
7 MS05DT2	DTS	Begin of line	Jun 19 2004 05:37:48	35.41245	30.48817	35	24.7470	30	29.2902	1934	LINE 2	
7	DTS	End of line	Jun 19 2004 13:04:28	35.35472	30.82908	35	21.2832	30	49.7448	1967		
8 MS05DT3	DTS	Begin of line	Jun 19 2004 15:41:50	35.39150	30.82258	35	23.4900	30	49.3548	1942	LINE 3	
8	DTS	End of line	Jun 19 2004 23:17:54	35.44987	30.47455	35	26.9922	30	28.4730	1741		
9 MS05DT4	DTS	Begin of line	Jun 20 2004 00:35:14	35.42457	30.48353	35	25.4742	30	29.0118	1844	LINE 4	
9	DTS	End of line	Jun 20 2004 08:02:18	35.36813	30.82047	35	22.0878	30	49.2282	1991		
10 MS05DT5	DTS	Begin of line	Jun 20 2004 11:08:05	35.40340	30.82195	35	24.2040	30	49.3170	1954	LINE 5	
10	DTS	End of line	Jun 20 2004 18:38:51	35.45818	30.48340	35	27.4908	30	29.0040	1741		
11 MS05DT6	DTS	Begin of line	Jun 20 2004 19:47:48	35.44430	30.47208	35	26.6580	30	28.3248	1786	LINE 6	
11	DTS	End of line	Jun 21 2004 03:07:20	35.38133	30.80177	35	22.8798	30	48.1062	1991		Kazan mv
12 MS06GT	Pistoncorer	Bottom	Jun 21 2004 07:59:54	35.43087	30.56487	35	25.8522	30	33.8922	1684		Kazan mv
13 MS07GT	Pistoncorer	Bottom	Jun 21 2004 10:51:36	35.43198	30.56188	35	25.9188	30	33.7128	1663		Kazan mv
14 MS_ES1	3.5 kHz	Begin of line	Jun 23 2004 11:30:45	32.36765	31.40668	32	22.0590	31	24.4008	1030		Isis 3.5 kHz survey
14	3.5 kHz	End of line	Jun 23 2004 12:03:07	32.35342	31.37485	32	21.2052	31	22.4910	1003		
15 MS_ES2	3.5 kHz	Begin of line	Jun 23 2004 12:03:09	32.35342	31.37485	32	21.2052	31	22.4910	1003		
15	3.5 kHz	End of line	Jun 23 2004 12:16:28	32.35003	31.39958	32	21.0018	31	23.9748	1003		
16 MS_ES3	3.5 kHz	Begin of line	Jun 23 2004 12:16:30	32.35003	31.39958	32	21.0018	31	23.9748	1003		
16	3.5 kHz	End of line	Jun 23 2004 12:42:48	32.36203	31.38850	32	21.7218	31	23.3100	975		
17 MS_ES4	3.5 kHz	Begin of line	Jun 23 2004 12:43:38	32.36250	31.38810	32	21.7500	31	23.2860	981		
17	3.5 kHz	End of line	Jun 23 2004 12:48:48	32.36648	31.38358	32	21.9888	31	23.0148	990		
18 MS08PT	Pistoncorer	Bottom	Jun 23 2004 13:49:36	32.36098	31.38947	32	21.6588	31	23.3682	978	FAILED	Isis mv
18 MS09PC	Pistoncorer	Bottom	Jun 23 2004 17:11:38	32.36092	31.38958	32	21.7000	31	23.4000	977		Isis mv
19 MS10DT1	DTS	Begin of line	Jun 23 2004 20:32:12	32.39408	31.39703	32	23.6448	31	23.8218	1090	SOL 1	Isis deep-tow survey

Station Label	Type	Event	Date/ Time	Lat	Lon	LAT(DEG)	LAT(MIN)	LO(DEC)	LO(MIN)	Depth	Remarks	Where
19	DTS	End of line	Jun 24 2004 00:33:02	32.26078	31.27958	32	15.6468	31	16.7748	818		
20	MS10DT2	Begin of line	Jun 24 2004 01:55:24	32.22942	31.28812	32	13.7652	31	17.2872	712	SOL2	
20	DTS	End of line	Jun 24 2004 06:46:29	32.38325	31.42178	32	22.9950	31	25.3068	1050		
21	MS10DT3	Begin of line	Jun 24 2004 08:25:39	32.41555	31.39830	32	24.9330	31	23.8980	1148	SOL 3	
21	DTS	End of line	Jun 24 2004 12:52:46	32.25017	31.31442	32	15.0102	31	18.8652	773		
22	MS10DT4	Begin of line	Jun 24 2004 14:43:57	32.25437	31.29175	32	15.2622	31	17.5050	794	SOL 4	
22	DTS	End of line	Jun 24 2004 18:57:00	32.38728	31.40783	32	23.2368	31	24.4698	1062		
23	MS10DT5	Begin of line	Jun 24 2004 20:09:19	32.37838	31.43707	32	22.7028	31	26.2242	1038	SOL 5	
23	DTS	End of line	Jun 25 2004 00:23:01	32.24195	31.31503	32	14.5170	31	18.9018	748		
24	MS10DT6	Begin of line	Jun 25 2004 02:48:26	32.34048	31.38450	32	20.4288	31	23.0700	1014	SOL 6 ?	
24	DTS	End of line	Jun 25 2004 04:02:32	32.38020	31.41902	32	22.8120	31	25.1412	1044		
25	MS11PT	Pistoncorer	Jun 25 2004 07:06:52	32.35987	31.39148	32	21.5922	31	23.4888	989	MS11PT	Isis mv
26	MS12PT	Pistoncorer	Jun 25 2004 11:27:15	32.35690	31.38460	32	21.4140	31	23.0760	1007	MS12PT	Isis mv
27	MS13PT	Pistoncorer	Jun 25 2004 13:40:34	32.36477	31.39912	32	21.8862	31	23.9472	995	MS13PT	Isis mv
28	MS14DT1	Begin of line	Jun 25 2004 19:00:18	32.34163	31.46800	32	20.4978	31	28.0800	922	MS14DT line 1	Osiris & Amon deep tow survey
28	DTS	End of line	Jun 26 2004 01:24:00	32.41933	31.75868	32	25.1598	31	45.5208	1343		
29	MS14DT2	Begin of line	Jun 26 2004 03:08:11	32.39458	31.76007	32	23.6748	31	45.6042	1352	MS14DT line 2	
30	DTS	End of line	Jun 26 2004 09:28:29	32.32125	31.48753	32	19.2750	31	29.2518	858		
31	MS14DT3	Begin of line	Jun 26 2004 11:10:56	32.32688	31.46597	32	19.6128	31	27.9582	885	MS14DT line 3	
31	DTS	End of line	Jun 26 2004 17:12:26	32.40348	31.74415	32	24.2088	31	44.6490	1361		
32	MS14DT4	Begin of line	Jun 26 2004 19:13:50	32.38267	31.76440	32	22.9602	31	45.8640	1337	MS14DT Line 4	
32	DTS	End of line	Jun 27 2004 01:47:48	32.30447	31.47352	32	18.2682	31	28.4112	843		
33	MS14DT5	Begin of line	Jun 27 2004 02:44:52	32.30993	31.42010	32	18.5958	31	25.2060	898	MS14DT line 5	
33	DTS	End of line	Jun 27 2004 04:58:59	32.39218	31.37382	32	23.5308	31	22.4292	1090		
34	MS15CT	Begin	Jun 27 2004 06:29:25	32.36105	31.38948	32	21.6630	31	23.3688	980	FAILED	Isis mv
34		Bottom	Jun 27 2004 06:37:50	32.36088	31.38972	32	21.6528	31	23.3832	977		
34		End	Jun 27 2004 06:43:36	32.36087	31.38970	32	21.6522	31	23.3820	977		
34	MS16CT	Begin	Jun 27 2004 07:11:24	32.36115	31.38933	32	21.6690	31	23.3598	977	ABORTED	Isis mv
34		Bottom	Jun 27 2004 07:25:11	32.36102	31.38960	32	21.6612	31	23.3760	977	stopped at 715 mtr	
34		End	Jun 27 2004 07:40:58	32.35900	31.38920	32	21.5400	31	23.3520	986		
35	MS17PT	Pistoncorer	Jun 27 2004 08:34:22	32.36645	31.38483	32	21.9870	31	23.0898	998	MS17PT	Isis mv
36	MS18BV	Boxcorer	Jun 27 2004 11:59:51	32.36107	31.38938	32	21.6642	31	23.3628	977	MS18BV	Isis mv
37	MS19GT	Gravitycorer	Jun 27 2004 13:53:11	32.36097	31.38952	32	21.6582	31	23.3712	986	MS19GT	Isis mv
38		Begin	Jun 27 2004 15:37:33	32.25757	31.39413	32	15.4542	31	23.6478	718	CTD cable test	
38		Bottom	Jun 27 2004 15:44:46	32.25743	31.39417	32	15.4458	31	23.6502	718	Break in cable at 382m	

Station Label	Type	Event	Date/Time	Lat	Lon	LAT(DEG)	LAT(MIN)	LO(DEG)	LO(MIN)	Depth	Remarks	Where
38	CTD salt- nutrients- en oxygen samples	End	Jun 27 2004 15:52:17	32.25755	31.39395	32	15.4530	31	23.6370	718		
39	DTS	Begin of line	Jun 27 2004 19:09:27	32.28247	31.48655	32	16.9482	31	29.1930	759	MS20DT line 1	Osiris & Amon deep tow survey
39	DTS	End of line	Jun 28 2004 01:50:22	32.36485	31.79273	32	21.8910	31	47.5638	1197		
40	DTS	Begin of line	Jun 28 2004 03:20:06	32.34010	31.79463	32	20.4060	31	47.6778	1045	MS20DT line 2	
40	DTS	End of line	Jun 28 2004 09:52:50	32.25957	31.49323	32	15.5742	31	29.5938	700		
41	DTS	Begin of line	Jun 28 2004 10:54:35	32.27005	31.48797	32	16.2030	31	29.2782	727	MS20DT line 3	
41	DTS	End of line	Jun 28 2004 17:24:46	32.34785	31.77425	32	20.8710	31	46.4550	1036		
42	DTS	Begin of line	Jun 28 2004 19:30:29	32.37277	31.77232	32	22.3662	31	46.3392	1231	MS20DT Line 4	
42	DTS	End of line	Jun 29 2004 04:39:56	32.30450	31.35337	32	18.2700	31	21.2022	890		
43	Pistoncorer	Bottom	Jun 29 2004 07:59:57	32.34497	31.65008	32	20.6982	31	39.0048	1022	MS21PC	between Osiris & Amon
44	Pistoncorer	Bottom	Jun 29 2004 11:07:54	32.35670	31.44502	32	21.4020	31	26.7012	1006	MS22PT	beside Isis mv
45	CTD salt- nutrients- en oxygen samples	Begin	Jun 29 2004 12:33:32	32.36083	31.38935	32	21.6498	31	23.3610	979	MS23CT	Isis mv
45	CTD salt- nutrients- en oxygen samples	Bottom	Jun 29 2004 13:07:20	32.36092	31.38957	32	21.6552	31	23.3742	988		(third attempt)
45	CTD salt- nutrients- en oxygen samples	End	Jun 29 2004 13:47:39	32.36092	31.38957	32	21.6552	31	23.3742	986		
46	Pistoncorer	Bottom	Jun 29 2004 15:03:34	32.36098	31.38952	32	21.6588	31	23.3712	981	MS24PT	Isis mv
47	CTD salt- nutrients- en oxygen samples	Begin	Jun 30 2004 05:18:31	31.96947	30.13632	31	58.1682	30	8.1792	495	MS25CT	North Alex mv
47	CTD salt- nutrients- en oxygen samples	Bottom	Jun 30 2004 05:27:14	31.96948	30.13635	31	58.1688	30	8.1810	495		
47	CTD salt- nutrients- en oxygen samples	End	Jun 30 2004 06:19:14	31.96945	30.13642	31	58.1670	30	8.1852	495		
47	Pistoncorer	Bottom	Jun 30 2004 07:51:47	31.96950	30.13617	31	58.1700	30	8.1702	495	MS26PT	North Alex mv
48	Pistoncorer	Bottom	Jun 30 2004 13:16:20	31.79832	29.46167	31	47.8992	29	27.7002	1389	MS27PC	Migeon M8
49	CTD salt- nutrients- en oxygen samples	Begin	Jul 01 2004 05:09:02	32.10920	28.17747	32	6.5520	28	10.6482	2897	MS28CT	Chefren mv
49	CTD salt- nutrients- en oxygen samples	Bottom	Jul 01 2004 05:59:42	32.10895	28.17788	32	6.5370	28	10.6728	2897		
49	CTD salt- nutrients- en oxygen samples	End	Jul 01 2004 07:41:50	32.10900	28.17762	32	6.5400	28	10.6572	2897		
50	Boxcorer	Bottom	Jul 01 2004 12:20:20	32.11015	28.17698	32	6.6090	28	10.6188	2923	MS29BV	Chefren mv
51	Pistoncorer	Bottom	Jul 01 2004 15:16:23	32.10898	28.17783	32	6.5388	28	10.6698	2897	MS30PT	Chefren mv
52	3.5 kHz	Begin of line	Jul 01 2004 19:19:17	32.08288	28.19852	32	4.9728	28	11.9112	2770	MS31ES SOL1	Menes Caldera 3.5 kHz survey
52	3.5 kHz	End of line	Jul 01 2004 22:01:05	32.18593	28.11690	32	11.1558	28	7.0140	2908	EOL1	
53	3.5 kHz	Begin of line	Jul 01 2004 23:34:07	32.15342	28.10037	32	9.2052	28	6.0222	2877	SOL2	
53	3.5 kHz	End of line	Jul 02 2004 02:17:10	32.10468	28.24152	32	6.2808	28	14.4912	2821	EOL2	
54	3.5 kHz	Begin of line	Jul 02 2004 02:46:49	32.15740	28.23717	32	9.4440	28	14.2302	2836	SOL3	
54	3.5 kHz	End of line	Jul 02 2004 04:55:27	32.08337	28.14620	32	5.0022	28	8.7720	2816	EOL3	

Station Label	Type	Event	Date/ Time	Lat	Lon	LAT(DEG)	LAT(MIN)	LON(DEG)	LON(MIN)	Depth	Remarks	Where
55 MS32CT	CTD salt- nutrients- en oxygen samples	Begin	Jul 02 2004 06:02:47	32.13618	28.15710	32	8.1708	28	9.4260	2923	MS32CT	Cheops mv
55	CTD salt- nutrients- en oxygen samples	Bottom	Jul 02 2004 06:54:22	32.13592	28.15705	32	8.1552	28	9.4230	2923	(contaminated)	
55	CTD salt- nutrients- en oxygen samples	End	Jul 02 2004 08:28:56	32.13615	28.15667	32	8.1690	28	9.4002	2923		
56 MS33BV	Boxcorer	Bottom	Jul 02 2004 12:00:07	32.13408	28.15800	32	8.0448	28	9.4800	2923	MS33BV CAMERA	Cheops mv
57 MS34PT	Pistoncorer	Bottom	Jul 02 2004 15:14:00	32.11233	28.17253	32	6.7398	28	10.3518	2943	MS34PT	Chefren mv
58 MS35PC	Pistoncorer	Bottom	Jul 03 2004 06:28:27	32.26672	27.63328	32	16.0032	27	37.9968	3051	MS35PC	Migeon M2 (Herodotus AP)
59 MS36PT	Pistoncorer	Bottom	Jul 03 2004 12:48:11	32.10902	28.17785	32	6.5412	28	10.6710	2897	MS36PT - FAILED to trip	Chefren mv
59 MS37PT	Pistoncorer	Bottom	Jul 03 2004 15:59:14	32.10898	28.17782	32	6.5388	28	10.6692	2897	MS37PT -- empty	Chefren mv
60 MS38ES1	3.5 kHz	Begin of line	Jul 03 2004 18:36:37	32.08290	28.12407	32	4.9740	28	7.4442	2821	MS38ES1	Menes Caldera 3.5 kHz survey
60	3.5 kHz	End of line	Jul 03 2004 21:14:23	32.18305	28.18687	32	10.9830	28	11.2122	2877		
61 MS38ES2	3.5 kHz	Begin of line	Jul 03 2004 21:58:31	32.15960	28.20775	32	9.5760	28	12.4650	2831	MS38ES2	
61	3.5 kHz	End of line	Jul 04 2004 00:09:17	32.11667	28.11158	32	7.0002	28	6.6948	2877		
62 MS38ES3	3.5 kHz	Begin of line	Jul 04 2004 02:13:22	32.16665	28.13142	32	9.9990	28	7.8852	2908	MS38ES3	
62	3.5 kHz	End of line	Jul 04 2004 04:12:43	32.08335	28.19895	32	5.0010	28	11.9370	2780		
63 MS39CT	CTD salt- nutrients- en oxygen samples	Begin	Jul 04 2004 05:10:56	32.13605	28.15715	32	8.1630	28	9.4290	2923	MS39CT	Cheops mv
63	CTD salt- nutrients- en oxygen samples	Bottom	Jul 04 2004 06:31:41	32.13605	28.15715	32	8.2000	28	9.4000	2923	(problems with tubes, etc)	
63	CTD salt- nutrients- en oxygen samples	End	Jul 04 2004 07:52:09	32.13617	28.15722	32	8.2000	28	9.4000	2923		
64 MS40PT	Pistoncorer	Bottom	Jul 04 2004 09:45:08	32.13605	28.15717	32	8.2000	28	9.4000	2923	MS40PT -- empty	Cheops mv
65 MS41GT	Pistoncorer	Bottom	Jul 04 2004 12:47:19	32.13600	28.15712	32	8.2000	28	9.4000	2923	MS41GT	Cheops mv
66 MS42ES1	3.5 kHz	Begin of line	Jul 04 2004 14:55:02	32.13597	28.15708	32	5.0000	28	7.5000	2826	MS42ES	Cheops mv
66	3.5 kHz	End of line	Jul 04 2004 17:27:51	32.08342	28.12502	32	11.0000	28	11.2000	2877		
67 MS43PC	Pistoncorer	Bottom	Jul 05 2004 06:10:45	32.18338	28.18682	32	0.1000	29	28.9000	1695	MS43PC	Migeon M6b -- central Nile fan
68 MS44PC	Pistoncorer	Bottom	Jul 05 2004 08:22:28	32.00167	29.48163	32	1.9000	29	29.0000	1683	MS44PC	Migeon M6a -- central Nile fan
69 MS45PC	Pistoncorer	Bottom	Jul 05 2004 11:37:32	32.03168	29.48330	32	1.9008	29	28.9980	1606	MS45PC	Migeon M7 -- central Nile fan
70 MS46PC	Pistoncorer	Bottom	Jul 05 2004 14:22:22	32.00103	29.48122	32	0.0618	29	28.8732	1700	MS46PC	Migeon M6b -- central Nile fan
71 MS47GT	Gravitycorer	Bottom	Jul 06 2004 06:27:48	32.10907	28.17777	32	6.5442	28	10.6662	2899	MS47GT	Chefren mv
72 MS48CT	CTD salt- nutrients- en oxygen samples	Begin	Jul 06 2004 08:37:57	32.10875	28.17762	32	6.5250	28	10.6572	2899	MS48CT (ME CTD)	Chefren mv

Station Label	Type	Event	Date/ Time	Lat	Lon	LAT(DEC)	LAT(MIN)	LO(DEC)	LO(MIN)	Depth	Remarks	Where
72	CTD salt- nutrients- en oxygen samples	Bottom	Jul 06 2004 10:17:45	32.10902	28.17768	32	6.5412	28	10.6608	2902		
72	CTD salt- nutrients- en oxygen samples	End	Jul 06 2004 10:48:45	32.10902	28.17767	32	6.5412	28	10.6602	2902		
73 MS49GC	Gravitycorer	Bottom	Jul 06 2004 14:02:32	32.10902	28.17785	32	6.5412	28	10.6710	2899	MS49GC -- FAILURE	Chefren mv
74 MS50ES1	3.5 kHz	Begin of line	Jul 06 2004 15:47:18	32.10833	28.16050	32	6.4998	28	9.6300	2912	MS50ES Line 1	Cheops mv
74	3.5 kHz	End of line	Jul 06 2004 17:06:33	32.16653	28.16057	32	9.9918	28	9.6342	2922		
74 MS50ES2	3.5 kHz	Begin of line	Jul 06 2004 17:12:00	32.16668	28.15673	32	10.0008	28	9.4038	2925	MS50ES Line 2	
74	3.5 kHz	End of line	Jul 06 2004 18:09:39	32.10830	28.15697	32	6.4980	28	9.4182	2899		
74 MS50ES3	3.5 kHz	Begin of line	Jul 06 2004 18:20:07	32.10827	28.15320	32	6.4962	28	9.1920	2899	MS50ES Line 3	
74	3.5 kHz	End of line	Jul 06 2004 19:34:34	32.16667	28.15338	32	10.0002	28	9.2028	2928		
75 MS51PC	Pistoncorer	Bottom	Jul 07 2004 06:18:34	32.36175	28.05003	32	21.7050	28	3.0018	2938	MS51PC -- FAILURE	Migeon site -- distal lobe of Nile fan
76 MS52CT	CTD salt- nutrients- en oxygen samples	Begin	Jul 07 2004 09:27:49	32.10873	28.17777	32	6.5238	28	10.6662	2899		Chefren mv
76	CTD salt- nutrients- en oxygen samples	Bottom	Jul 07 2004 11:26:43	32.10902	28.17773	32	6.5412	28	10.6638	2899		
76	CTD salt- nutrients- en oxygen samples	End	Jul 07 2004 12:42:12	32.10747	28.17682	32	6.4482	28	10.6092	2899		
77 MS53GC	Gravitycorer	Bottom	Jul 07 2004 14:40:40	32.13613	28.15720	32	8.1678	28	9.4320	2925	MS53GC -- FAILURE	Cheops mv
78 MS54ES1	3.5 kHz	Begin of line	Jul 07 2004 16:43:07	32.14223	28.12490	32	8.5338	28	7.4940	2912	MS54ES Line 1	Cheops mv
78	3.5 kHz	End of line	Jul 07 2004 17:55:27	32.14230	28.19153	32	8.5380	28	11.4918	2902		
78 MS54ES2	3.5 kHz	Begin of line	Jul 07 2004 18:01:10	32.13952	28.19187	32	8.3712	28	11.5122	2912	MS54ES Line 2	Cheops mv
78	3.5 kHz	End of line	Jul 07 2004 19:11:30	32.13985	28.12510	32	8.3910	28	7.5060	2918		
78 MS54ES3	3.5 kHz	Begin of line	Jul 07 2004 19:24:25	32.13608	28.12498	32	8.1648	28	7.4988	2860	MS54ES Line 3	Cheops mv
78	3.5 kHz	End of line	Jul 07 2004 20:35:26	32.13635	28.19152	32	8.1810	28	11.4912	2912		
78 MS54ES4	3.5 kHz	Begin of line	Jul 07 2004 20:44:12	32.13670	28.19178	32	8.2020	28	11.5068	2912	MS54ES Line4	Cheops mv
78	3.5 kHz	End of line	Jul 07 2004 21:43:47	32.14337	28.14578	32	8.6022	28	8.7468	2948		
79 MS54ES5	3.5 kHz	Begin of line	Jul 07 2004 22:12:14	32.14857	28.15012	32	8.9142	28	9.0072	2951	MS54ES Line 5	Cheops mv
79	3.5 kHz	End of line	Jul 07 2004 22:54:29	32.12292	28.16992	32	7.3752	28	10.1952	2954		
80 MS55ES1	3.5 kHz	Begin of line	Jul 07 2004 23:23:43	32.10943	28.17688	32	6.5658	28	10.6128	2899	MS55ES within circle with r=320m	Chefren mv
80	3.5 kHz	End of line	Jul 08 2004 04:32:27	32.10717	28.17700	32	6.4302	28	10.6200	2897		
81 MS56CT	CTD salt- nutrients- en oxygen samples	Begin	Jul 08 2004 05:09:50	32.13657	28.15675	32	8.1942	28	9.4050	2925	MS56CT	Cheops mv -- repeat of MS32CT

Station Label	Type	Event	Date/ Time	Lat	Lon	LAT(DEG)	LAT(MIN)	LON(DEG)	LON(MIN)	Depth	Remarks	Where
81	CTD salt- nutrients- en oxygen samples	Bottom	Jul 08 2004 06:04:22	32.13613	28.15718	32	8.1678	28	9.4308	2925		
81	CTD salt- nutrients- en oxygen samples	End	Jul 08 2004 07:36:25	32.13607	28.15685	32	8.1642	28	9.4110	2925		
82 MS57GC	Gravitycorer	Bottom	Jul 08 2004 09:20:31	32.10885	28.17793	32	6.5310	28	10.6758	2899	MS57GC	Chefren mv
83 MS58CT	CTD salt- nutrients- en oxygen samples	Begin	Jul 08 2004 10:59:37	32.13600	28.15720	32	8.1600	28	9.4320	2925	MS58CT	Cheops mv
83	CTD salt- nutrients- en oxygen samples	Bottom	Jul 08 2004 12:37:30	32.13615	28.15713	32	8.1690	28	9.4278	2925		
83	CTD salt- nutrients- en oxygen samples	End	Jul 08 2004 13:32:18	32.13575	28.15687	32	8.1450	28	9.4122	2925		
84 MS59PT	Pistoncorer	Bottom	Jul 08 2004 15:36:11	32.16333	28.14165	32	9.7998	28	8.4990	2925	MS59PT	northern floor of Menes Caldera
85 MS60CT	CTD salt- nutrients- en oxygen samples	Begin	Jul 09 2004 03:21:15	31.96948	30.13625	31	58.1688	30	8.1750	495	MS60CT	North Alex
85	CTD salt- nutrients- en oxygen samples	Bottom	Jul 09 2004 03:29:45	31.96953	30.13623	31	58.1718	30	8.1738	492		
85	CTD salt- nutrients- en oxygen samples	End	Jul 09 2004 04:15:36	31.96947	30.13623	31	58.1682	30	8.1738	492		
86 MS61BV	Boxcorer	Bottom	Jul 09 2004 07:22:02	31.96917	30.13677	31	58.1502	30	8.2062	492	MS61BV	North Alex
87 MS62GC	Pistoncorer	Bottom	Jul 09 2004 08:25:47	31.96950	30.13633	31	58.1700	30	8.1798	495	MS62GC -- poor recovery	North Alex
88 MS63GC	Pistoncorer	Bottom	Jul 09 2004 10:30:54	31.96967	30.13650	31	58.1802	30	8.1900	498	MS63GC -- FAILURE	North Alex
89 MS64PT	Pistoncorer	Bottom	Jul 09 2004 11:42:02	31.96933	30.13650	31	58.1598	30	8.1900	495	MS64PT -- repeat of MS62GC and MS63GC	North Alex
90 MS65DT1	DTS	Begin of line	Jul 09 2004 18:48:03	32.51355	30.23317	32	30.8130	30	13.9902	1701	MS65DT	Pockmark area in Central Nile Fan
91	DTS	End of line	Jul 10 2004 00:18:49	32.59237	30.46875	32	35.5422	30	28.1250	1782	EOL1	
92 MS65DT2	DTS	Begin of line	Jul 10 2004 02:57:15	32.55670	30.48018	32	33.4020	30	28.8108	1700	SOL 2	
93	DTS	End of line	Jul 10 2004 09:17:46	32.46312	30.20513	32	27.7872	30	12.3078	1635	EOL 2	
94 MS65DT3	DTS	Begin of line	Jul 10 2004 10:57:43	32.49280	30.23423	32	29.5680	30	14.0538	1661	SOL 3	
94	DTS	End of line	Jul 10 2004 16:14:30	32.57547	30.47617	32	34.5282	30	28.5702	1730	EOL 3	
95 MS65DT4	DTS	Begin of line	Jul 10 2004 18:03:42	32.54082	30.49312	32	32.4492	30	29.5872	1706	SOL 4	
95	DTS	End of line	Jul 11 2004 01:07:37	32.43255	30.17553	32	25.9530	30	10.5318	1607	EOL 4	
96 MS66PC	Pistoncorer	Bottom	Jul 11 2004 12:12:52	33.03167	31.79873	33	1.9002	31	47.9238	1630	MS66PC	Reference core north central Nile Fan (for Coolen)



## **10 References**

- Aloisi, G., Bouloubassi, I., Heijs, S.K., Pancost, R.D., Pierre, C., Sinninghe Damsté, J.S., Gottschal, J.C., Forney, L.J. and Rouchy, J-M., 2002, CH<sub>4</sub>-consuming microorganisms and the formation of carbonate crusts at cold seeps. *Earth and Planetary Science Letters*, **203**:195-203.
- Bellaïche, G., Loncke, L., Gaullier, V., Mascle, J., Courp, T., Moreau, A., Radan, S., Sardou, O., 2001, Le Cône sous marin du Nil et son réseau de chenaux profonds: nouveaux résultats, *C.R. Acad. Sci. Paris, Sciences de la Terre et des Planètes*, 333, 399-404
- Bellaïche, G., Zitter, T., Droz, L., Gaullier, V., Mart, Y., Mascle, J. et l'équipe scientifique embarquée, 1999. Le cône sous-marin profond du Nil: principaux résultats de la campagne "Prismed II" du N.O. "l'Atalante", *C. R. Acad. Sc. Paris*, t. 329, série II a, 727-733.
- Blondel, P., and Murten, B.J., 1998, Handbook of seafloor imagery. John Wiley and Sons Ltd, West Sussex, England, 314 p.
- Boetius, A., Ravensschlag, K., Schubert, C., Rickert, D., Widdel, F., Gieseke, A., Amann, R., Jørgensen, B.B., Witte, U., Pfannkuche, O. (2000) A marine microbial consortium apparently mediating anaerobic oxidation of methane. *Nature* 407, 623-626.
- Charlou, J.L., Donval, J.P., Zitter, T., Roy, N., Jean Baptiste, P., Foucher J.P., Woodside J and Medinaut party. 2003. Evidence of methane venting and geochemistry of brines on mud volcanoes of the eastern Mediterranean. *Deep-Sea Research I*, 50:941-958.
- Cita, M.B., Ryan, W.B.F., and Paggi, L., 1981, Prometheus mud breccia: An example of shale diapirism in the Western Mediterranean Ridge. *Ann. Geol. Pays Hellen.*, **30**:543-570.
- Cita, M.B., Ivanov, M., and Woodside, J., (eds.), 1996, The Mediterranean Diapiric Belt; special issue of *Marine Geology*, **132**(1/4):1-276.
- Dählmann, A., and de Lange, G.J., 2003, Fluid-sediment interactions at the eastern Mediterranean mud volcanoes: a stable isotope study from ODP Leg 160. *Earth and Planetary Science Letters*, **212**(3/4):377-391.
- De Lange, G.J., and Brumsack, H.J. (1998) The occurrence of gas hydrates in Eastern Mediterranean mud dome structures as indicated by porewater composition. In Henriet, J.-P., and Mienert, J. (eds.) *Gas Hydrates: Relevance to World Margin Stability and Climate Change*. Geological Society, London, Special Publications, **137**:167-175.
- De Lange, G.J., 1992, Shipboard routine and pressure-filtration system for pore-water extraction from suboxic sediments. *Mar. Geol.*, **109**:77-81.
- De Lange, G.J., 1983, Geochemical evidence of a massive slide in the southern Norwegian Sea. *Nature*, **305**:420-422.
- De Lange, G.J., and Ten Haven, H.L., 1983, Recent sapropel formation in the eastern Mediterranean. *Nature*, **305**:797-798.
- Foucher, J.-P., Mascle, J., Loncke, L., Woodside, J., Boetius, A., and the Nautinil shipboard party, 2004, Fluid seeps of the Nile Deep Sea Fan: First results of the NAUTINIL (2003) Dive expedition. Extended abstract in *Rapp. Comm. int. Mer Médit.*, **37**:29
- Gaullier, V., Mart, Y., Bellaïche, G., Mascle, J., Vendeville, B., Zitter, T. and the second leg "PRISMED II" scientific party, 2000. Salt tectonics in and around the Nile deep sea fan : insights from the Prismed II cruise.: in :Vendeville, B., Mart, Y. and Vigeresse, J.L.

- (eds) *Salt, Shale and Igneous diapirs in and around Europe*. Geological Society, London, Special publications, 174, 110-129.
- Grasshoff, K., Ehrhardt, M., and Kremling, K., 1983, Methods of seawater analysis. VCH, Weinheim.
- Haese, R.R., Meile, C., van Cappellen, P., and de Lange, G.J., 2003, Carbon geochemistry of cold seeps: Methane fluxes and transformation in the sediments from Kazan mud volcano, eastern Mediterranean Sea. *Earth and Planetary Science Letters*, **212**(3/4):361-375.
- Huguen, C., Ondreas, H., Sibuet, M., Foucher, J.-P., Woodside, J., Mascle, J., and the Nautinil shipboard scientific party, 2004, Seepage activity of the Napoli mud volcano: evidence from observations made during the MEDINAUT (1998) and NAUTINIL(2003) dive expeditions. Extended abstract in *Rapp. Comm. int. Mer Médit.*, **37**:38.
- Johnson, H.P., and Helferty, M., 1990, The geological interpretation of sidescan sonar. *Reviews in Geophysics*, **28**:357-380.
- Jongsma, D., Fortuin, A.R., Huson, W., Troelstra, S.R., Klaver, G.T., Peters, J.M., van Harten, D., de Lange, G.J., and Ten Haven, L., 1983, Discovery of an anoxic basin within the Strabo Trench, Eastern Mediterranean. *Nature*, **305**:795-797.
- Loncke, L., 2002, Le Delta Profond du Nil : Structure et évolution depuis le Messinien, Thèse de Doctorat de l'Université P. et M. Curie (Paris 6), 180p.
- Loncke, L., Gaullier, V., Bellaiche, G., and Mascle, J., (2002) Recent depositional pattern of the Nile deep-sea fan from echo-character mapping: interactions between turbidity currents, mass-wasting processes and tectonics, *Am. Assoc. of Petroleum Geologists Bull.*, *in press*.
- Loncke, L., Gaullier, V., Bellaiche, G., and Mascle, J., Recent depositional pattern of the Nile deep-sea fan: control from turbidity currents, mass-wasting processes and tectonics, *CIESM Workshop series* 13. 71-75
- Loncke, L., Mascle, J., and the Fanil scientific parties, Mud Volcanoes, gas chimneys, pockmarks and mounds in the Nile deep-sea fan (Eastern Mediterranean), *Marine Petroleum Geology*, **21**:669-689.
- Mascle, J., Zitter, T., Bellaiche, G., Droz, L., Gaullier, V., Mart, Y. & the Prismed Scientific Party, (2001) The Nile deep sea fan: preliminary results from a swath bathymetry survey. *Marine and Petroleum Geology*, **18**, 471-479.
- Mascle J., Benkhelil J., Bellaiche G., Zitter T., Woodside J., and Loncke L., 2000. Marine geologic evidence for a Levantine-Sinai plate, a new piece of the Mediterranean puzzle, *Geology*, **28**, 779-782.
- MEDINAUT/MEDINETH Shipboard Scientific Party, (2000) Linking Mediterranean Brine Pools and Mud volcanism. *Eos Trans. Am. Geophys. Union* 625-632.
- MEDRIFF Consortium, 1995, Three brine lakes discovered in the seafloor of the eastern Mediterranean, *Eos, Transactions, American Geophysical Union*, **76**:313-318.
- Olu – Le Roy, K., Sibuet, M., Levitre, G., Gofas, S., Salas, C., Fiala-Médioni, A., Foucher, J.-P., and Woodside, J., (2004) Cold seep communities in the deep eastern Mediterranean Sea: composition and spatial distribution on mud volcanoes. *Deep-Sea Research – I*, *in press*.
- Pancost R., Sinninghe Damsté J.S., De Lint S., Van Der Maarel M.J.E.C., Gottschal J.C. and the Medinaut Shipboard Scientific Party, 2000, Biomarker evidence for widespread

- anaerobic methane oxidation in Mediterranean sediments by a consortium of methanogenic archae and bacteria. *Appl. Env. Microbiol.* **66**:1126-1132.
- Sardou, O., and Mascle, J., 2003, Cartography by multibeam echo-sounder of the Nile deep-sea Fan and surrounding areas (2 sheets). Special publication CIESM, Monaco.
- Stoll, M.H.C., Bakker, K., Nobbe, G.H., and Haese, R.R., 2001, Continuous-Flow Analysis of Dissolved Inorganic Carbon Content in Seawater. *Anal. Chem.*, **73**:4111-4116.
- Volgin, A.V., and Woodside, J.M., (1996) Sidescan sonar images of mud volcanoes from the Mediterranean Ridge: Causes of variation in backscatter intensity; *Marine Geology*, vol. 132, no. 1/4, pp 39-53.
- Werne, J.P., Baas, M., and Sinninghe Damsté, J.S., 2002, Molecular isotope tracing of carbon flow and trophic relationships in a methane-supported benthic microbial community. *Limnol. Oceanogr.*, **47**(6):1694-1701.
- Woodside, J.M., Ivanov, M.K., Limonov, A.F., and Shipboard Scientists of the Anaxiprobe Expeditions, (1998) Shallow gas and gas hydrates in the Anaximander Mountains regions, eastern Mediterranean Sea; In Henriot, J.-P., and Mienert, J. (eds.) *Gas Hydrates: Relevance to World Margin Stability and Climate Change*. Geological Society, London, Special Publications, vol. 137, pp 177-193.
- Zitter, T.A.C., 2004, Mud volcanism and fluid emissions in eastern Mediterranean neotectonic zones. PhD Thesis, Vrije Universiteit te Amsterdam, 140p.